Glial Glutamate Transporters in Human Epileptic Hippocampus

By

Lars Petter B-W Bjørnsen

Thesis

Medical Research Curriculum
Department of Anatomy
Institute of Basic Medical Sciences
University of Oslo
Oslo, Norway

Supervisor: Prof. Niels Chr. Danbolt

Acknowledgements

The work included in this thesis has been performed at the Department of Anatomy of the Institute of Basic Medical Sciences, University of Oslo, and Department of Neurosurgery, Yale School of Medicine, Yale University, USA.

My main supervisor Niels Christian Danbolt deserves my deepest thanks for enthusiastic guidance, encouragement, continuous support, and friendship. I am grateful for having had the opportunity to work in his lab since 1999. I extend my thanks to my supervisor and friend Dr Tore Eid who has contributed with support and discussions concerning my work at Yale. I am deeply grateful to my supervisor at Neurosurgery Department at Yale, Professor Nihal de Lanerolle, for letting me be a part of his lab. A special thank to Knut Petter Lehre for always being willing to help and answer questions. I appreciate the contribution of all colleagues and staff members to creating a friendly and stimulating atmosphere at the institute of Basic Medical Sciences in Oslo and at Yale University. A special thank to Silvia Holmseth, who has been working alongside me at the lab.

I wish to thank Ilona Kovacs for technical assistance.

Research scholarship and travel support were provided by the Norwegian Research Council through the Medical Research Curriculum, The Norwegian Top Research Program, Tom Wilhelmsen's Foundation, and The Norwegian Epilepsy Association.

Table of contents

Abbreviations

CA = Ammon's horn

EAAT = Excitatory Amino Acid Transporter

GLAST = Glutamate-Aspertate-Transporter

GLT = Glutamate Transporter

ML = Molecular Layer

MTLE = Mesial Temporal Lobe Epilepsy

PTLE = Paradoxical Temporal Lobe Epilepsy

SDS = Sodium Dodecyl Sulfate

SDS-PAGE = Sodium Dodecyl Sulfate – polyacrylamide gel electrophoresis

TLE = Temporal Lobe Epilepsy

Aims of present study

The overall interest in Professor Danbolt's research group at the Department of Anatomy, University of Oslo, is the control of neurotransmitter concentrations and diffusion in the extracellular space in between synapses in the central nervous system. My research has focused on the transporter proteins moving the transmitter amino acids (GABA and glutamate) across cell membranes, and on the roles of these transporter proteins in normal brain physiology and temporal lobe epilepsy. Changes in transporter function and expression have been reported in all neurological diseases, and these changes appear to be part of the pathogenetic processes ultimately leading to nerve cell damage and neurological and psychological disabilities (for review see: Danbolt, 2001).

In 1999 I applied for a summer research scholarship that was announced by the Norwegian Research Council. Professor Jon Storm-Mathisen at the Department of Anatomy was my lecturer and I had talked to him about starting research. I did not get the scholarship, but Professor Storm-Mathisen wanted students in his lab and he gave me economic compensation for doing research in his lab that summer. My project was to study changes in expression of glutamate and GABA transporters in rat brain after injection of amphetamine. For an inexperienced researcher like me it turned out to be a project way over my head, but that summer I really got a good introduction to basic lab techniques.

After that summer I started to work as a Medical Student Research Fellow under Professor Niels Chr. Danbolt and gradually during my year at Medical School I felt more competent as a researcher. I have contributed on different projects that involved transporter expression after immobilization stress, corticosterone injections (see abstract 1), and worked on developing an ELISA procedure using a robot. The results form the immobilization stress project was presented as a poster on the International Society for Neurochemistry 18th Biennial Meeting, Buenos Aires, Argentina, and the ELISA procedure was later used to test antibody specificity (Paper 2). My main project at Professor Danbolt's lab was later localization and quantification of the two GABA transporters in the rat brain (unpublished). This research project is in collaboration with Prof. D. Furness form Keele, UK.

I was later enrolled in the Medical Research Curriculum and because Professor Danbolt was collaborating with a lab at Yale University School of Medicine I got the opportunity to spend almost a year in USA doing research. I did my research at Professor de Lanerolle's lab at Yale School of Medicine and had Dr. Tore Eid as my supervisor. The main goal in this lab is to investigate proteins and enzymes in hippocampus that are involved in temporal lobe epilepsy. Because the lab is affiliated with the internationally recognized The Epilepsy Surgery Program at Yale-New Haven Hospital, we had access to hippocampus tissue from patients with mesial temporal lobe epilepsy.

Since high extracellular glutamate concentrations have been identified as a likely trigger of epileptic seizures in mesial temporal lobe epilepsy (MTLE), it was a good opportunity to investigate if these high glutamate levels could be the result of down-regulation of glutamate transporters (paper 1).

I addition to my main project I worked on two other project at Yale involving the human epileptic hippocampus. I looked at perivascular expression of aquaporin 4 (AQP4) using electron microscopy (paper 3) and investigated the distribution of GABA transporters (GAT1 and GAT3) using immunohistochemistry, Western blotting and electron microscopy (unpublished).

Overall my research has involved GABA or glutamate transporter proteins in normal brain physiology and temporal lobe epilepsy. I have learned and used techniques like membrane protein purification, confocal imaging, electron microscopy, Western blotting, antibody production, and immunohistochemistry. In addition to using rats, human tissue from epileptic patients has given me more clinical knowledge. It is after all patients that bring research to life. Research has given me an appreciation and enthusiasm for problem solving and basic science and I intend to continue research activity throughout my career, applying these skills to my work in the clinic.

Papers

Abstract 1

AP14-12

Immobilization stress increases the hippocampal protein levels of the GABA transporter GAT1

H. Beckstrøm, L. P. Bjørnsen, S. Arancibia*,
L. Tapia-Arancibia* and N. C. Danbolt
*Department Anatomy, Institute of Basic Medical Sciences, University of Oslo, Norway; *Laboratoire de Plasticité Cérébrale, Université de Montpellier II, Montpellier, France*

GABA and glycine are the major inhibitory neurotransmitters in the mammalian brain and spinal cord, respectively, while glutamate is the major excitatory transmitter. These transmitters are cleared from the extracellular fluid by Na^+-dependent cellular uptake. GABA uptake is mediated by four different transporters (GAT1, GAT2, GAT3 and GAT4), while glycine and glutamate uptake are mediated by two (GLYT1 and GLYT2) and five (GLAST, GLT, EAAC, EAAT4 and EAAT5) different transporters, respectively. A number of reports have been published on the effects of stress on GABA, glutamate or glycine receptors, but few data is available on the effect of stress on the uptake of these transmitters. Here we show the effects of immobilization stress on the expression of GAT1, GAT3, GLYT1, GLT and GLAST. Rats were stressed by immobilization for 7 h. Transporter immunoreactivities were determined in hippocampus, hypothalamus and frontal cortex by quantitative immunoblotting 3, 7, 15 and 24 h after termination of immobilization stress. GAT1 immunoreactivity was significantly increased in hippocampus by a maximum of 57 ± 18% (mean ± SEM) after 3 h. This effect was still detectable after 24 h. There were no significant effect on the immunoreactivities of the other transporters, with a possible exception of GAT3 in the hypothalamus. Injection (i.p.) of corticosterone-21-acetate (10 mg/kg) did not result in a similar up regulation of GAT1. In conclusion, our data show that immobilization stress up-regulates preferentially GAT1 in the hippocampus.

Comments on abstract 1

Beckstrøm, H. // **Bjørnsen, L. P**. // Arancibia, S. // Tapia-Arancibia, L. // Danbolt, N. C. - Immobilization stress increases the hippocampal protein levels of the GABA transporter GAT1-Journal of Neurochemistry-2001-78-Supplement: 1- p. 37-Abstract

This was a project where I collaborated with Dr. Henning Beckstrøm to investigate changes in GABA, glycine, and glutamate transporters during stress. I was responsible for carrying out the part of the project that involved corticosterone-21-acetate. I injected the corticosterone into the rats, prepared the rat brain tissue, and performed the Western blot analysis. I also visited our colleagues S. Aranicibia and L.

Tapia-Arncibia at Laboratoire de Plasticité, Univeristé de Montpellier, Montpellier, France, to pick up tissue samples for the project. The immobilization stress was performed using special restraining devices in France.

Paper 1

Glial Glutamate Transporters in Human Epileptogenic Hippocampus

LP Bjørnsen [3], T Eid[1,2], S Holmseth[3], NC Danbolt[3], D.D. Spencer[1], NC de Lanerolle[1]
[1] Department of Neurosurgery and [2] Laboratory Medicine, Yale University School of Medicine, New Haven, Connecticut, USA; [3] CMBN at Department of Anatomy, Institute of Basic Medical Sciences, University of Oslo, Blindern, Norway

Corresponding author: Dr. Nihal C. de Lanerolle, Department of Neurosurgery FMB414, Yale University School of Medicine, 333 Cedar Street, New Haven, Connecticut 06520-8082, USA. Tel: 203-785-3258, Fax: 203-737-2159, email: nihal.delanerolle@yale.edu

Abstract

Glutamate is the major excitatory neurotransmitter in the brain and is implicated in the pathogenesis of neurodegenerative diseases. High extracellular glutamate concentrations have been identified as a likely trigger of epileptic seizures in mesial temporal lobe epilepsy (MTLE), and these high glutamate levels could be the result of malfunctioning and /or down-regulation of glutamate transporters. Five glutamate transporters have been cloned and are responsible for the removal of potentially excitotoxic excess glutamate from the extracellular space. This study aimed to investigate the differences in distribution of the two glial glutamate transporters that are predominantly responsible for removal of synatically released glutamate, in hippocampal seizure foci with and without sclerosis. The distribution of EAAT1 (GLAST) and EAAT2 (GLT) in hippocampi of patients with medically intractable temporal lobe epilepsy was studied by means of immunohistochemistry, electron microscopy and Western blotting. Western blotting showed no significant differences between non-sclerotic and sclerotic hippocampi for both EAAT1 and EAAT2. Immunocytochemistry only detected EAAT1 and EAAT2 in astrocytes in non-sclerotic and sclerotic hippocampi. There was weaker immunoreactivity for both glutamate transporters in areas associated with neuronal loss, especially in CA1. In areas with less pronounced neuronal loss, like CA2, subiculum and parts of the dentate ML, showed no decrease and even an apparent increase in immunoreactivity. Such compensatory changes in immunoreactivity may account of the lack of differences between the groups in immunoblot studies because the blots shows the average concentrations in the samples. These data suggest that differences in glial glutamate transporter distribution between the two groups of hippocampi may be an insufficient explanation for the high levels of extracellular glutamate in sclerotic seizure foci observed in in vivo dialysis studies.

Keywords: Astrocytes, Glutamate, Hippocampus, Temporal Lobe Epilepsy, MTLE, EAAT, GLAST, GLT

Introduction

Glutamate has long been thought to play a major role in the initiation and spread of seizure activity (Meldrum, 1994). Animal studies have shown that the administration to the hippocampus of glutamate or glutamate analogues triggers seizures, while co-injection of glutamate antagonists blocks the seizures (Olney JW., 1978; Olney *et al*, 1986).

Temporal lobe epilepsy (TLE) is among the most common of the chronic seizure disorders (Hauser *et al.*, 1975), and since this form of epilepsy is often intractable (Chadwick D., 1990) many of these patients undergo anteromedial temporal lobectomy with hippocampectomy for seizure control (Spencer *et al.*, 1984). Approximately 70% of the resected hippocampi are characterized by pronounced neuronal loss and astroglial proliferation, especially in areas CA1, CA3 and the dentate hilus (de Lanerolle *et al.*, 1994). These neuropathological features are the hallmarks of hippocampal sclerosis, a distinctive characteristic of patients with mesial temporal lobe epilepsy (MTLE) (Sommer W., 1880). Hippocampal sclerosis is believed to play a key-role in the generation of seizures in MTLE (Mathern *et al.*, 1997; de Lanerolle and Lee, 2005).

In the sclerotic hippocampus changes in NMDA and AMPA receptors have been observed (de Lanerolle *et al.*, 1998; Musshoff *et al.*, 2000) and intracellular recordings from dentate granule cells in the human MTLE hippocampus have revealed a glutamate dependent hyperexcitability in these neurons (Williamson A, 1994). Elevated levels of extracellular glutamate are observed in patients with various epilepsies (e.g. Janjua *et al.*, 1992; Ferrie *et al.*, 1999) and in vivo microdialysis studies of patients with MTLE have shown that the extracellular concentration of glutamate rises in sclerotic hippocampi just before a seizure and remains high for at least 15 minutes after the cessation of electrographic seizure activity (During and Spencer, 1993). These results indicate that there may be an impaired glutamate uptake capacity and thus possible malfunctioning and/or down-regulation of glutamate transporters (Meldrum *et al.*, 1999).

Synaptically released glutamate is normally taken up by astrocytes and rapidly converted to the nonexcitotoxic amino acid glutamine (Broman *et al.*, 2000). The glutamate uptake system (for review see Danbolt, 2001) consists of at five different transporter proteins and represents the only mechanism for removal of glutamate from the extracellular fluid in the brain. Five different glutamate (excitatory amino acid) transporters have been identified: EAAT1 (GLAST) (Storck *et al.*, 1992; Tanaka, 1993), EAAT2 (GLT) (Pines *et al.*, 1992), EAAT3 (EAAC1) (Kanai and Hediger, 1992), EAAT4 (Fairman *et al.*, 1995), and EAAT5 (Arriza *et al.*, 1997). EAAT1 and EAAT2 are expressed by astrocytes (Danbolt *et al.*, 1992; Levy *et al.*, 1993; Chaudhry *et al.*, 1995;

Lehre *et al.*, 1995), while EAAT3 is neuronal and probably predominantly postsynaptic (Rothstein *et al.*, 1994). EAAT4 is a neuronal postsynaptic glutamate transporter in Purkinje cell spines (Yamada *et al.*, 1996; Nagao *et al.*, 1997; Dehnes et al., 1998) and EAAT5 is primarily expressed in the retina (Arriza *et al.*, 1997). Although both neurons and glia contain glutamate transporters, it is generally accepted that more than 90 % of the forebrain glutamate uptake activity is mediated by EAAT2 (Danbolt et al., 1992; Haugeto et al., 1996; Tanaka et al., 1997; For review and discussion see Danbolt 2001) ().

Reduced expression of glutamate transporters has been shown to cause or be associated with seizures in animal models. A relationship between glutamate transporter dysfunction and epilepsy was established by Tanaka and colleagues, who found that mutant mice lacking EAAT2 had increased extracellular glutamate levels and developed spontaneous seizures (Tanaka *et al.*, 1997). Several studies on animal models have later linked glutamate transporter expression and epilepsy, but the results of these studies have been contradictory. The majority show a decrease in EAAT1 and EAAT2 mRNA and protein (e.g. Samuelsson *et al.*, 2000; Ueda *et al.*, 2001; Ingram *et al.*, 2001), and an increase in EAAT3 mRNA and protein (e.g. Ghijsen *et al.*, 1999; Ueda *et al.*, 2001; Crino *et al.*, 2002;Gorter *et al.*, 2002) in animal epileptic models. Some have on the other hand found an increase in EAAT1 mRNA (Nonaka *et al.*, 1998) and decreased EAAT3 mRNA (Akbar *et al.*, 1998), while Simantov et al. found a down-regulation of EAAT3 and a modest increase in expression of EAAT2 in restricted hippocampal regions (Simantov *et al.*, 1999).

There are a few studies reporting on glutamate transporters in human epileptic patients. Tessler and colleagues (Tessler *et al.*, 1999) found no change in the level of the mRNA or protein, by using *in situ* hybridization and Western blotting techniques respectively, for EAAT1 and EAAT2 in hippocampus and temporal cortex in temporal lobe epilepsy (TLE) patients compared to post mortem controls. In a study by Mathern and colleagues using immunocytochemical methods coupled with neuronal counting and image analysis, no changes in EAAT1 immunoreactivity (IR) were observed in hippocampi from TLE patients with hippocampal sclerosis compared with TLE patients without hippocampal sclerosis. Decreased EAAT2-IR was, in the same study, associated with neuronal loss. An increased EAAT3-IR was seen in areas where neurons were spared and a decrease in areas with neuronal loss (Mathern *et al.*, 1999). A recent study from Proper et al. showed a general decrease in EAAT1-IR and EAAT2-IR in the sclerotic hippocampus when compared with the non-sclerotic hippocampus or post mortem controls (Proper *et al.*, 2002). This decrease was accompanied by a decrease in mRNA levels for both transporters. An increase in neuronal EAAT3 protein levels in the resistant areas (CA2, granule cell layer and subiculum) in the hippocampal sclerosis group was also observed. Using immmunohistochemistry and quantitative western blots Eid et al. found no difference in EAAT2 expression between non-MTLE and MTLE hippocampi (Eid *et al.*, 2004).

The aim of the present study is to further explore the differences in glial glutamate transporter distribution in the hippocampus between non-sclerotic and sclerotic hippocampi in TLE patients. The two glial transporters (EAAT1 and EAAT2) were studied by immunoblotting, immunohistochemistry and electron microscopic methods.

Methods

Patient Tissue

Patients with medically intractable temporal lobe epilepsy underwent phased presurgical evaluation at the Yale-New Haven Hospital, and appropriate candidates underwent anteromedial temporal lobectomy with hippocampectomy according to standard procedures (Spencer DD, 1984). Informed consent from each patient and institutional approval were obtained for the use of tissue in this project. The surgically resected hippocampi were classified into two groups: (1) mesial temporal lobe epilepsy (MTLE) and (2) non-MTLE as described by Eid et al. (Eid *et al.*, 2004). The MTLE hippocampus was characterized by pronounced neuronal loss (>50%) and extensive astroglial proliferation most pronounced in the hippocampal subfields CA1, CA3, and hilus (Kim JH, 2001). Reorganization of peptidergic neurons (neurons containing dynorphin, somatostatin, neuropeptide Y, and substance P) in the dentate gyrus was also seen (de Lanerolle *et al.*, 1994). On the other hand the non-MTLE hippocampi were recognized by a modest (<25%) neuronal loss throughout all hippocampal subfields, minimal astroglial proliferation, and no reorganization of peptidergic neurons in the dentate gyrus (Kim JH, 2001). They were obtained from patients with a mass lesion in the temporal lobe outside the hippocampus (MaTLE) and those with no clear etiology, described previously as paradoxical temporal lobe epilepsy –PTLE (de Lanerolle *et al.*, 1997).

Tissue preparation

Immediately after surgical resection two 5 mm thick slices were cut from the mid-portion of the hippocampus. One of the samples was immersed into a fixative containing 4 % formaldehyde and 15 % (v/v) of a saturated picric acid solution in 0.1 M phosphate buffer pH 7.4 (PB) for 1 hour, followed by immersion into 5 % acrolein in PB for 3 hours. Thereafter the tissue was rinsed and stored in PB at 4 °C. Fifty-micrometer coronal sections were cut on a Vibratome and processed for immunohistochemistry. The other sample was rapidly frozen on dry ice, stored at –80 °C, and later used for Western blots.

Hippocampal Nomenclature

The mesial temporal lobe consists of the hippocampus, parahippocampal gyrus, entorhinal cortex and amygdala. The hippocampus is commonly divided into the subiculum, Ammon's horn and dentate gyrus (Lorente de Nó R., 1934). The Ammon's horn is further subdivided into the areas CA1, CA2 and CA3, while the dentate gyrus is subdivided into the hilus, granule cell layer and molecular layer (Amaral and Insauti, 1990).

Antisera and chemicals

Antibodies against GLAST and GLT were prepared by immunizing rabbits with synthetic peptides (A522-541 (PYQLIAQDNEPEKPVADSET) for GLAST and B563-573 (SVEEEPWKREK) for GLT) coupled to keyhole limpet hemocyanin with glutaraldehyde (Lehre *et al.*,

1995; Danbolt *et al.*, 1998). The corresponding anti-peptide antibodies were referred to as anti-A522 (rabbit 8D0161; Ab,314) and anti-B563 (rabbit 1B0707; Ab,355). These antibodies were tested and characterized by Western blotting (Fig. 1) and immunohistochemical methods, and cross-reacted with human GLAST and GLT, respectively. Unless otherwise specified, all other chemicals were obtained from Sigma-Aldrich (St. Louis, MO).

Immunohistochemistry and electron microscopy
Vibratome sections were incubated free-floating in anti-A522 (200 ng/ml) or anti-B563 (200 ng / ml) antibodies for 24 hours (RT), and then processed according to the avidin-biotin peroxidase method (Hsu *et al.*, 1981) using a commercially available kit (Vectastain Elite, Vector Laboratories, Burlingame, CA). Immunstained sections from each patient were mounted on slides, dehydrated and coverslipped for light microscopic analysis. Control sections incubated without the primary antibody or by replacing it with preimmune sera were not immunostained. Additional immunostained sections were processed for electron microscopy. After immunostaining as described above the sections were treated with 2 % osmium tetroxide in PB, stained *en bloc* with 2 % uranyl acetate in water, dehydrated and flat-embedded in Durcupan ACM. Sections were cut on an ultramicrotome, transferred to 500-mesh copper grids (Electron Microscopic Sciences, Fort Washington, PA, USA), contrast-stained with lead citrate and examined in a transmission electron microscope (Jeol 1200 EX II) at 60 kV.

Western blot Analysis
Sections containing all hippocampal subregions were cut from frozen non-MTLE and MTLE specimens. The tissue was homogenized in 10 tissue volumes of SDS-solubilization buffer (1 % SDS with 150 mM NaCl and 10 mM PB pH 7.4, 5mM EDTA, and 1 mM PMSF) using a FastPrep® Instrument (Qbiogene, Inc., Ca) and the FastRNA® Pro Green Kit (Qbiogene, Inc., Ca). The homogenates were then incubated for 10 min and centrifuged (1000 x g, 10 min, 15°C). The supernatant solutions were stored at 80°C. The sample protein concentrations were determined using BCA Protein Assay Kit (Pierce, #23227) and the determination was preformed according to manufacturer's protocol. Bovine serum albumin (BSA) was used as standard and the spectrophotometer (GeneQuant pro, Amersham) was set to 562 nm. The extracts were then subjected to SDS-PAGE (Laemmli, 1970) and electroblotted (Towbin *et al.*, 1979) to nitrocellulose (100v, 1h). The Protein homogenates were diluted to a final protein concentration of 2 mg/ml in a loading buffer (10 % sucrose, 2 % (w/v) SDS (pure C12; Pierce 28312), 0.001 % (w/v) bromophenol blue, 62.5 mM Tris-HCl pH 6.8, and 5% 2-mercaptoethanol) and applied at different concentration on precast polyacrylamide gels (Criterion, 10% Tris-HCl, BIORAD). The gels were run (200V, 40 min) in Criterion™ Cell Electrophoresis Module (BIORAD). Immunostaining of blots was done as previously described (Lehre *et al.*, 1995) at room temperature. The immunolabeling of the blots was preformed using Supersignal West Dura Extended Duration Substrate (Pierce, cat#34075). First the nitrocellulose blots were washed (1x1min) in TBST (150mM NaCl, 0.05% (v/v) Tween 20, 0.05% (w/v) sodium azide and 10mM Tris-HCl pH 8), blocked (30 min) in TBST with 4 % (w/v) skimmed milk powder (Nestle, Carnation, instant nonfat dry milk), washed (1 x 1 min) with TBST and incubated (overnight) with primary antibodies (200 ng / ml anti-A522 or 200 ng / ml anti-B563) in TBST with 1% BSA (Sigma A-7888) and 0.05% (w/v) sodium azide. The blots were washed (1x1 min and 3x5-10 min) in TBST without azide, incubated 1 hour with peroxidase conjugated (HRP-Conjugated) anti-rabbit IgG (Anti-rabbit IgG peroxidase conjugate, A-1949, Sigma, diluted 1:30000) in TBST with 4 % dry milk (without azide) on a shaker. The blots were incubated for 5 min in Supersignal Substrate according to manufacturers protocol (Pierce, Prod # 34075), after they had been washed (1x1 min and 3x5-10 min) with TBST (without azide). The blots were read at a Kodak Image 2000 R and the intensity of the bands was calculated for GLAST and GLT using the Kodak software. A standard curve was made with increasing concentrations of homogenized hippocampal tissue from a non-MTLE patient to determine the linear range and 3, 6, and 12 µg protein were used from each patient. Both antibodies gave a strong single band consistent with the expected molecular mass of the glial glutamate transporters. Substitution of the primary antibodies with normal serum completely abolished the staining. The blots were assessed using a two-tailed Mann-Whitney U test (Statview Software, SAS Institute, NC).

Results
Clinical characteristics of patients
The demographic and clinical characteristics of the patients used in this study were similar to those in a larger sample reported previously (de Lanerolle *et al.*, 2003) (Table 1). Similar numbers of males and females were studied in the non-MTLE group, but the male:female relationship was 5:8 in the MTLE group. Eight of the 10 non-MTLE hippocampi were of the PTLE category (Table 1). The ages at surgery of the patients in the MTLE group were not significantly different (MTLE mean 37 years ± 4 SEM and non-MTLE 26 years ± 5 SEM, $p = 0.082$, Mann-Whitney U, two-tailed test). The duration of seizure history prior to surgery was also not significantly different (MTLE 27 ±2 and non-MTLE 19 ±4 years, $p = 0.0585$, Mann-Whitney U, two-tailed test). All MTLE patients had hippocampal sclerosis characterized by significant neuronal loss easily seen in area CA1 (neuronal counts not shown) compared to non-MTLE. There was no difference between groups as regards the antiepileptic drugs they were on at the time of surgery.

Western blotting
Western blot studies of the transporters GLAST and GLT were carried out on whole hippocampal sections from non-MTLE and MTLE hippocampi to determine if there was an overall difference in the levels of these transporters between patient groups (figure 1). No statistically significant difference in the expression of GLAST and GLT between the non-MTLE and MTLE hippocampi was observed (GLAST: $p = 0.27$, GLT: $p = 0.95$, Mann-Whitney U, two-tailed test). However, since such a result may also be produced in the face of regional changes in distribution, which may be compensatory, an immunohistochemical study of the distribution of GLAST and GLT was undertaken.

Cellular localization of GLAST and GLT

In both non-MTLE and MTLE hippocampi both EAAT1 and EAAT2 were localized to astrocytes, being seen in both somata and processes of these cells (Fig. 2D, 2E, 3D, 3E). The staining was around neurons sometimes outlining them (Fig. 2C-F, 3C-F). No neuronal labeling was detected.

At the ultrastructural level localization of EAAT1 and EAAT2 the immunoreactivity was studied in area CA1 of the hippocampus in both MTLE and non-MTLE patients (Fig. 4). CA1 was chosen as sclerosis is most prominent in this area of the hippocampus. Only astrocytes were labeled, processes (Fig.4A) as well as somata. Labeled astrocytic processes could be seen to separate unlabeled pyramidal cell bodies and terminals (Fig. 4B, C, D). The immunostained somata contained the organelles typical for astrocytes. Though they were adjacent to strongly labeled astrocytic processes, the axon terminals themselves always appeared completely unlabeled (Fig. 4B, 4D). The labeling was entirely intracellular. In moderately reacted preparations the diaminobenzidine reaction product appeared concentrated close to the inner surface of the plasma membrane sparing the outer lamina (Fig 4E). The extracellular space always was free of reaction product. Fibrous astrocytes in white matter were also labeled (Fig. 4F). Strong immunolabeling for EAAT1 and EAAT2 was also seen at the endothelial-astrocyte interface with the labeling on the astrocyte membrane (Fig. 4E). Such labeling was seen in both non-MTLE and MTLE tissue.

Regional distribution of immunolabeling

The pattern of immunolabeling for EAAT1 and EAAT2 in non-MTLE differed somewhat from the MTLE group. Overall, there was weaker EAAT1 than EAAT2 immunostaining. EAAT1 and EAAT2 were expressed in all subfields of both non-MTLE and MTLE hippocampi. The immunoreactivity was homogeneous and seen in all sublayers, but a patchy pattern, was seen in some subareas such as CA1 for both EAAT1 and EAAT2 in non-MTLE and MTLE (Fig. 2A, 2B, 3A, 3B), as earlier described for GLT in post mortem material (Milton *et al.*, 1997; Proper *et al.*, 2002).

Dentate gyrus and hilus

The staining of both GLAST and GLT was mainly around pyramidal cells in hilus (not shown) and granule cells (figure 2c-d and 3c-d), outlining the neurons, and individual labeled astrocyte cell bodies were seen in the dentate molecular layer and polymorphic layer (not shown) in both non-MTLE (Fig. 2C, 3C) and MTLE (Fig. 2D, 3D). In MTLE compared to non-MTLE a loss of GLAST immunoreactivity was visually observed throughout these two regions (Fig. 2B). The immunoreactivity for GLT in the molecular layer of MTLE hippocampi, was less uniform than in the non-MTLE, with some regions of the molecular layer showing even stronger labeling (Fig. 3B).

Some areas of the hilus in MTLE also retained EAAT1 and EAAT2 immunoreactivity and individual labeled astrocytes were seen in these resistant areas (not shown). Blood vessels were outlined by the immunostaining for both EAAT1 and EAAT2 in all hippocampi (Fig 2C, 2D, 3C, and 3D).

Hippocampal area CA1

The CA1 region in the MTLE is clearly sclerotic and smaller in size then the non-MTLE hippocampus (Fig 2B, 3B). The staining of both EAAT1 and EAAT2 were mainly around pyramidal cells in non-MTLE (Fig 2E, 3E). The neurons were outlined, but not as clearly as around the granule cells. It was hard to distinguish individual astrocytes due to an intricate meshwork of labeling in stratum radiatum, stratum pyramidale, and stratum oriens in non-MTLE hippocampi (not shown). In the MTLE hippocampi, the intensity of immunoreactivity for both GLAST and GLT appeared reduced in astrocyte cell bodies compared the non-MTLE area CA1, and this was associated with the neuronal loss and astroglial proliferation in CA1 (Fig. 2F, 3F).

Hippocampal area CA3, CA2 and subiculum

The immunostaining for both GLAST and GLT in these regions was also mainly in fine processes around pyramidal neurons, but individual astrocytes were seen in stratum radiatum, stratum oriens, and subiculum in both non-MTLE and MTLE (not shown). Blood vessels were outlined by the staining for both GLAST and GLT in both groups of hippocampi, specially pronounced in subiculum. In the MTLE hippocampi, weaker immunoreactivity for GLAST was apparent in CA3 and CA2, whereas for GLT no noticeable differences were observed. The subiculum did not show any loss of immunoreactivity for either transporter in either group of hippocampi (Fig. 2B, 3B). Individual astrocytes cell bodies labeled for GLAST and GLT were observed in MTLE. (not shown).

White matter and alveus

A few astrocytes labeled with GLAST and GLT were seen in alveus and the white matter in both non-MTLE and MTLE groups (not shown).

Discussion

In this study we demonstrate both at the light microscopic and ultrastructural level that in the human hippocampus both EAAT1 and EAAT2 are found in astrocytes. No immunoreativity for these two proteins was observed in neurons. This finding is fully consistent with the localization of EAAT1 and EAAT2 in the rat hippocampus (Lehre *et al.*, 1995). In contrast, one study of the human hippocampus has reported EAAT2 mRNA in neurons as well. This has not been corroborated in the immunohistochemical studies by these same workers or by in situ hybridization or immunohistochemistry in any other studies (Lehre *et al.*, 1995; Mathern *et al.*, 1999; Tessler *et al.*, 1999).

Prior studies of the distribution of EAAT1 and EAAT2 in surgically removed human sclerotic hippocampi compared to non-sclerotic hippocampi have concluded that there is a reduction in EAAT2 (Proper *et al.*, 2002; Mathern *et al.*, 1999), a slight or no reduction in EAAT1 (Proper *et al.*, 2002; Mathern *et al.*, 1999) or essentially no-change in these transporters (Tessler *et al.*, 1999). The Western blot data presented in the current study suggests that there is no change in the levels of either EAAT1 or EAAT2, though immunohistochemical localization shows weaker staining in sclerotic regions like CA1 and the hilus compared to that in non-sclerotic hippocampi. This apparent discrepancy needs explanation.

Careful perusal of previous reports of reduced astrocyte glutamate transporters in the sclerotic hippocampus from patients with TLE, show that the

actual evidence for such reduction is not compelling. Firstly the two studies that report a reduction of glutamate transporters, especially of EAAT2, do so on the basis of immunohistochemistry on fixed tissue (4% formaldehyde for 24 - 48 hr), whereas those that assessed transporter levels in parallel with immunoblots report no change (Tessler *et al.*, 1999 and this study). It is well known that fixatives reduce the antigenicity of molecules and do not provide a reliable basis for quantification (Danbolt, 2001).

Evaluation of immunohistochemical data also presents further issues for discussion. The data presented in Proper et al (Proper *et al.*, 2002) show that staining levels for EAAT1 quantified as a Relative Optical Density (ROD) measure show a reduction only for the dentate polymorphic layer (PML) in the sclerotic compared to the non-sclerotic hippocampus, despite the demonstration in their immunohistochemical photomicrographs of reductions in staining in area CA1 and CA3/CA2 (see Fig. 2 Proper *et al.*, 2002). Mathern et al (Mathern *et al.*, 1999) also find no difference in EAAT1 immunostaining levels between sclerotic and non-sclerotic hippocampi. Thus in essence all previous studies concur with our data that there is no difference in EAAT1 levels. Comparisons that report reductions relative to autopsy controls must be interpreted with caution as postmortem changes are in general likely to results in changes of glutamate transporter levels due to autolytic effects (Beckstrøm *et al.*, 1999).

EAAT2 is the predominant glutamate transporter in the hippocampus (Danbolt et al., 1992; Haugeto et al., 1996; Tanaka et al., 1997; For review and discussion see Danbolt, 2001). Proper et al (Proper *et al.*, 2002) report on the basis of immunohistochemical staining that EAAT2 levels in areas CA1, CA2, CA3 and CA4 were reduced. Unlike for EAAT1, the immunohistochemical patterns and well as their ROD quantification are generally in concordance for EAAT2. However, in situ hybridization studies by the same group show no quantitative change in EAAT2 in areas CA1 and CA2 (Fig 6B Proper *et al.*, 2002) between sclerotic and non-sclerotic hippocampi. Even though the granule cell layer in the sclerotic hippocampus appears visually to have a considerable reduction in mRNA (see Fig. 5F and 5G Proper *et al.*, 2002) no quantitative difference is recorded (Fig. 6B Proper *et al.*, 2002). Thus the data for EAAT2 as presented in this study is equivocal at best. In a study using similar surgical tissue and patient types and fixed similar to that of the study by Proper et al., Mathern and co-workers found a reduction in EAAT2 only in the hilar area of sclerotic hippocampi (see Fig. 11 Mathern *et al.*, 1999). No depletion of EAAT2 is shown for CA1 either in gray value measures or immunoreactivity pattern shown in the illustrated figures (Fig 6E and F Mathern *et al.*, 1999). Tessler et al (1999) also found no difference in EAAT2 levels between epileptic hippocampi and postmortem controls; this study did not distinguish between sclerotic and non-sclerotic hippocampi (Tessler *et al.*, 1999). On the basis of these studies it would be reasonable to conclude that there is no appreciable difference in EAAT2 levels as well between sclerotic and non-sclerotic hippocampi.

However, in the immunohistochemical localization studies shown in this paper as well as others, why does there appear to be reduced immunoreactivity in areas such as CA1 and the hilus in sclerotic hippocampi, while immunoblot analyses show no difference? There are some possible explanations for this. The first may be that in areas such as CA1 where there is an apparent reduction in staining intensity, this may only be reflective of a redistribution of the transporter throughout the astrocytic processes in the sclerotic hippocampi rather than a true reduction in level. Evidence in support of this is that ultrastructural localization studies show EAAT2 immunoreactivity throughout astrocytic process despite apparent loss suggestive in light microscopy (present study). Likewise confocal immunohistochmical studies reveal EAAT2 immunoreactivity throughout astrocyte processes, even though staining in somata is reduced (Eid *et al.*, 2004). Such redistribution of EAAT2 transporter in epileptic surgical tissue has previously been suggested by others (Tessler *et al.*, 1999). An alternative possibility is that there may be compensatory changes in the expression of transporters in its different regions. Such a possibility is recognized in suggestive upregulation of transporter in subiculum and molecular layer (our study) with the apparent down regulation in other areas.

Previous studies of the distribution of glutamate transporters (Proper *et al.*, 2002; Mathern *et al.*, 1999) have postulated a reduction in glutamate transporters to explain the striking physiological observation that there are elevated levels of extracellular glutamate in the epileptogenic (sclerotic) hippocampus (During and Spencer, 1993; Cavus *et al.*, 2005) during seizures. Our own findings, like those of Tessler et al. (Tessler *et al.*, 1999) find little support for a role of glutamate transporters in this phenomenon.

On the contrary, there are several plausible alternative explanations for such elevated extracellular glutamate levels. One possibility may be related to the down regulation of glutamine synthetase in astrocytes in sclerotic areas of the hippocampus, which has been argued as a possible cause (Eid *et al.*, 2004). Alternatively, or in addition, increased levels of inflammatory factors such as interleukin 1β and chemokines in sclerotic hippocampi are now recognized as able to cause the release of glutamate from astrocytes, which may be the source of the increased glutamate (data reviewed in de Lanerolle and Lee, 2005). These mechanisms may be more pertinent to elevated extracellular glutamate in sclerotic seizure foci than alterations in transporter levels or their function and certainly merit further study.

Acknowledgements
This work was supported by grants from NIH to DDS and NCdeL, the Norwegian Top Research Program (Toppforskningsprogrammet) to NCD and the Medical Research Curriculum at University of Oslo, the Norwegian Epilepsy Association and the Norwegian Research Council to L.P.B. We thank Ms. Ilona Kovacs for expert technical assistance.

References

Akbar, M.T., Rattray, M., Williams, R.J., Chong, N.W.S., and Meldrum, B.S., 1998. Reduction of GABA and glutamate transporter messenger RNAs in the severe-seizure genetically epilepsy-prone rat, Neuroscience, 85, pp. 1235-1251

Amaral, D. G. and Insauti, R., 1990. Hippocampal

Formation, In: The Human Nervous System, Ed: G. Paxinos, Academic Press, New York, pp. 711-756.

Arriza, J.L., Eliasof, S., Kavanaugh, M.P., and Amara, S.G., 1997. Excitatory amino acid transporter 5, a retinal glutamate transporter coupled to a chloride conductance, Proceedings of the National Academy of Sciences of the United States of America, 94, pp. 4155-4160

Beckstrøm, H., Julsrud, L., Haugeto, Ø., Dewar, D., Graham, D.I., Lehre, K.P., Storm-Mathisen, J., and Danbolt, N.C., 1999. Interindividual differences in the levels of the glutamate transporters GLAST and GLT, but no clear correlation with Alzheimer's disease, Journal of Neuroscience Research, 55, pp. 218-229

Broman J, Hassel B, Rinvik E, Ottersen OP. 2000. Biochemistry and anatomy of transmitter glutamate. In: Ottersen OP, Storm-Mathisen J, eds. Glutamate. Amsterdam: Elsevier Science, pp. 1-44

Cavus, I., Kasoff, W.S., Cassaday, M.P., Jacob, R., Gueorguieva, R., Sherwin, R.S., Krystal, J.H., Spencer, D.D., and Abi-Saab, W.M., 2005. Extracellular metabolites in the cortex and hippocampus of epileptic patients, Ann Neurol, 57, pp. 226-35

Chadwick D., 1990. The epidemiology of drug resistant epilepsy and adverse effects of antiepileptic drugs., Acta Neurochir Suppl (Wien), 50, pp. 32-37

Chaudhry, F.A., Lehre, K.P., van Lookeren Campagne, M., Ottersen, O.P., Danbolt, N.C., and Storm-Mathisen, J., 1995. Glutamate transporters in glial plasma membranes: highly differentiated localizations revealed by quantitative ultrastructural immunocytochemistry, Neuron, 15, pp. 711-720

Crino, P.B., Jin, H., Shumate, M.D., Robinson, M.B., Coulter, D.A., and Brookskayal, A.R., 2002. Increased expression of the neuronal glutamate transporter (EAAT3/EAAC1) in hippocampal and neocortical epilepsy, Epilepsia, 43, pp. 211-218

Danbolt, N.C., 2001. Glutamate uptake, Progress in Neurobiology, 65, pp. 1-105

Danbolt, N.C., Lehre, K.P., Dehnes, Y., Chaudhry, F.A., and Levy, L.M., 1998. Localization of transporters using transporter-specific antibodies, Methods in Enzymology, 296, pp. 388-407

Danbolt, N.C., Storm-Mathisen, J., and Kanner, B.I., 1992. An [Na+ + K+]coupled L-glutamate transporter purified from rat brain is located in glial cell processes, Neuroscience, 51, pp. 295-310

de Lanerolle, N.C., Eid, T., von Campe, G., Kovacs, I., Spencer, D.D., and Brines, M., 1998. Glutamate receptor subunits GluR1 and GluR2/3 distribution shows reorganization in the human epileptogenic hippocampus, European Journal of Neuroscience, 10, pp. 1687-1703

de Lanerolle, N.C., Kim, J.H., Williamson, A., Spencer, S.S., Zaveri, H.P., Eid, T., and Spencer, D.D., 2003. A retrospective analysis of hippocampal pathology in human temporal lobe epilepsy: evidence for distinctive patient subcategories, Epilepsia, 44, pp. 677-687

de Lanerolle, N.C. and Lee, T.S., 2005. New facets of the neuropathology and molecular profile of human temporal lobe epilepsy, Epilepsy Behav, 7, pp. 190-203

de Lanerolle, N.C., Williamson, A., Meredith, C., Kim, J.H., Tabuteau, H., Spencer, D.D., and Brines, M.L., 1997. Dynorphin and the kappa 1 ligand, Epilepsy Res, 28, pp. 189-205

de Lanerolle NC, K.J.B.ML., 1994. Cellular and molecular alterations in partial epilepsy., Clin Neurosci, 2, pp. 64-81

Dehnes Y, Chaudhry FA, Ullensvang K, Lehre KP, Storm-Mathisen J, Danbolt NC (1998) The glutamate transporter EAAT4 in rat cerebellar Purkinje cells: a glutamate-gated chloride channel concentrated near the synapse in parts of the dendritic membrane facing astroglia. J Neurosci 18: 3606-3619.

During, M.J. and Spencer, D.D., 1993. Extracellular hippocampal glutamate and spontaneous seizure in the conscious human brain, Lancet, 341, pp. 1607-1610

Eid T, Thomas MJ, Spencer DD, Runden-Pran E, Lai JC, Malthankar GV, Kim JH, Danbolt NC, Ottersen OP, de Lanerolle NC., 2004. Loss of glutamine synthetase in the human epileptogenic hippocampus: possible mechanism for raised extracellular glutamate in mesial temporal lobe epilepsy, Lancet., 363(9402), pp. 28-37

Fairman, W.A., Vandenberg, R.J., Arriza, J.L., Kavanaugh, M.P., and Amara, S.G., 1995. An excitatory amino-acid transporter with properties of a ligand-gated chloride channel, Nature, 375, pp. 599-603

Ferrie, C.D., Bird, S., Tilling, K., Maisey, M.N., Chapman, A.G., and Robinson, R.O., 1999. Plasma amino acids in childhood epileptic encephalopathies, Epilepsy Research, 34, pp. 221-229

Ghijsen, W.E.J.M., Belo, A.I.D.A., Zuiderwijk, M., and da Silva, F.H.L., 1999. Compensatory change in EAAC1 glutamate transporter in rat hippocampus CA1 region during kindling epileptogenesis, Neuroscience Letters, 276, pp. 157-160

Gorter, J.A., Van Vliet, E.A., Proper, E.A., De Graan, P.N.E., Ghijsen, W.E.J.M., Da Silva, F.H.L., and Aronica, E., 2002. Glutamate transporters alterations in the reorganizing dentate gyrus are associated with progressive seizure activity in chronic epileptic rats, Journal of Comparative Neurology, 442, pp. 365-377

Haugeto Ø, Ullensvang K, Levy LM, Chaudhry FA, Honoré T, Nielsen M, Lehre KP, Danbolt NC (1996) Brain glutamate transporter proteins form homomultimers. J Biol Chem 271: 27715-27722.

Hauser WA, Kurland LT., 1975. The epidemiology of epilepsy in Rochester, Minnesota, 1935 through 1967., Epilepsia., 16(1), pp. 1-66

Hsu S, Raine L, Fanger H., 1981. The use of avidin-biotin-peroxidase complex (ABC) in immunoperoxidase techinques: a comparison between ABC and unlabeled antibody (PAP) procedures, J Histochem Cytochem., 29, pp. 577-580

Ingram, E.M., Wiseman, J.W., Tessler, S., and Emson, P.C., 2001. Reduction of glial glutamate transporters in the parietal cortex and hippocampus of the EL mouse, Journal of Neurochemistry, 79, pp. 564-575

Janjua NA, Itano T, Kugoh T, Hosokawa K, Nakano M, Matsui H, Hatase O., 1992. Familial increase in plasma glutamic acid in epilepsy., Epilepsy Res., 11(1), pp. 37-44

Kanai, Y. and Hediger, M.A., 1992. Primary structure and functional characterization of a high-affinity glutamate transporter , Nature, 360, pp. 467-471

Kim JH., 2001. Pathology of epilepsy, Exp Mol Pathol., 70(3), pp. 345-367

Laemmli, U.K., 1970. Cleavage of structural proteins during the assembly of the head of bacteriophage T4, Nature, 227, pp. 680-685

Lehre, K.P., Levy, L.M., Ottersen, O.P., Storm-Mathisen, J., and Danbolt, N.C., 1995. Differential expression of two glial glutamate transporters in the rat brain: quantitative and immunocytochemical observations, Journal of Neuroscience , 15, pp. 1835-1853

Levy, L.M., Lehre, K.P., Rolstad, B., and Danbolt, N.C., 1993. A monoclonal antibody raised against an [Na+ - K+]coupled L- glutamate transporter purified from rat brain confirms glial cell localization, FEBS Letters, 317, pp. 79-84

Lorente de Nó R., 1934. Studies on the structure of thecerebral cortex: II continuation of the study of the ammonic system, J Psychol Neurol (Leipzig), 46, pp. 113-77

Mathern, G.W., Mendoza, D., Lozada, A., Pretorius, J.K., Dehnes, Y., Danbolt, N.C., Nelson, N., Leite, J.P., and Chimelli, L., 1999. Hippocampal GABA and glutamate transporter immunoreactivity in patients with temporal lobe epilepsy, Neurology, 52, pp. 453-472

Mathern GW, Babb TL, Armstrong DL., 1997. Hippocampal sclerosis, In Engel J, Pedley TA, eds. Epilepsy: a comprehensive textbook. Philadelphia: Lippincott-Raven, pp. 133-155

Meldrum, B.S., 1994. The role of glutamate in epilepsy and other CNS disorders, Neurology, 44, pp. 14-23

Meldrum, B.S., Akbar, M.T., and Chapman, A.G., 1999. Glutamate receptors and transporters in genetic and acquired models of epilepsy, Epilepsy Research, 36, pp. 189-204

Milton, I.D., Banner, S.J., Ince, P.G., Piggott, N.H., Fray, A.E., Thatcher, N., Horne, C.H.W., and Shaw, P.J., 1997. Expression of the glial glutamate transporter EAAT2 in the human CNS: an immunohistochemical study, Molecular Brain Research, 52, pp. 17-31

Musshoff, U., Schünke, U., Köhling, R., and Speckmann, E.J., 2000. Alternative splicing of the NMDAR1 glutamate receptor subunit in human temporal lobe epilepsy, Molecular Brain Research, 76, pp. 377-384

Nagao, S., Kwak, S., and Kanazawa, I., 1997. EAAT4, a glutamate transporter with properties of a chloride channel, is predominantly localized in Purkinje cell dendrites, and forms parasagittal compartments in rat cerebellum, Neuroscience, 78, pp. 929-933

Nonaka, M., Kohmura, E., Yamashita, T., Shimada, S., Tanaka, K., Yoshimine, T., Tohyama, M., and Hayakawa, T., 1998. Increased transcription of glutamate-aspartate transporter (GLAST/glut-1) mRNA following kainic acid-induced limbic seizure (vol 55, pg 54, 1998), Molecular Brain Research, 60, p. 310

Olney JW., 1978. Neurotoxicity of exitatory amino acids., In: McGeer EG, Olney JW, McGeer PL, eds. Kaini acid as a tool in neurobiology. New York: Raven Press, pp. 37-70

Olney JW, Collins RC, Sloviter RS., 1986. Excitotoxic mechanisms of epileptic brain damage, Adv Neurol., 44, pp. 857-77

Pines, G., Danbolt, N.C., Bjørås, M., Zhang, Y., Bendahan, A., Eide, L., Koepsell, H., Storm-Mathisen, J., Seeberg, E., and Kanner, B.I., 1992. Cloning and expression of a rat brain L-glutamate transporter, Nature, 360, pp. 464-467

Proper, E.A., Hoogland, G., Kappen, S.M., Jansen, G.H., Rensen, M.G., Schrama, L.H., van Veelen, C.W., van Rijen, P.C., van Nieuwenhuizen, O., Gispen, W.H., and de Graan, P.N., 2002. Distribution of glutamate transporters in the hippocampus of patients with pharmaco-resistant temporal lobe epilepsy, Brain, 125, pp. 32-43

Rothstein, J.D., Martin, L., Levey, A.I., Dykes-Hoberg, M., Jin, L., Wu, D., Nash, N., and Kuncl, R.W., 1994. Localization of neuronal and glial glutamate transporters, Neuron, 13, pp. 713-725

Samuelsson, C., Kumlien, E., Flink, R., Lindholm, D., and Ronne-Engstrom, E., 2000. Decreased cortical levels of astrocytic glutamate transport protein GLT-1 in a rat model of posttraumatic epilepsy, Neurosci Lett, 289, pp. 185-188

Simantov, R., Crispino, M., Hoc, W., Broutman, G., Tocco, G., Rothstein, J.D., and Baudry, M., 1999. Changes in expression of neuronal and glial glutamate transporters in rat hippocampus following kainate-induced seizure activity, Molecular Brain Research, 65, pp. 112-123

Sommer W., 1880. Erkrankung des Ammonshorns as aetiologisches Momnet der Epilepsie, Arch Psychiatr Nervenkr, 10, pp. 631-675

Spencer DD, Spencer SS, Mattson RH, Williamson PD, Novelly RA., 1984. Access to the posterior medial temporal lobe structures in the surgical treatment of temporal lobe epilepsy., Neurosurgery , 15(5), pp. 667-671

Storck, T., Schulte, S., Hofmann, K., and Stoffel, W., 1992. Structure, expression, and functional analysis of a Na+-dependent glutamate/aspartate transporter from rat brain, Proceedings of the National Academy of Sciences of the United States of America, 89, pp. 10955-10959

Tanaka, K., 1993. Cloning and expression of a glutamate transporter from mouse brain, Neuroscience Letters, 159, pp. 183-186

Tanaka, K., Watase, K., Manabe, T., Yamada, K., Watanabe, M., Takahashi, K., Iwama, H., Nishikawa, T., Ichihara, N., Hori, S., Takimoto, M., and Wada, K., 1997. Epilepsy and exacerbation of brain injury in mice lacking the glutamate transporter GLT-1, Science, 276, pp. 1699-1702

Tessler, S., Danbolt, N.C., Faull, R.L.M., Storm-Mathisen, J., and Emson, P.C., 1999. Expression of the glutamate transporters in human temporal lobe epilepsy, Neuroscience, 88, pp. 1083-1091

Towbin, H., Staehelin, T., and Gordon, J., 1979. Electrophoretic transfer of proteins from polyacrylamide gels to nitrocellulose sheets: Procedure and some applications, Proceedings of the National Academy of Sciences of the United States of America, 76, pp. 4350-4354

Ueda, Y., Doi, T., Tokumaru, J., Yokoyama, H., Nakajima, A., Mitsuyama, Y., Ohyanishiguchi, H., Kamada, H., and Willmore, L.J., 2001. Collapse of extracellular glutamate regulation during epileptogenesis: down-regulation and functional failure of glutamate transporter function in rats with chronic seizures induced by kainic acid, Journal of Neurochemistry, 76, pp. 892-900

Williamson A., 1994. Electrophysiology of epileptic human neocortical and hippocampal neurons maintained in vitro., Clin Neurosci, 2, pp. 47-52

Yamada, K., Watanabe, M., Shibata, T., Tanaka, K., Wada, K., and Inoue, Y., 1996. EAAT4 is a post-synaptic glutamate transporter at Purkinje cell synapses, Neuroreport, 7, pp. 2013-2017.

Comments to Paper 1

This is my main project and I have focused on this paper in my thesis.

NB: Table, Figures and Figure Texts are placed in the main part of the thesis (Results for Paper 1)

SPECIFICITY OF ANTIBODIES: UNEXPECTED CROSS-REACTIVITY OF ANTIBODIES DIRECTED AGAINST THE EXCITATORY AMINO ACID TRANSPORTER 3 (EAAC) GLUTAMATE TRANSPORTER

S. HOLMSETH,[a] Y. DEHNES,[a] L. P. BJØRNSEN,[a] J.-L. BOULLAND,[a] D. N. FURNESS,[b] D. BERGLES[c] AND N. C. DANBOLT[a]*

[a]Departments of Anatomy, Institute of Basic Medical Sciences, University of Oslo, P.O. Box 1105, Blindern, N-0317 Oslo, Norway

[b]MacKay Institute of Communication and Neuroscience, Keele University, Keele, Staffs ST5 5BG, UK

[c]Department of Neuroscience, Johns Hopkins University School of Medicine, WBSB 813, 725 North Wolfe Street, Baltimore, MD 21205, USA

Abstract—Specific antibodies are essential tools for identifying individual proteins in complex biological samples. While generation of antibodies is often straightforward, determination of the antibody specificity is not. Here we illustrate how complicated this can be by describing the production and characterization of antibodies to the excitatory amino acid transporter 3 glutamate transporter. We synthesized 13 peptides corresponding to parts of the excitatory amino acid transporter 3 sequence and immunized 36 different animals (6 sheep and 30 rabbits). All sera were affinity purified against the relevant immobilized peptide. Antibodies to the peptides were obtained in almost all cases. Immunoblotting with tissue extracts from wild type and excitatory amino acid transporter 3 knockout animals revealed that most of the antibodies did not recognize the native excitatory amino acid transporter 3 protein, and that some antibodies recognized non-excitatory amino acid transporter 3 proteins. Several immunization protocols were tried, but strong reactions with excitatory amino acid transporter 3 were only seen with antibodies to the C-terminal peptides. In contrast, good antibodies were obtained to several parts of excitatory amino acid transporter 2 (GLT). The C-terminal excitatory amino acid transporter 3 antibodies labeled only neurons in tissue sections. However, rabbits immunized with an excitatory amino acid transporter 3-peptide corresponding to residues 479–498 produced antibodies that labeled axoplasm and microtubules therein particularly strongly. On blots, these antibodies recognized both excitatory amino acid transporter 3 and a slightly smaller, but far more abundant protein that turned out to be tubulin. The antibodies were fractionated on columns with immobilized tubulin. One fraction contained antibodies apparently specific for excitatory amino acid transporter 3 while another fraction contained antibodies recognizing both excitatory amino acid transporter 3 and tubulin despite the lack of primary sequence identity between the two proteins. Addition of free peptide to the incubation solution blocked immunostaining of both excitatory amino acid transporter 3 and tubulin. Conclusions: (1) Not all antibodies to synthetic peptides recognize the native protein. (2) The specificity of an antibody is hard to predict. Unwanted reactivity can be highly specific and thereby hard to recognize. In this case, cross-reactivity was discovered because antibodies to different epitopes gave different labeling patterns.

Key words: glutamate uptake, neurotransmitter transport, immunocytochemistry, antibodies, tubulin, specificity testing, oligodendrocyte.

The amino acid glutamate is the major excitatory neurotransmitter in the mammalian CNS. The only significant mechanism for inactivation of extracellular glutamate appears to be cellular uptake mediated by a family of glutamate transporter proteins (excitatory amino acid transporter (EAAT)1–5; for review see: Danbolt, 2001). EAAT3 is expressed in neurons (Kanai and Hediger, 1992; Rothstein et al., 1994; Shashidharan et al., 1997; He et al., 2001), including GABAergic ones, in most parts of the nervous system. EAAT3 is concentrated in the neuronal cell bodies (somata) and dendrites apparently avoiding the nerve terminals. Later studies (Conti et al., 1998; Kugler and Schmitt, 1999) have confirmed these findings, but have reported that astrocytes of the cerebral cortex and white matter also express EAAT3 (Conti et al., 1998). Kugler and Schmitt (1999) detected the protein in oligodendrocytes and noted co-localization with tubulin using an antibody directed to a synthetic peptide corresponding to residues 480–499 of rat EAAT3.

We have previously produced antibodies to EAAT1, EAAT2 and EAAT4, and used them to identify the transporter proteins in tissue sections and protein extracts (e.g. Danbolt et al., 1992; Levy et al., 1993; Lehre et al., 1995; Dehnes et al., 1998; Lehre and Danbolt, 1998a). In parallel with this work, we have also generated antibodies to EAAT3 by immunizing animals with synthetic peptides corresponding to different parts of the EAAT3 protein sequence. Here we describe the production and testing of the latter antibodies in order to demonstrate some of the difficulties in determining the specificity of an antibody. We show that rabbits immunized with a peptide corresponding

*Corresponding author. Tel: +47-22-85-10-83; fax: +47-22-85-12-78.
E-mail address: n.c.danbolt@medisin.uio.no (N. C. Danbolt).

Abbreviations: BSA, bovine serum albumin; CHAPS, 3-[(3-cholamidopropyl)dimethylammonio]-1-propanesulphonate; EAAC1, rabbit glutamate transporter (Kanai and Hediger, 1992); EAAT, excitatory amino acid transporter (=glutamate transporter); EDTA, sodium ethylenediamine tetraacetate; HEPES, 4-(2-hydroxyethyl)-1-piperazineethanesulfonic acid; HSA, human serum albumin; KLH, keyhole limpet hemocyanin, map, multiple antigenic peptide; MBP, myelin basic protein; MBS, *m*-maleimido benzoyl-*N*-hydroxysuccinimide ester NaPi, sodium phosphate buffer with pH 7.4; PMSF, phenylmethanesulfonyl fluoride; SDS, sodium dodecyl sulfate; SDS-PAGE, sodium dodecyl sulfate-polyacrylamide gel electrophoresis; TBST, Tris-buffered saline with 0.1% Triton X-100.

0306-4522/06$30.00+0.00 © 2005 IBRO. Published by Elsevier Ltd. All rights reserved.
doi:10.1016/j.neuroscience.2005.07.022

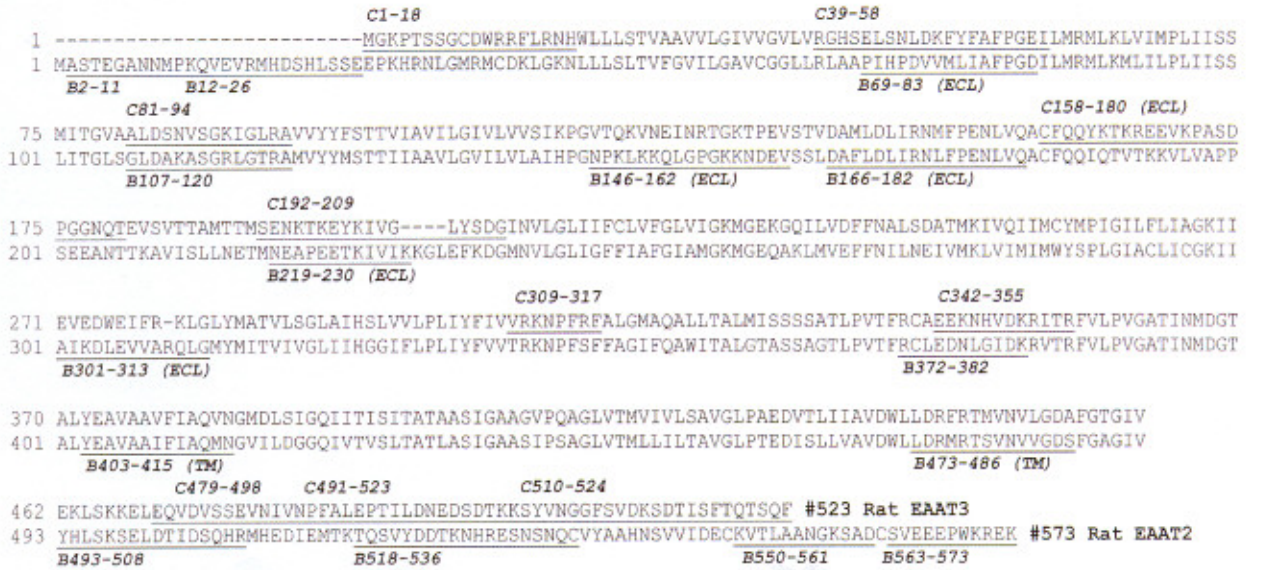

Fig. 1. Sequence alignment of rat EAAT2 and rat EAAT3. The amino acid sequences used for peptide synthesis are underlined and the peptide names given either above (EAAT3) or below (EAAT2) the sequences. Some peptides represent parts of putative extracellular (ECL) or transmembrane (TM) domains as indicated. All the other peptides are selected from putative intracellular domains. The peptides C468–482 and C486–499 correspond to parts of rabbit EAAT3 differing from rat EAAT3 and are therefore not shown in this figure. Peptide C510–524 is also from rabbit, but this sequence is identical to rat, corresponding to rat amino acids 509–523. To avoid confusion, we have kept this peptide's original (rabbit) numbering, as it is used throughout this paper. Peptide C1–13 is not shown because of the overlap with C1–18.

to residues 479–498 of rat EAAT3 gave rise to antibodies recognizing both EAAT3 and tubulin. Using antibodies specific to EAAT3, no EAAT3 immunoreactivity was detected in oligodendrocytes in contrast to the previous report based on antibodies to EAAT3 residues 480–499 (Kugler and Schmitt, 1999).

EXPERIMENTAL PROCEDURES

Materials

Sodium dodecyl sulfate (SDS) of high purity (>99% C12 alkyl sulfate) and bis(sulfosuccinimidyl) suberate were obtained from Pierce (Rockford, IL, USA). *N,N'*-methylene-bisacrylamide, acrylamide, ammonium persulfate, TEMED and alkaline phosphatase substrates (nitroblue tetrazolium and 5-bromo-4-chloro-3-indolyl phosphate) were from Promega (Madison, WI, USA). Biotinylated anti-rabbit, anti-sheep and anti-mouse immunoglubulins, streptavidin-biotinylated horseradish peroxidase complex, and colloidal gold-labeled anti-rabbit and anti-mouse immunoglubulins, electrophoresis equipment, molecular mass markers for sodium dodecyl sulfate–polyacrylamide gel electrophoresis (SDS-PAGE), nitrocellulose sheets (0.22 m pores, 100% nitrocellulose), Protein A-Sepharose Fast Flow and Sephadex G-50 fine were from Amersham Biosciences (Buckinghamshire, UK). Alexa fluor goat anti-rabbit 555 and goat anti-mouse 488 were from Molecular Probes (Eugene, OR, USA). Paraformaldehyde and glutaraldehyde EM grade was from TAAB (Reading, UK). Fluoromount G and Lowicryl HM20 were from Electron Microscopy Sciences (Fort Washington, PA, USA). Alkaline phosphatase-conjugated monoclonal antibodies to rabbit and sheep IgG, anti-beta-tubulin, bovine serum albumin (BSA), 3-[(3-cholamido-propyl)dimethylammonio]-1-propanesulphonate (CHAPS), dithiotreitol (DTT), EDTA, guanosine-5'-triphosphate (GTP), HEPES, human serum albumin (HSA), keyhole limpet hemocyanin (KLH), *m*-maleimido benzoyl-*N*-hydroxysuccinimide ester (MBS), phenylmethanesulfonyl fluoride (PMSF), rabbit serum albumin, thyroglobulin, Trizma base, Trisma–HCl and tubulin were obtained from Sigma (St. Louis, MO, USA). Other reagents were obtained from Fluka (Buchs, Switzerland). Anti-myelin basic protein (MBP) and anti-CNPase were from Sternberger Monoclonals (Lutherville, MD, USA).

Peptides

Peptides representing parts of EAAT2 (Pines et al., 1992; 573 amino acid residues) and EAAT3 are referred to by capital letters "B" and "C," respectively, followed by numbers indicating the corresponding amino acid residues in the sequences (given in parentheses). The first EAAT3-peptides were made based on the rabbit sequence which is 524 amino acid residues long (Kanai and Hediger, 1992). The rat sequence was used when it became available (Bjørås et al., 1996) and is 523 residues long (lacking residue 191 in the rabbit sequence). The peptide sequences are shown in Fig. 1. Note that the C510–524 peptide is numbered according to the rabbit sequence although identical to the rat 509–523. The following two rabbit peptides are not shown in Fig. 1 because the sequences are different: C468–482 (KELEQMDVSSEVNIV-*amide*) and C486–499 (ALESATLDNEDSDT-*amide*).

Only the peptides representing the C-termini of the native proteins were synthesized as free C-terminal acids (B563–573, C491–523 and C510–524). The remaining peptides shown were synthesized as C-terminal amides. B301–313 and C1–13 were also synthesized as multiple antigenic peptides (map). Map-peptides were used for immunization without coupling to carrier protein while the other peptides were coupled to either KLH, rabbit serum albumin or thyroglobulin with either glutaraldehyde (with or without reduction with sodium borohydride) or MBS as described previously (Danbolt et al., 1998). The production of gold particles (Frens, 1973) and the conjugation of gold to immunogenes (Pow and Crook, 1993) were performed as described.

Antigenicity profiles (Fig. 2) were calculated for rat EAAT2 and EAAT3 according to Jameson and Wolf (1988) using the Protean program (DNASTAR, Inc.).

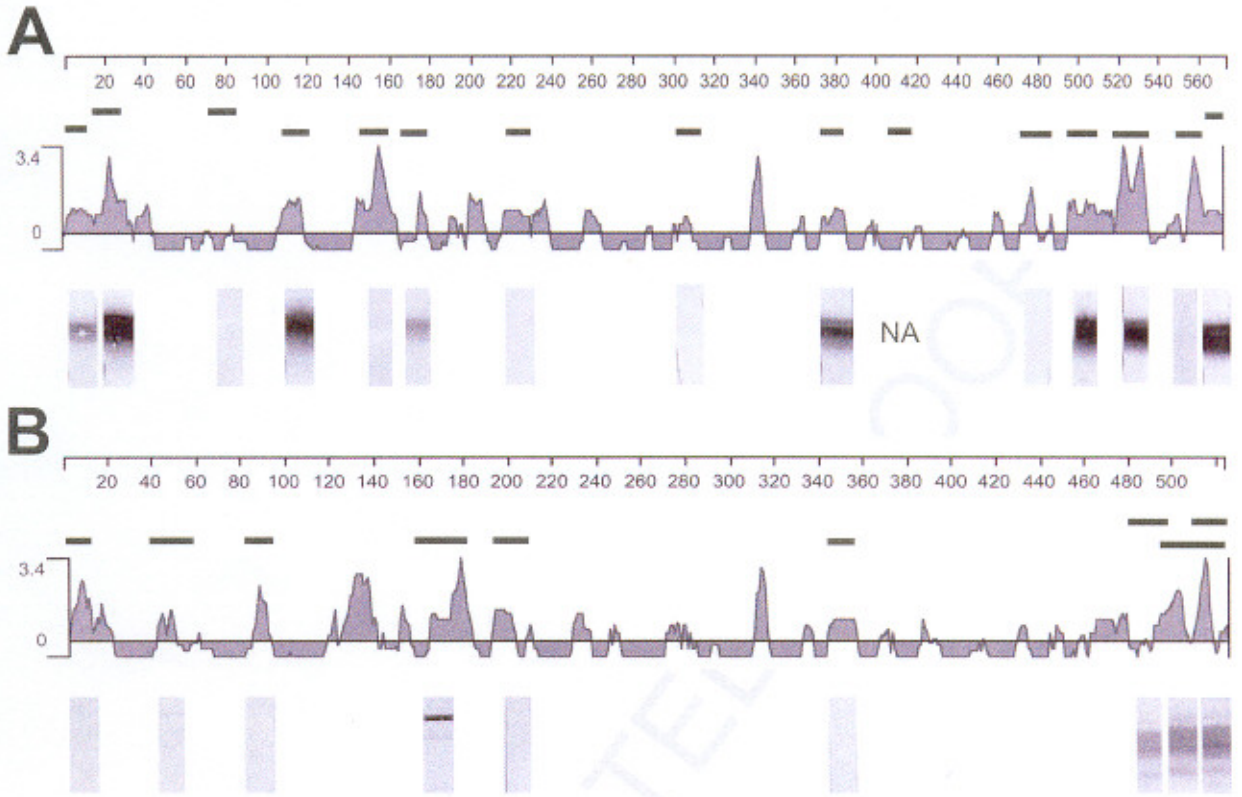

Fig. 2. Comparison of antibody production to EAAT2 (A) and EAAT3 (B). Antigenicity profiles (Jameson and Wolf, 1988) were used to help find the most antigenic amino acid sequences in the proteins. The amino acid sequences of the two transporters are represented by numbered lines above the profiles. Peptides corresponding to parts of the sequences were synthesized as indicated by short horizontal black lines between the numbered lines and the antigenicity profiles. Sequence information is given in Fig. 1. All peptides shown (except B403–415) gave rise to antibodies as determined be the amount of protein isolated by affinity purification. The purified antibodies were subsequently tested by immunoblotting (see Table 2 for antibody concentrations) as shown below the profiles. The nitrocellulose blots represent PAGE separated SDS extracts of rat hippocampus, and the blots were cut into identical strips. (A) Antibodies from left to right: anti-B2 (+); anti-B12B (+); anti-B69, anti-B107 (+); anti-B146; anti-B166 (+); anti-B219; anti-B301; anti-B372 (+); anti-B473; anti-B493 (+); anti-B518 (+); anti-B550 and anti-B563 (+). Each strip contained 1.75 μg protein rat hippocampus protein except the strip for anti-B166 which had 17.5 μg. (B) Antibodies from left to right: anti-C1; anti-C39; anti-C81; anti-C158; anti-C192; anti-C342; anti-C479P (+); anti-C491B (+) and anti-C510A (+). All the strips had 35 μg rat hippocampus protein. Please note: (1) Lack of labeling reaction does not imply lack of antibody, but lack of reactivity toward the native proteins. (2) EAAT2 was recognized by antibodies to eight of the 15 EAAT2-peptides, but EAAT3 by only three of 13 EAAT3-peptides. NA, no antibody; (+), positive reaction with native proteins.

Animals, immunizations and collection of tissue

All animal experimentation was carried out in accordance with the National Institutes of Health Guide for the Care and Use of Laboratory Animals (NIH Publications No. 80-23) revised 1996 and the European Communities Council Directive of 24 November 1986 (86/609/EEC). Formal approval to conduct the experiments described was obtained from the animal subjects review board of our institutions.

Rabbits and sheep. Chinchilla rabbits (Chbb:CH) and New Zealand rabbits (obtained from B&K Universal, Sollentuna, Sweden) were kept in the animal facility at the Institute of Basic Medical Sciences (University of Oslo, Oslo, Norway). The sheep were kept at the Governmental Institute of Public Health (SIFF) or at the School of Veterinary Medicine (Oslo, Norway). The animals (Table 1) were immunized and bled as described previously (Danbolt et al., 1998), but using s.c. rather than intracutaneous injections.

Rats and mice. Adult male Wistar rats (10–12 weeks old) were obtained from B&K Universal. Mice lacking EAAT3 (Peghini et al., 1997) were bred and kept in the animal facility at the John Hopkins University (Baltimore, USA) until they reached 4 weeks of age. Fresh tissue for biochemical studies was obtained from rats and mice killed humanely using approved procedures. Brain tissue for immunocytochemistry was obtained from animals that had been killed by injection of pentobarbital followed by perfusion fixation (see Immunocytochemistry below).

Glutamate transporter antibody purification and nomenclature

Antibodies against the peptides could be isolated from the antisera in most cases, albeit in highly variable amounts (0–300 μg/ml serum; data not shown). Testing of crude antisera was usually done (data not shown), but all antibodies presented here have been affinity purified as described previously on columns containing covalently immobilized antigen (Lehre et al., 1995; Danbolt et al., 1998). Sera from rabbits immunized with multiple peptides were passed through one affinity column for each of the peptides used for immunization. Rabbit 82356 (Table 1) may serve as an example. This rabbit was immunized with three peptides (C468–482, C486–499 and C510–524), and the serum was passed through three affinity columns which were eluted separately. This

Table 1. Overview over EAAC antibody production

Animal no.	Peptide(s)	Carrier	Coupling reagent	Antibody, ID no.
20580*	C1-18+C39+C81+C468+C486+C510	KLH, map	GA, MBS	
26693	C1-18+C39+C81+C158+C192+C342+C468+C486+C510	TG	GA, red.	Anti-C510, ab243
				Anti-C158+C192, ab158
26697*	C1-18+C39+C81+C158+C192+C342+C468+C486+C510	RSA and liposomes (i.v.)	GA, red.	Anti-C158+C192, ab161: anti-C510, ab240
			NHS (i.v.)	
26699	C1-18+C39+C81+C158+C192+C342+C468+C486+C510	KLH	GA, red.	Anti-C510, ab239
26719	C1-18+C39+C81+C158+C192+C342+C468+C486+C510	RSA	GA, red.	Anti-C510, ab238
69738*	C510	RSA	GA, red.	Anti-C510, ab136
80820	C510			
82356	C468+C486+C510	KLH	GA, red.	Anti-C510, ab52
84172	C468+C510		GA, red.	Anti-C510, ab234
89058	C1-13+C39	map		
89350	C1-13	map		
89780	C39	KLH		
0B0620	C479	KLH	GA, red.	
0B0715	C479	KLH	GA, red.	Anti-C479, ab334
0B0717	C479	KLH	GA, free	Anti-C479, ab333
0B0721	C479	KLH	GA, free	Anti-C479, ab335, 359, 545 and 547
1B0683	C491	KLH	GA, free	Anti-C491, ab10 and 371
1B0696*	C1-13+C39+C81+C158+C192	Gold-TG	GA, free	
1B0716*	C1-13+C39+C81+C158+C192	Gold-TG	GA, free	
1B0764*	C1-13+C39+C81+C158+C192	Gold-TG	GA, free	
1B0784	C491	KLH	GA, free	
1B0853*	C1-13+C39+C81+C158	Gold-TG	GA, free	
1B1012*	C1-13+C39+C81+C158	Gold-TG	GA, free	
1B1225*	C1-13+C39+C81+C158	Gold-TG	GA, free	
7D0988	C491	KLH	GA, free	Anti-C491, ab236
7D0993	C491	KLH	GA, free	Anti-C491, ab237
JQ51	C491	KLH	GA, free	
JR26	C491	KLH	GA, free	
MB303	C81	KLH	GA, red.	
MB3459	C1-18+C39+C81+C468+C486+C510		GA, red.	
Sh3016	C1-13-map+C39-MBS-KLH+C510-GA-KLH	map, KLH	MBS and GA, red.	
Sh4131	C491	KLH	GA, free	Anti-C491, ab256: anti-C510, ab340
Sh4430	C158+C192+C510	KLH	MBS	Anti-C158, ab209: anti-C192, ab211
Sh I	C510	KLH	GA, red.	
Sh II	C468	KLH	GA, red.	
Sh III	C486	KLH	GA, red.	

Most of the EAAC peptide sequences gave rise to antibodies recognizing the peptides they were directed against, but only a few of these labeled EAAC protein (listed in "Antibody, ID no."). Although some very weak antibodies were obtained for C158–180 and C192–209, the by far best antibodies were obtained from sequences close to the C-terminal (C479–498, C491–523 and C510–524; see also Fig. 1). Changing the carrier protein or coupling reagent did not seem to change this trend, and this was true whether the animals were immunized with one peptide or a mix of different ones. Peptide-conjugates were mixed with Freund's Complete Adjuvant (FCA) at the first immunization and Freund's Incomplete Adjuvant (FIA) at the subsequent ones, except for those animals marked with asterisk (*). These animals received FIA supplemented with muramyl dipeptide at all immunizations. Abbreviations: GA, glutaraldehyde (reduced with NaBH4 or free); NHS, N-hydroxysuecinimide; TG, thyroglobulin.

resulted in three different antibody fractions which were named according to the antigen immobilized on the respective affinity column: anti-C468 (Ab,50), anti-C486 (Ab,51) and anti-C510 (Ab,52). (The parentheses contain the database identification numbers). Only the latter antibody is listed in Table 1 because it was the only one which recognized EAAT3.

An overview of the antibodies used in the present report is given in Table 2. To make this manuscript easier to read, the antibodies have been given short systematic and informative names. However, these names do not contain sufficient information to identify them unequivocally in our records. Therefore we have also included the unique database identification numbers.

The antiserum from rabbit (Rb) 0B0721 to C479–498 (19.09.2002) was subjected to a four stage purification process (see Results) which included absorption against tubulin. Purified antibodies were quantified spectrophotometrically at 280 nm using bovine IgG as the standard.

Table 2. Primary antibodies used

Antibody ID no.	Animal number	Antibody names used in the present report	Ligand on affinity column	Reference date	Conc. used for blot labeling (μg/ml)
Ab,109	Rb 89350	Anti-C1	C1–18	1994-07-16	3
Ab,125	Rb 89780	Anti-C39	C39–58	1994-07-16	3
Ab,206	Rb 26693	Anti-C81	C81–94	1996-07-08	3
Ab,245	Rb 26693	Anti-C158	C158–180	1997-12-17	3
Ab,166	Rb 26699	Anti-C342	C342–355	1996-05-27	3
Ab,50	Rb 82356	Anti-C468	C468–482	1993-06-20	3
Ab,336	Rb 0B0620	Anti-C479A	C479–498	2001-07-26	1
Ab,334	Rb 0B0715	Anti-C479B	C479–498	2001-07-26	1
Ab,333	Rb 0B0717	Anti-C479C	C479–498	2001-07-26	1
Ab,335	Rb 0B0721	Anti-C479D	C479–498	2001-07-26	1
Ab,545	Rb 0B0721	Anti-C479-KLH	KLH	2002-09-19	
Ab,547	Rb 0B0721	Anti-C479-Tub	Tubulin	2002-09-19	
Ab,359	Rb 0B0721	Anti-C479P	C479–498	2002-09-19	3
Ab,371	Rb 0B0683	Anti-C491B	C491–523	2003-01-03	1
Ab,237	Rb 7D0993	Anti-C491A	C491–523	1997-12-14	1
Ab,126	Rb 69738	Anti-C510A	C510–523	1993-04-04	1
Ab,340	Sh 4131	Anti-C510B	C510–523	2001-08-16	1
Ab,48	Rb 81024	Anti-B2	B2–11	1993-06-15	1
Ab,152	Rb 68518	Anti-B12A	B12–26	1995-09-14	0.2
Ab,360	Rb 26970	Anti-B12B	B12–26	2002-07-10	0.2
Ab,130	Rb 89606	Anti-B107	B107–120	1995-04-23	1
Ab,528	Rb 8D0155	Anti-B146	B146–162	1998-08-01	1
Ab,311	Rb 84204	Anti-B166	B166–182	1998-08-01	10
Ab,42	Rb 68550	Anti-B219	B219–230	1993-01-30	1
Ab,132	Rb 89330	Anti-B301	B301–313	1995-07-25	1
Ab,63	Rb 82898	Anti-B372	B372–384	1994-06-05	1
Ab,64	Rb 82898	Anti-B473	B473–486	1993-08-09	1
Ab,97	Rb 84946	Anti-B493	B493–508	1994-05-29	0.5
Ab,94	Rb 84932	Anti-B518	B518–536	1993-12-28	1
Ab,356	Rb 1B0707	Anti-B550	B550–561	2002-09-05	3
Ab,355	Rb 1B0707	Anti-B563	B563–573	2002-09-05	0.5

Electrophoresis and immunoblotting

Brain and kidney tissues were rapidly dissected out from rats and mice and directly homogenized in five to 15 volumes of 20 mM sodium phosphate buffer (NaPi) pH 7.4 containing 1% (w/v) SDS and 1 mM PMSF. The mixture was sonicated (30 s; dr. Hielscher UP 50H®) to reduce viscosity (by breaking up DNA). Brain tissue was homogenized in a Dounce glass–glass homogenizer while kidney tissue was first homogenized by means of a Polytron PT1200® homogenizer (which is able to break up connective tissue) and then further treated in a Dounce glass–glass homogenizer. Undissolved kidney tissue components were sedimented by centrifugation (3000 r.p.m., 41 °C, 5 min). These extracts are referred to below as brain or kidney SDS-extracts. Protein concentrations were determined with the bicinchoninic acid assay (BCA assay; Smith et al., 1985).

The SDS-extracts were diluted in SDS-sample buffer (Laemmli, 1970) to 1 mg/ml and subjected to SDS-PAGE which was performed as described before (Laemmli, 1970; Lehre et al., 1995) with separating gels consisting of 7.5 or 10% acrylamide. The molecular mass markers were used in non-reduced form. After electrophoresis the proteins were either silver stained (Danbolt et al., 1990) or electroblotted onto nitrocellulose membranes (Towbin et al., 1979; Lehre et al., 1995). The blots were immunostained with alkaline phosphatase-conjugated secondary antibodies (Lehre et al., 1995).

Light microscopical immunocytochemistry

This was performed as described previously (Danbolt et al., 1998; Boulland et al., 2004). Briefly, animals were deeply anesthetized and fixed by transcardiac perfusion with 0.1 M NaPi containing either 4% formaldehyde or 4% formaldehyde and 0.05% glutaraldehyde. Free floating vibratome sections (40 μm thick) were treated with 1 M ethanolamine–HCl (pH 7.4), blocked with 10% newborn calf serum and 3% (w/v) BSA in TBST (300 mM NaCl, 0.5% Triton X-100 and 100 mM Tris–HCl pH 7.4), and incubated overnight with primary antibodies diluted in TBST with 3% newborn calf serum and 1% BSA), followed by secondary antibodies diluted in blocking solution. Anti-glutamate transporter antibodies were used in different concentrations as indicated. The mouse monoclonal anti-CNPase and anti-MBP from Sternberger Monoclonals were both used at 1:500 dilutions. The secondary antibodies (biotinylated anti-rabbit, anti-sheep and anti-mouse, and fluorescently tagged GAM Alexa 468 and GAR Alexa 555) were all used at 1:1000 dilutions. When fluorescently marked secondary antibodies were used, the sections were mounted in Fluoromount G water base, and observed in a Zeiss Axioplan 2 microscope equipped with a Zeiss LSM 5 Pa confocal scanner head. Pinhole size was around 1 area unit, optimized for each wavelength to ensure confocality. When biotinylated secondary antibodies were used, then the sections were developed with the biotin–streptavidin–peroxidase system and diaminobenzidine as described (Danbolt et al., 1998). Control sections incubated with preimmune IgG instead of anti-peptide antibodies, or with antibodies preab-

sorbed with the peptide used for immunization, showed no labeling.

Postembedding

Postembedding immunogold labeling was performed on freeze-substituted low temperature resin-embedded tissue, from rats perfusion fixed as above with 4% formaldehyde and 0.05% glutaraldehyde, as described previously (Dehnes et al., 1998) Ultrathin sections were cut, collected on nickel grids and labeled by sequential immersion for 10 min each at room temperature unless otherwise stated, in small drops of the following solutions: Tris-buffered saline with 0.1% (w/v) Triton X-100 (TBST), 2–3% HSA in TBST, primary antibody diluted as appropriate in HSA–TBST (4 °C overnight), three times in TBST, gold-conjugated secondary antibody in HSA–TBST diluted 1:20 (1–2 h), three times in TBST and two times in distilled water. They were stained with uranyl acetate and lead citrate and examined in a Tecnai 12 transmission electron microscope.

ELISA-procedure for antibody testing

The procedure was performed by a Tecan Genesis 200 Workstation robot. The microtiterplates were kept on a horizontal shaker at room temperature during all incubations. Each well in the 96 well microtiterplate was first incubated (2 h) with 50 μl TBS (10 mM Tris–HCl pH 8.0, 150 mM NaCl, 0.05% NaN_3) containing 3 μg antigen per ml and then washed with TBS (4 cycles, 50 s) to remove unbound antigen. To block free binding sites, the wells were incubated with TBS (380 μl/well) containing 20% NCS (when not stated otherwise) for 2 h with agitation and washed in TBS with 0.05% (v/v) Tween 20 (TBST) (4 cycles, 50 s). Antibody fractions to be tested were diluted in blocking solution to the desired concentration. 50 μl was added to each well and was incubated for 60 min and then washed with TBST (eight cycles, 50 s). The wells were incubated for 60 min with 50 μl TBST containing 20% NCS and alkaline phosphatase-conjugated anti-rabbit diluted 1:1000. A final washing with TBST (eight cycles, 50 s) was followed by addition of 100 μl *p*-nitrophenyl phosphate (1 mg/ml) in 0.1 M diethanolamine–HCl buffer (pH 9.8) with 1 mM $MgCl_2$. The OD405 was measured after 60 min. Background levels in each assay were determined by using BSA as the coating antigen.

RESULTS

Anti-peptide antibodies are usually obtained, but they often fail to recognize the parent protein

Animals were immunized with synthetic peptides corresponding to parts of the EAAT3-sequence (Fig. 1, Table 1). The amounts of antibodies which could be isolated by antigen affinity chromatography varied greatly. For example, rabbit 80886 which was immunized with B403–415 did not produce any detectable amounts of anti-peptide antibodies while about 0.2 mg anti-C491 antibodies (Ab.237) was isolated from each ml of serum from rabbit 7D0993 (data not shown).

Because the antibodies were affinity purified, it follows that all the antibodies shown here (Table 2) did recognize the peptides used to generate them. In spite of this, only a minority of the affinity purified antibodies recognized the EAAT3 protein on immunoblots (Fig. 2B). Only peptides in the C-terminal region generated antibodies recognizing EAAT3. The two peptides from the putative second extracellular loop (C158 and C192) also generated antibodies to the EAAT3 proteins, but their reaction is too weak to be seen in Fig. 2B and too weak to be useful. The other peptides showed no detectable signal.

The peptide sequence is the main factor, but is hard to predict

It is interesting to note that the ability of a peptide antibody to recognize both the peptide and the parent protein seemed to be a property of the peptides and not of the immunization protocol used. The last column to the right in Table 1 lists the peptides giving rise to antibodies recognizing EAAT3-protein. It can be seen that even when animals were immunized with mixtures of peptides, it was the same peptides that gave rise to the good antibodies.

Consequently, in order to produce good anti-peptide antibodies, the key factor is to select the right parts of the sequence for peptide synthesis. Unfortunately, this is difficult as shown in Fig. 2. The EAAT3 and EAAT2 proteins are about 60% identical and the predicted antigenicity profiles are similar. Like EAAT3, peptides selected from the C-terminal region of EAAT2 were excellent immunogens while, similarly, weak antibodies were obtained to the second extracellular loop (B166), but not to the first one (B69 and C39). But in contrast to EAAT3, peptides from the N-terminus (B2 and B12) and from both the first (C107) and the third (B372) intracellular loops gave rise to good antibodies. This could not be predicted prior to immunization and testing.

Antibodies recognizing unrelated proteins are frequently obtained

Because the purpose of the immunoblotting was to maximize the probability of detecting possible immunoreactivity toward non-EAAT3-proteins, the samples were made from whole tissue directly homogenized in SDS to ensure that the immunoblots would contain as many of the tissue antigens as possible. Examples of labeling patterns are shown in Fig. 3. The antibodies generated by immunization and purification with five of the peptides (C1–13, C1–18, C39–58, C81–94 and C468–482) did not recognize EAAT3, but did frequently bind to other proteins (examples are shown in Fig. 3A, strips 1–4) and are therefore not discussed further. Strong reaction with the EAAT3-protein was observed with the majority of the antibodies obtained after immunization with the C479–498, C491–523 and C510–523 (Fig. 3A, strips 5–11; Fig. 3B, strips 1–3).

The anti-C491 and the anti-C510 antibodies labeled one relatively broad fuzzy band at around 70 kDa on immunoblots of brain (Fig. 3A, strips 8–11) and kidney (Fig. 3B, strips 2 and 3). The labeling intensity of this band was weak compared with the band immunopositive for antibodies to EAAT2 (Fig. 3A, strip 12). The weak labeling was due to the low amounts of EAAT3-protein in brain tissue and not the result of low affinity of the antibodies, because high labeling intensities were obtained when they were tested on immunoblots of transfected HeLa cells (data not shown) and on blots containing purified EAAT3-protein (data not shown).

The anti-C479 antibodies labeled the same band as the anti-C491 and the anti-C510 antibodies, but also a

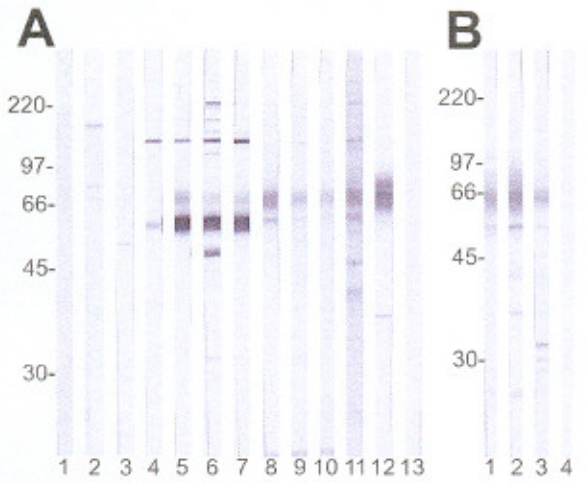

Fig. 3. Specificity testing of EAAT3 antibodies by immunoblotting. Whole rat tissue was solubilized with SDS, subjected to SDS-PAGE and blotted onto nitrocellulose. The nitrocellulose sheets were cut into identical strips (each with 16 μg protein) which were labeled with the following antibodies: A (hippocampus): (1) anti-C1; (2) anti-C39; (3) anti-C158; (4) anti-C479A; (5) anti-C479B; (6) anti-C479CI; (7) anti-C479D; (8) anti-C491B; (9) anti-C491A; (10) anti-C510A; (11) anti-C510B; (12) anti-B12A (positive control); (13) no primary antibody (negative control. (B) (kidney): (1) anti-C479P; (2) anti-C491B; (3) anti-C510A; (4) no primary antibody (negative control). Note the strong labeling of an extra band just below the EAAT3 labeling in panel A (strips 5–7). For antibody concentrations see Table 2.

broad band just below the 66 kDa marker (Fig. 3A, lanes 5–7). This band was labeled with higher intensity than that of the upper band.

Uncovering of the identity of the lower anti-C479 positive band

It was important to uncover the identity of the protein represented by the lower band recognized by the anti-C479 antibodies because the strong labeling suggested it is abundant, and expression of such high concentrations of an EAAT3 variant would be a major discovery. We therefore attempted to immunoisolate the molecular species using procedures we have successfully applied to transporter proteins (Dehnes et al., 1998; Lehre and Danbolt, 1998b) in order to subject the purified protein to partial protein sequencing. However, we found that the water solubility of the unknown protein varied with the buffer composition during homogenization, in contrast to EAAT3, which was always found in the pellet, and always soluble with CHAPS (data not shown).

The variable water solubility suggested reversible attachment to cytoskeletal proteins. To obtain information about the protein's localization, the different EAAT3-antibodies were used to label vibratome sections of brain tissue. All the anti-C491 and anti-C510 antibodies and three of the anti-C479 antibodies labeled neuronal cell bodies and dendrites in tissue sections. Examples using anti-C491B, anti-C479D and anti-C479P antibodies are illustrated (Fig. 4). One particularly striking difference between the three anti-C479 antibodies and the rest was the dense labeling of axons. The labeling of dendritic cytoplasm was also somewhat stronger. Axonal labeling was particularly evident in white matter tracts (Fig. 4D). At the electron microscopical level, label was found to be associated with axonal and dendritic microtubules (Fig. 4E).

The antibodies were then tested in a robotic ELISA assay for reactivity toward proteins present in high concentrations in axons. A strong and specific reaction to tubulin was observed, but not to any of the other proteins tested, including another abundant cytoskeletal protein, actin. This result indicated that the anti-C479 antibodies recognized both tubulin and EAAT3 despite of being affinity purified against the C479–498 peptide.

Fractionation of the anti-C479 antiserum

In order to separate antibodies to EAAT3 from the antibodies to tubulin, another aliquot of crude serum from one of the same rabbits (0B0721) was first fractionated by absorption on a column containing glutaraldehyde-treated bovine serum proteins to remove polyreactive antibodies and antibodies recognizing aldehyde-treated proteins in general (Fig. 4F). Then it was passed through a column with immobilized KLH (the carrier protein to which the peptide was conjugated during immunization), and subsequently through columns containing immobilized tubulin and the C479–498 peptide. The antibodies that were retained on the various columns were eluted with low pH-buffer and tested in an ELISA assay. The immunoreactivities of the antibody fractions obtained are shown in Table 3. The antibodies eluted with low pH from the KLH-column (referred to as "anti-C479KLH") reacted both with the C479–498 peptide and with KLH. The antibodies eluted from the tubulin-column ("anti-C479-Tub") reacted both with tubulin and with the C479–498 peptide, while the antibodies collected from the peptide-column reacted only with the peptide and neither with KLH nor with tubulin. These latter antibodies are referred to below as the "anti-C479P."

The anti-C479P antibodies were then tested on both immunoblots and tissue sections (Figs. 3, 4, 5, 6 and 7). As can be seen in Fig. 4I (strip 2) these absorbed antibodies displayed the same labeling profile as the anti-C491 antibodies (strip 3). They did not recognize the lower band labeled by the non-absorbed anti-C479 antibodies (strip 1). Consequently, absorption against tubulin removed the antibodies labeling the lower band. The absorption also removed the antibodies giving rise to labeling of axons (Figs. 4G, 4H and 7D).

Reaction of the antibodies with proteins from wild-type and EAAT3 knockout mice

To verify that the band expected to represent EAAT3 really did so, the antibodies were tested by immunoblotting with protein extracts from wild-type (Fig. 5A) and EAAT3 knockout mice (Fig. 5B). The bands detected in the wild type (Fig. 5A, strips 1–5) were exactly as would be observed in rat tissue. In contrast, neither the absorbed anti-C479 nor anti-C491 antibodies showed detectable reaction with blots of tissue from genetically modified mice deficient in

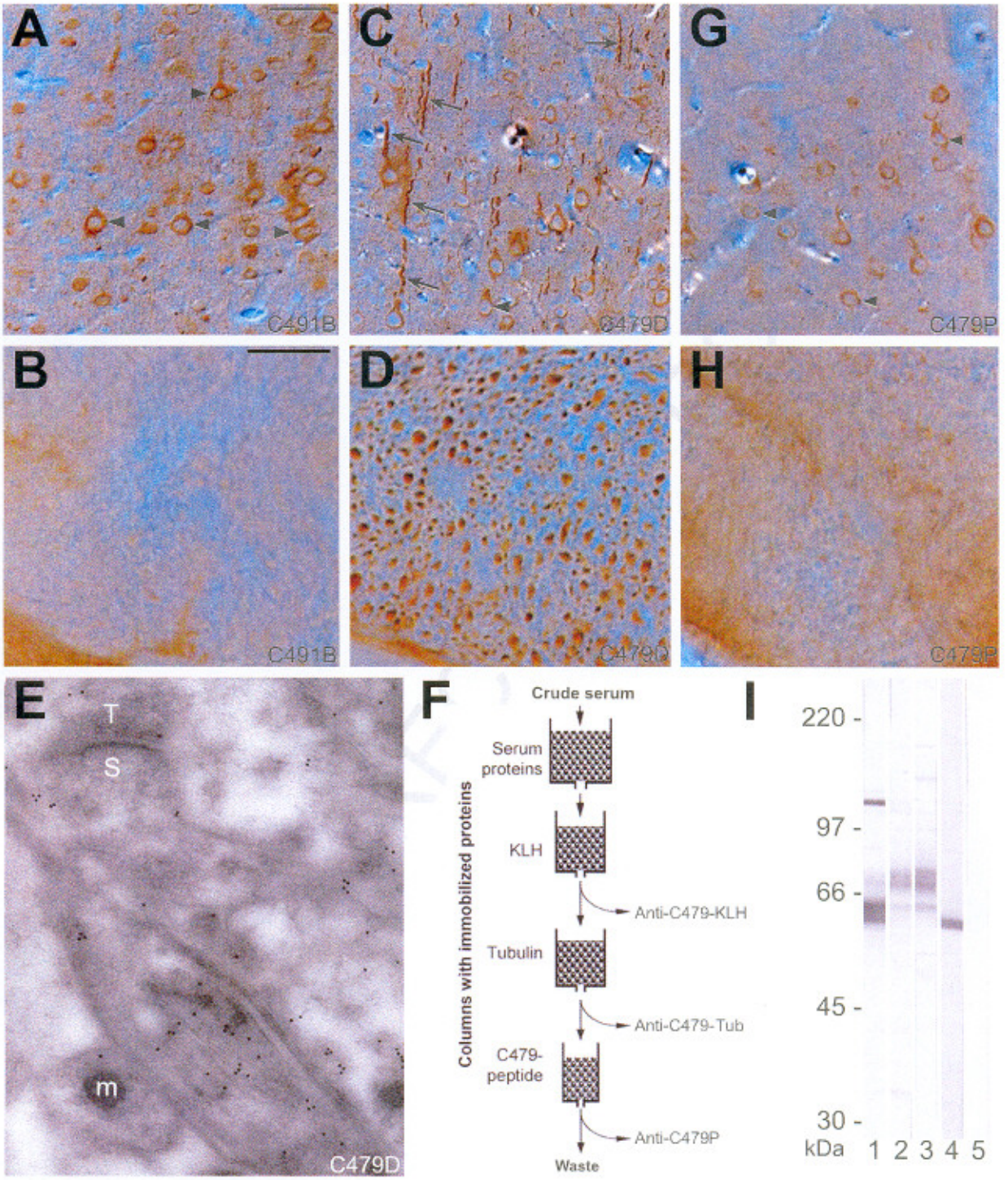

Fig. 4. Immunocytochemical labeling of rat brain sections (A, C and G: neocortex layer 4; panels B, D and H: white matter of the pyramidal tract; panel E: hippocampus CA1) using 3 μg/ml anti-C491B (panels A and B), 1 μg/ml anti-C479D (panels C, D and E) and 10 μg/ml anti-C479P (G and H). The latter antibody was purified as shown in panel F: 10 ml anti-C479 serum (bleeding 26.09.2001 of rabbit 0B0721; database ID: serum, 70). The serum was passed through a column with aldehyde-treated bovine serum proteins to remove polyreactive antibodies and antibodies to aldehyde-treated proteins in general. Then the absorbed serum was first passed through a column with immobilized carrier protein (KLH), then on a column with tubulin and finally on a column with the C479-peptide in order to collect the desired antibodies. The antibodies bound to the last three columns were eluted with low pH-buffer and neutralized. The amounts of anti-C479-KLH, anti-C479-Tub and anti-C479P antibodies collected were 4.26 mg, 0.7 mg and 0.8 mg, respectively. Their specificity was tested by ELISA (see Table 3), by immunocytochemistry (panels G and H) and by immunoblotting (panel I: rat hippocampus, 16 μg protein

Table 3. Testing of fractionated anti-C479 antiserum (0B0721) by ELISA

	Antigen coating in the microtiterplate wells		
	C479	Tubulin	KLH
Anti-C479-KLH (14 μg/ml)	3.96	0.05	3.86
Anti-C479-KLH (1.4 μg/ml)	3.97	0.00	3.63
Anti-C479-Tub (4 μg/ml)	3.95	3.86	0.06
Anti-C479-Tub (0.4 μg/ml)	0.83	0.52	0.00
Anti-C479P (4 μg/ml)	3.96	0.03	0.03
Anti-C479P (0.4 μg/ml)	3.94	0.00	0.00
Anti-C491B (1 μg/ml)	0.31	0.01	0.01

C479-498 peptide, purified tubulin and KLH were immobilized in the wells of microtiter plates. The plates were used to test the immunoreactivities of the various antibody fractions from the separation experiment described in Fig. 4. Table shows the absorbance values obtained (average of duplicate determinations). Note that the antibodies collected on the last column (containing C479-peptide) were devoid of tubulin reactivity. The anti-C491B antibodies did not react with tubulin. The slight reactivity towards the C479–498 peptide shows that some of the antibodies directed to the C491–523 peptide react with the overlapping part of the sequence.

EAAT3 (Fig. 5B, strips 3 and 4) while tubulin labeling only was present with the non-absorbed anti-C479 (strip 2) and EAAT2 was detected, as expected, with anti-B12 (strip 1). Labeling with anti-tubulin antibody (strip 5) produced a band consistent with that observed with the non-absorbed anti-C479.

Screening of antibodies for reactivity toward tubulin

Tubulin was purified from rabbit brain and immunoblotted with a number of antibodies. Some of these tests are shown in Fig. 6. Of the anti-glutamate transporter antibodies tested, only the unabsorbed anti-C479 antibodies recognized tubulin. No reaction was observed with any of the anti-B12 or anti-C491 antibodies.

Preabsorption of the anti-C479D and the anti-C479Tub antibodies

As shown in Table 3, the tubulin-reactive antibodies in the anti-C479 antisera bound to both tubulin and the C479–498 peptide. This indicated that the antiserum contained a mixture of antibodies. Some of these were specific for the peptide (anti-C479P) and some had a dual specificity in that they could bind both the peptide and tubulin. To test this further, anti-C479D and anti-C479Tub antibodies were preincubated with free C479-498 peptide prior to incubation with immunoblots and sections. As expected, the free peptide was able to block all binding of the antibodies to all

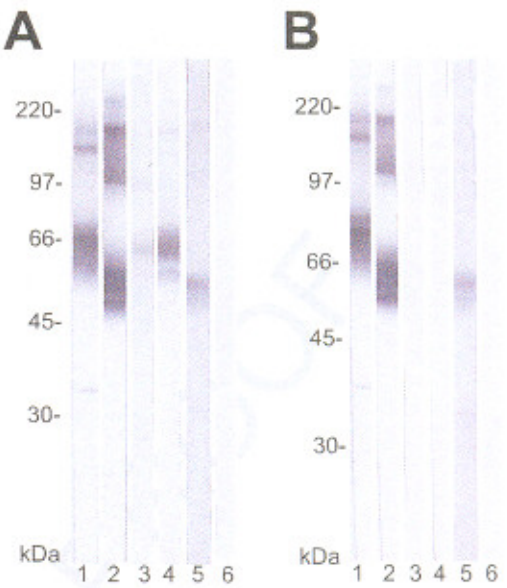

Fig. 5. Immunoblotting of antibodies with brain protein from wild type (panel A) and EAAT3-knockout mice (panel B): (strip 1) anti-B12 antibodies to EAAT2; (strip 2) unabsorbed anti-C479D; (strip 3) absorbed anti-C479P; (strip 4) anti-C491B; (strip 5) monoclonal anti-tubulin (Sigma-Aldrich) 1:200; (strip 6) no primary antibody. Note that the labeling of the EAAT3-band is absent on the Western blot of proteins from the EAAT3-knockout. Also note the difference in labeling intensity obtained with the anti-C479P and anti-C491B in mice. The anti-C479 antibodies show almost no reaction, while they label the rat EAAT3 almost as strongly as the anti-C491 antibodies (compare strips 1 and 2 in Fig. 3B or strips 2 and 3 in Fig. 4I). The unabsorbed anti-C479D antibodies recognize tubulin in both wild-type and EAAT3-knockout.

tissue proteins. Thus, the peptide also abolished the binding of the antibodies to tubulin (data not shown).

Double labeling with anti-EAAT3 antibodies and oligodendrocyte markers

It has been reported (Kugler and Schmitt, 1999) that EAAT3 is expressed in oligodendrocytes. This study is based on antibodies to a peptide corresponding to EAAT3 residues 480–499. Because our peptide (C479–498), covers almost the same sequence, it is natural to ask if their antibodies also cross-react with tubulin. This has not been tested, and the antibody has not been available to us. However, the authors show in their article that they have performed double labeling with a monoclonal anti-tubulin antibody and observe colocalization of labeling. On this background, we wanted to check if our antibodies also labeled oligodendrocytes. Vibratome sections were double labeled with rabbit antibodies to EAAT3 and with mouse

per strip): anti-C479D (not absorbed; strip 1), anti-C479P (after tubulin absorption; strip 2), anti-C491B (strip 3), a monoclonal anti-tubulin antibody (1:200) from Sigma-Aldrich (strip 4) and negative control (no primary antibody; strip 5). Note that both EAAT3 antibodies labeled neurons (arrowheads), but that the latter antibody labeled axons and dendrites stronger than the former and labeled microtubules at the electron microscopical level (E). Absorption against tubulin removes both the tubulin reactivity and the axonal labeling in tissue sections. There was no evidence of myelin labeling. Scale bars = 50 μm in panels A, C and G and 10 μm in panels B, D and H. Letters (T, S, m) in panel E indicate nerve terminal, dendritic spine and mitochondrion, respectively. The animals were perfusion fixed with 0.1 M NaPi containing 4% formaldehyde (panels A–D, H) or 4% formaldehyde and 0.05% glutaraldehyde (panel E).

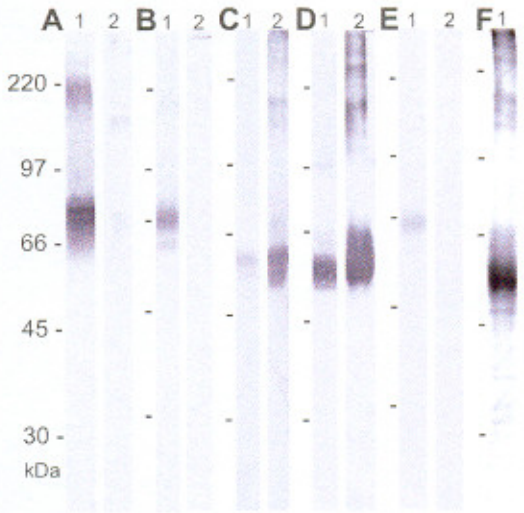

Fig. 6. Immunoblotting (panels A–E) of antibodies with brain proteins and purified tubulin. Tubulin was purified from rabbit brain according a published procedure (Weisenberg, 1980). The purity was checked by SDS-PAGE and silver staining (panel F). Lane 2 in panels A–E contains each 5 μg of the purified tubulin, while lane 1 contains 5 μg total rat forebrain protein. The blots were immunolabeled with anti-B12 (panel A), anti-C491B (panel B), anti-tubulin (1:100; Sigma-Aldrich) (panel C), anti-C479D (panel D) and anti-C479P (panel E). Note that no reaction with tubulin is seen with the anti-B12, anti-C491B and the anti-C479P, while strong reaction is seen with the anti-tubulin and anti-C479D antibodies.

antibodies to oligodendrocyte markers (CNPase and MBP). No co-localization between oligodendrocyte markers and EAAT3 was detected (Fig. 7A–D). The antibody produced by Kugler and Schmitt (1999) must be different from our anti-C479D, because none of our anti-EAAT3 antibodies label myelin or oligodendrocyte cell bodies.

DISCUSSION

This paper illustrates that immunization with an antigen may lead to the generation of antibodies that recognize not only the antigen, but also molecules that appear completely unrelated to the antigen. While it might be expected that two molecules which share some sequence similarity could be recognized by antibodies raised against one of them, in this case the cross-reactivity between anti-EAAT3 antibodies and tubulin could not have been predicted from existing knowledge.

Clearly, as reported here, animals frequently produce antibodies that have the ability to bind to the antigen-columns and also to bind to unrelated proteins on immunoblots. Consequently, the generation of antibodies with oligo- or poly-reactivity is something that frequently occurs. We have seen this also in connection with the production of antibodies to other transporter proteins, e.g. a monoclonal polyreactive IgG antibody (Danbolt et al., 1998). This is in line with studies of autoantibodies in systemic lupus erythematosus where certain peptide sequences bind anti-DNA antibodies (Sibille et al., 1997; James et al., 1999).

Another issue this raises relates to preabsorption with the relevant antigen which is considered by many to be a key test of antibody specificity. The results presented here show that this test is of little value when the antibody is already affinity purified against the immobilized antigen, because only the antibodies recognizing the antigen have been collected and the rest eliminated. Since antibodies have a finite number of binding sites (IgG molecules have two), it follows that antigen added in excess, will always saturate the antibody binding sites and thereby completely block the labeling of tissue sections, even when the antibody has affinity for other tissue antigens. As we show here, the anti-C479-Tub fraction labels both EAAT3 and tubulin in sections. Preabsorption with C479-peptide blocks all labeling of the sections, including that directed against tubulin.

A third point illustrated here is that it is hard to predict in advance if sequence differences between species are going to matter for antibody binding. The rat 479–498 sequence and the rat 491–523 sequence both differ with one amino acid from the corresponding mouse sequences:

479 NIVNPFALEPTILDNEDSDTK 498 Rat

491 LDNEDSDTKKSYVNGGFSVDKSDTISFTQTSQF 523 Rat

479 NIVNPFALEPTTLDNEDSDTKKSYVNGGFAVD-KSDTISFTQTSQF 523 Mouse

The anti-C491 antibodies detect mouse and rat EAAT3 with about the same strength, while anti-C479 antibodies do not recognize the mouse protein to any significant degree.

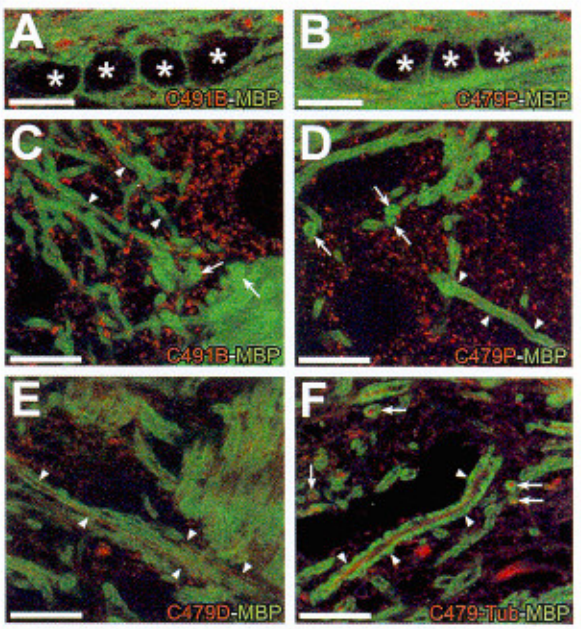

Fig. 7. Double labeling with anti-EAAT3 antibodies (red) and MBP (green). (A, B) Neither 1 μg/ml anti-C491B nor 10 μg/ml anti-C479P labels oligodendrocytes (asterisks) in corpus callosum. Panels C and D show that neither anti-C491B nor anti-C479P labels axons in rat thalamus. There is no red color inside longitudinally (arrowheads) or transversally cut (arrows) myelin sheets (green). Panels E and F show that both the anti-C479D and the anti-C479Tub antibodies label axons inside myelin sheets. Rat tissue perfusion fixed with 4% formaldehyde in 0.1 M NaPi. Scale bars=10 μm.

A fourth point illustrated is that generation of good anti-peptide antibodies mainly depend on the selection of the best part of the protein sequence. This, however, is hard as shown in Fig. 2. The difference between EAAT2 and EAAT3 was not predicted in advance. Our conclusion is that the most efficient way to produce anti-peptide antibodies is to use a "shotgun" approach: synthesize several peptides, mix them together before conjugation to carrier protein and inject them all into the same rabbits. By separating the various antibodies from the ensuing antisera, it is easy to find out which are the best peptides. Then these can be injected alone into new rabbits if larger amounts of antibody are needed. This approach conserves the number of animals used. Further, if good antibodies are not obtained, it is better to try new peptides rather than trying unsuccessful peptides in new rabbits.

Concluding remarks

Polyreactivity is a well-known phenomenon which comes in various disguises. As this paper demonstrates, antibody specificity is no trivial matter. Because the cross-reactivity can be highly specific, it may be hard to discover. It also follows from this that cross-reactivity depends on the presence of the cross-reacting molecular species. Thus, an antibody may be specific in one organ and not in another due to differences in the expression of proteins cross-reacting with the antibody. Often, antibodies tested in one organ in animals of a certain age and species are used to study other organs in animals of different ages or species using different immunocytochemical protocols. On this background it is unacceptable that immunocytochemical papers are published with little or no information on the antibodies used.

If sharp and beautiful pictures are obtained, investigators often tend to believe that the antibodies are specific. The main concern is that the cost involved in disproving spurious results from other laboratories is huge, and often much higher than the costs of proper testing in the first place. This problem is recognized, and the *Journal of Comparative Neurology* lists requirements that must be met in order to make a paper acceptable for publication (Saper and Sawchenko, 2003). Data presented in this paper suggest that these requirements should be taken seriously and perhaps be made stricter. The main difficulty is not to distinguish between antibodies that recognize the desired antigen and those antibodies that recognize other antigens, but to find out whether or not antibody molecules derived from a single clone recognize both the desired antigen and something else. This is costly and a solution to this problem may be to establish web-based database systems in which all antibodies used in scientific publications are listed (for general consideration on neuroscience databases, see Amari et al., 2002; Koslow and Subramaniam, 2005). Then it would be possible to track each antibody, and thereby make it possible to accumulate knowledge on the specificity of each antibody. This would be particularly valuable for monoclonal antibodies, but if such a system is established, then it could just as well include all antibodies because polyclonal ones are often produced in sufficient quantities to be used in a number of studies.

Acknowledgments—This work was supported by the Norwegian Top Research Program (Toppforskningsprogrammet), the Norwegian Research Council, EU BIOMED (contract QLG3-CT-2001-02004).

REFERENCES

Amari S, Beltrame F, Bjaalie JG, Dalkara T, De Schutter E, Egan GF, Goddard NH, Gonzalez C, Grillner S, Herz A, Hoffmann KP, Jaaskelainen I, Koslow SH, Lee SY, Matthiessen L, Miller PL, Da Silva FM, Novak M, Ravindranath V, Ritz R, Ruotsalainen U, Sebestra V, Subramaniam S, Tang Y, Toga AW, Usui S, Van Pelt J, Verschure P, Willshaw D, Wrobel A (2002) Neuroinformatics: the integration of shared databases and tools towards integrative neuroscience. J Integr Neurosci 1:117–128.

Bjørås M, Gjesdal O, Erickson JD, Torp R, Levy LM, Ottersen OP, Degree M, Storm-Mathisen J, Seeberg E, Danbolt NC (1996) Cloning and expression of a neuronal rat brain glutamate transporter. Mol Brain Res 36:163–168.

Boulland JL, Qureshi T, Seal RP, Rafiki A, Gundersen V, Bergersen LH, Fremeau RT Jr, Edwards RH, Storm-Mathisen J, Chaudhry FA (2004) Expression of the vesicular glutamate transporters during development indicates the widespread corelease of multiple neurotransmitters. J Comp Neurol 480:264–280.

Conti F, DeBiasi S, Minelli A, Rothstein JD, Melone M (1998) EAAC1, a high-affinity glutamate transporter, is localized to astrocytes and GABAergic neurons besides pyramidal cells in the rat cerebral cortex. Cereb Cortex 8:108–116.

Danbolt NC (2001) Glutamate uptake. Prog Neurobiol 65:1–105.

Danbolt NC, Lehre KP, Dehnes Y, Chaudhry FA, Levy LM (1998) Localization of transporters using transporter-specific antibodies. Methods Enzymol 296:388–407.

Danbolt NC, Pines G, Kanner BI (1990) Purification and reconstitution of the sodium- and potassium-coupled glutamate transport glycoprotein from rat brain. Biochemistry 29:6734–6740.

Danbolt NC, Storm-Mathisen J, Kanner BI (1992) An [Na^+ + K^+] coupled L-glutamate transporter purified from rat brain is located in glial cell processes. Neuroscience 51:295–310.

Dehnes Y, Chaudhry FA, Ullensvang K, Lehre KP, Storm-Mathisen J, Danbolt NC (1998) The glutamate transporter EAAT4 in rat cerebellar Purkinje cells: a glutamate-gated chloride channel concentrated near the synapse in parts of the dendritic membrane facing astroglia. J Neurosci 18:3606–3619.

Frens G (1973) Controlled nucleation for the regulation of the particle size in monodisperse gold suspensions. Nat Phys Sci 241:20–22.

He Y, Hof PR, Janssen WG, Rothstein JD, Morrison JH (2001) Differential synaptic localization of GluR2 and EAAC1 in the macaque monkey entorhinal cortex: a postembedding immunogold study. Neurosci Lett 311:161–164.

James JA, Mcclain MT, Koelsch G, Williams DG, Harley JB (1999) Side-chain specificities and molecular modelling of peptide determinants for two anti-Sm B/B′ autoantibodies. J Autoimmun 12: 43–49.

Jameson BA, Wolf H (1988) The antigenic index: a novel algorithm for predicting antigenic determinants. Comput Appl Biosci 4:181–186.

Kanai Y, Hediger MA (1992) Primary structure and functional characterization of a high-affinity glutamate transporter. Nature 360: 467–471.

Koslow SH, Subramaniam S (2005) Databasing the brain. From data to knowledge (neuroinformatics). John Wiley & Sons.

Kugler P, Schmitt A (1999) Glutamate transporter EAAC1 is expressed in neurons and glial cells in the rat nervous system. Glia 27: 129–142.

Laemmli UK (1970) Cleavage of structural proteins during the assembly of the head of bacteriophage T4. Nature 227:680–685.

Lehre K, Danbolt N (1998a) Determination of the number of glial glutamate transporter molecules and astroglial surface area in subregions of the rat hippocampus and cerebellum. Eur J Neurosci 10:14808

Lehre KP, Danbolt NC (1998b) The number of glutamate transporter subtype molecules at glutamatergic synapses: chemical and stereological quantification in young adult rat brain. J Neurosci 18: 8751–8757.

Lehre KP, Levy LM, Ottersen OP, Storm-Mathisen J, Danbolt NC (1995) Differential expression of two glial glutamate transporters in the rat brain: quantitative and immunocytochemical observations. J Neurosci 15:1835–1853.

Levy LM, Lehre KP, Rolstad B, Danbolt NC (1993) A monoclonal antibody raised against an [Na^+-K^+]coupled L-glutamate transporter purified from rat brain confirms glial cell localization. FEBS Lett 317:79–84.

Peghini P, Janzen J, Stoffel W (1997) Glutamate transporter EAAC-1-deficient mice develop dicarboxylic aminoaciduria and behavioral abnormalities but no neurodegeneration. EMBO J 16:3822–3832.

Pines G, Danbolt NC, Bjørås M, Zhang Y, Bendahan A, Eide L, Koepsell H, Storm-Mathisen J, Seeberg E, Kanner BI (1992) Cloning and expression of a rat brain L-glutamate transporter. Nature 360:464–467.

Pow DV, Crook DK (1993) Extremely high titre polyclonal antisera against small neurotransmitter molecules: rapid production, characterisation and use in light- and electron-microscopic immunocytochemistry. J Neurosci Methods 48:51–63.

Rothstein JD, Martin L, Levey AI, Dykes-Hoberg M, Jin L, Wu D, Nash N, Kuncl RW (1994) Localization of neuronal and glial glutamate transporters. Neuron 13:713–725.

Saper CB, Sawchenko PE (2003) Magic peptides, magic antibodies: guidelines for appropriate controls for immunohistochemistry. J Comp Neurol 465:161–163.

Shashidharan P, Huntley GW, Murray JM, Buku A, Moran T, Walsh MJ, Morrison JH, Plaitakis A (1997) Immunohistochemical localization of the neuron-specific glutamate transporter EAAC1 (EAAT3) in rat brain and spinal cord revealed by a novel monoclonal antibody. Brain Res 773:139–148.

Sibille P, Ternynck T, Nato F, Buttin G, Strosberg D, Avrameas A (1997) Mimotopes of polyreactive anti-DNA antibodies identified using phage-display peptide libraries. Eur J Immunol 27:1221–1228.

Smith PK, Krohn RI, Hermanson GT, Mallia AK, Gartner FH, Provenzano MD, Fujimoto EK, Goeke NM, Olson BJ, Klenk DC (1985) Measurement of protein using bicinchoninic acid. Anal Biochem 150:76–85.

Towbin H, Staehelin T, Gordon J (1979) Electrophoretic transfer of proteins from polyacrylamide gels to nitrocellulose sheets: Procedure and some applications. Proc Natl Acad Sci U S A 76:4350–4354.

Weisenberg RC (1980) Role of co-operative interactions, microtubule-associated proteins and guanosine triphosphate in microtubule assembly: a model. J Mol Biol 139:660–677.

(Accepted 12 July 2005)

Comments to Paper 2

Holmseth, Silvia // Dehnes, Yvette // **Bjørnsen, L.P.** // Boulland, Jean Luc // Bergles, Dwight // Furness N David // Danbolt, Niels Chr.- Specificity of antibodies – unexpected crossreactivity of antibodies directed against the EAAT3 (EAAC) glutamate transporter, Special Issue Article, Neuroscience

Specific antibodies are essential tools for identifying individual proteins in complex biological samples. While generation of antibodies is often straight forward, determinations of the antibody specificity is not. In this paper we illustrate how complicated this can be by describing the production and characterization of antibodies of the excitatory amino acid transporter 3 (EAAT3) glutamate transporter. I contributed on this paper by working on the ELISA-procedure for antibody testing. The procedure was performed by a Tecan Genesis 200 Workstation robot that I programmed. The antibodies were tested for reactivity toward proteins present in high concentrations in axons. A strong and specific reaction to tubulin was observed, but no to any of the other proteins tested, including another abundant cytoskeletal protein, actin. This result indicated that the anti-C479 antibodies recognized both tubulin and EAAT3 despite of being affinity purified against the corresponding peptide.

This paper show that not all antibodies to synthetic peptides recognize the native protein and that the specificity of an antibody is hard to predict. Unwanted reactivity can be highly specific and thereby hard to recognize.

Loss of perivascular aquaporin 4 may underlie deficient water and K^+ homeostasis in the human epileptogenic hippocampus

Tore Eid*[†‡§], Tih-Shih W. Lee[‡¶], Marion J. Thomas[‖**], Mahmood Amiry-Moghaddam[‖**], Lars P. Bjørnsen*[‖], Dennis D. Spencer*, Peter Agre[‡‡], Ole P. Ottersen[‖**], and Nihal C. de Lanerolle*

Departments of *Neurosurgery, [†]Laboratory Medicine, and [¶]Psychiatry, Yale University School of Medicine, New Haven, CT 06520; [‖]Centre for Molecular Biology and Neuroscience and Centre for Water Imbalance-Related Disorders and **Department of Anatomy, University of Oslo, N-0316 Oslo, Norway; and [††]Departments of Biological Chemistry and Medicine, The Johns Hopkins University School of Medicine, Baltimore, MD 21205

Contributed by Peter Agre, December 17, 2004

An abnormal accumulation of extracellular K^+ in the brain has been implicated in the generation of seizures in patients with mesial temporal lobe epilepsy (MTLE) and hippocampal sclerosis. Experimental studies have shown that clearance of extracellular K^+ is compromised by removal of the perivascular pool of the water channel aquaporin 4 (AQP4), suggesting that an efficient clearance of K^+ depends on a concomitant water flux through astrocyte membranes. Therefore, we hypothesized that loss of perivascular AQP4 might be involved in the pathogenesis of MTLE. Whereas Western blot analysis showed an overall increase in AQP4 levels in MTLE compared with non-MTLE hippocampi, quantitative ImmunoGold electron microscopy revealed that the density of AQP4 along the perivascular membrane domain of astrocytes was reduced by 44% in area CA1 of MTLE vs. non-MTLE hippocampi. There was no difference in the density of AQP4 on the astrocyte membrane facing the neuropil. Because anchoring of AQP4 to the perivascular astrocyte endfoot membrane depends on the dystrophin complex, the localization of the 71-kDa brain-specific isoform of dystrophin was assessed by immunohistochemistry. In non-MTLE hippocampus, dystrophin was preferentially localized near blood vessels. However, in the MTLE hippocampus, the perivascular dystrophin was absent in sclerotic areas, suggesting that the loss of perivascular AQP4 is secondary to a disruption of the dystrophin complex. We postulate that the loss of perivascular AQP4 in MTLE is likely to result in a perturbed flux of water through astrocytes leading to an impaired buffering of extracellular K^+ and an increased propensity for seizures.

dystrophin | epilepsy | seizures | astrocytes

Mesial temporal lobe epilepsy (MTLE) is one of the commonest forms of medically intractable epilepsies. MTLE is characterized by seizures that originate from mediobasal temporal lobe structures, particularly the hippocampus, and neurosurgical resection of the epileptogenic hippocampus is often used to treat this disorder. The resected, epileptogenic hippocampus in MTLE is typically indurated and atrophic and displays massive loss of neurons along with astroglial changes, particularly in areas CA1 and CA3 and the dentate hilus, a condition known as hippocampal (or Ammon's horn) sclerosis. Electrophysiological recordings from MTLE hippocampi have demonstrated that these hippocampi are hyperexcitable when compared with non-sclerotic hippocampi from patients with other types of temporal lobe epilepsy, such as mass associated temporal lobe epilepsy (patients with an extrahippocampal mass lesion) or paradoxical temporal lobe epilepsy (patients without a mass lesion and with seizures of unknown etiology). A fundamental question that remains to be resolved is why the MTLE hippocampus is hyperexcitable.

Studies of MTLE patient hippocampi have shown that the K^+ buffering capacity is diminished when compared with non-MTLE hippocampi (1). This decrease is most pronounced in sclerotic areas of the hippocampus, such as CA1, where patch clamp experiments have demonstrated impaired uptake of K^+ into astrocytes by means of inwardly rectifying K^+ channels (2, 3). The sclerotic, MTLE hippocampus also exhibits increased T2 signal density on magnetic resonance imaging and higher than normal apparent diffusion coefficient on diffusion-weighted imaging, suggesting that water accumulates in this structure (4). Moreover, the expression of mRNA for aquaporin 4 (AQP4) is increased in area CA1 of MTLE hippocampi compared with non-MTLE hippocampi (5).

Loss of AQP4 from the perivascular endfoot domain of astrocytes is associated with reduced clearance of extracellular K^+ and increased severity of seizures in an animal model of α-syntrophin deletion (6). This and other studies (7, 8) suggest that buffering of K^+ by means of inwardly rectifying K^+ channels on astrocytes depends on a parallel flux of water through the plasma membrane of these cells. Under conditions of high neuronal activity, K^+ and water are taken up by the astrocyte membrane facing the neuropil and siphoned into blood or cerebrospinal fluid through the endfoot membrane (9). Thus, in experimental models, a perturbation of the flux of K^+ and water exacerbates the potential for seizures. Here, we present data suggesting that a similar mechanism may operate in the hippocampus of patients with MTLE.

Materials and Methods

Tissue. Patients with medically intractable temporal lobe epilepsy underwent phased presurgical evaluation at the Yale–New Haven Hospital, and those selected for surgery had their hippocampus resected according to standard procedures (10). During the period of July 1996 to February 2002, a total of 86 hippocampi were resected. Twenty-four of these hippocampi were randomly selected for the present study, and they are therefore representative of the patient population that undergoes surgery at Yale. Informed consent from each patient and institutional approval were obtained for the use of tissue in this project (see Table 1).

Classification. Tissue classification was carried out separately by two investigators (T.E. and N.C.d.L.), and the samples were encoded for further use. Thus, the investigators performing the Western blots (M.J.T. and M.A.-M.) and quantitative electron microscopy (L.P.B.) were unaware of the patient categories until the experiments had been completed and the data were ready for statistical analysis.

Abbreviations: MTLE, mesial temporal lobe epilepsy; AQP4, aquaporin 4.

[‡]T.E. and T.-S.W.L. contributed equally to this work.

[§]To whom correspondence should be addressed at: Department of Neurosurgery, Yale University School of Medicine, 333 Cedar Street, P.O. Box 208082, New Haven, CT 06520-8082. E-mail: tore.eid@yale.edu.

Table 1. Characteristics of patients selected for the study

Case	Gender	Age, years	Years since first unprovoked seizure	AEDs at surgery	MRI findings	Pathology	Classification
1	M	39	16	ltg	Unremarkable	Unremarkable	Non-MTLE
2	F	22	10	tpm	Unremarkable	Unremarkable	Non-MTLE
3	F	46	28	cbz	Unremarkable	Unremarkable	Non-MTLE
4	M	40	4	lev, vpa	Unremarkable	Unremarkable	Non-MTLE
5	M	44	18	cbz, clo	R hippocampal sclerosis	Unremarkable	Non-MTLE
6	F	49	42	lev	Chiari I malformation; otherwise unremarkable	Unremarkable	Non-MTLE
7	F	38	30	cbz, tpm	Unremarkable	Unremarkable	Non-MTLE
8	M	35	17	ltg, cbz	Cavernous hemangioma, R amygdala, adjacent to hippocampal head; normal hippocampus	Cavernous hemangioma	Non-MTLE
9	M	27	1	cbz	L mesial temporal lobe mass lesion encroaching subbasal ganglia, replacing and involving amygdala and anterior hippocampus	Oligodendroglioma	Non-MTLE
10	F	10	5	ltg	R temporal lobe tumor involving basal ganglia and amygdala; bilateral hippocampal atrophy.	Low-grade astrocytoma	Non-MTLE
11	F	8	4	cbz	L temporal lobe tumor	Oligodendroglioma	Non-MTLE
12	M	47	22	cbz	R hippocampal atrophy	Hippocampal sclerosis	MTLE
13	F	36	14	cbz	L hippocampal sclerosis	Hippocampal sclerosis	MTLE
14	F	45	27	cbz, pri, gpn	R hippocampal atrophy	Hippocampal sclerosis	MTLE
15	M	40	39	cbz, pht	Unremarkable	Hippocampal sclerosis	MTLE
16	M	27	26	gpn, flb	R hippocampal atrophy	Hippocampal sclerosis	MTLE
17	M	24	16	tpm, pb	R hippocampal atrophy	Hippocampal sclerosis	MTLE
18	F	28	19	cbz	L hippocampal atrophy	Hippocampal sclerosis	MTLE
19	F	15	10	cbz, ltg	L hippocampal sclerosis with increased signal on FLAIR	Hippocampal sclerosis	MTLE
20	F	50	40	cbz	L hippocampal sclerosis with increased signal on FLAIR; bilateral small vessel ischemic changes	Hippocampal sclerosis	MTLE
21	F	36	26	ltg, pri	R hippocampal sclerosis with increased signal on FLAIR	Hippocampal sclerosis	MTLE
22	F	39	12	gpn, ltg	R hippocampal sclerosis	Hippocampal sclerosis	MTLE
23	M	46	10	ltg, lev	R hippocampal sclerosis	Hippocampal sclerosis	MTLE
24	F	51	33	cbz	L hippocampal sclerosis	Hippocampal sclerosis	MTLE

For non-MTLE, $n = 11$, and for MTLE, $n = 13$. M, male; F, female; AEDs, antiepileptic drugs; cbz, carbamazepine; clo, clonazepam; flb, felbamate; pht, phenytoin; lev, levetiracetam; li, lithium; ltg, lamotrigine; gpn, gabapentin; pb, phenobarbial; pri, primidone; tpm, topiramate; vpa, valproate; L, left; R, right; FLAIR, fluid-attenuated inversion recovery imaging.

The surgically resected hippocampi were classified into two groups (see ref. 11 for details): MTLE (group 1) and non-MTLE (group 2). In MTLE, the seizure activity is believed to originate from the hippocampus based on noninvasive studies, depth, and/or subdural electrode recordings. The MTLE hippocampus is characterized by pronounced neuronal loss (>50%) and extensive astroglial proliferation in the hippocampal subfields CA1, CA3, and hilus. Also, this category shows reorganization of peptidergic (dynorphin, somatostatin, neuropeptide Y, and substance P) neurons in the dentate gyrus. The non-MTLE hippocampi are recognized by a modest (<25%) neuronal loss throughout all hippocampal subfields, minimal astroglial proliferation, and no reorganization of peptidergic neurons in the dentate gyrus. The histological pattern in the non-MTLE hippocampi is similar to that of autopsy hippocampi. In ≈50% of the non-MTLE hippocampi, the seizures are thought to originate from a mass lesion (usually a tumor) outside the hippocampus but within the temporal lobe territory. In the remaining cases, no mass lesion is apparent and the hippocampi are selected for resection based on intracranial recordings of seizure onset.

Tissue Preparation. Immediately after surgical resection, two 5-mm-thick slices were cut from the center portion of the hippocampus. One of the samples was immersed into a fixative containing 4% paraformaldehyde and 15% (vol/vol) saturated picric acid in 0.1 M phosphate buffer, pH 7.4, for 1 h, followed by immersion into 5% acrolein in phosphate buffer, pH 7.4, for 3 h. Fifty-micrometer coronal sections were cut on a Vibratome and either (*i*) stored in a cryoprotection solution (FD NeuroTechnologies, Catonsville, MD) at −80°C until processed for preembedding immunohistochemistry or (*ii*) processed immediately for freeze substitution. The other sample was rapidly frozen on dry ice and cut coronally into 200-μm sections on a cryostat and stored at −80°C until used for Western blotting.

Antisera and Chemicals. Affinity-purified polyclonal (rabbit) antibodies against AQP4 (Chemicon) and monoclonal (mouse) antibodies against dystrophin (NovoCastra, Newcastle upon Tyne, U.K.) were used. The dystrophin antibody was made against a synthetic polypeptide consisting of the last 17 aa of the carboxyl terminus of the human dystrophin sequence (SSRGRNTPGKPMREDTM). This sequence is present in the astrocyte-specific form of dystrophin, Dp71 (12). Unless otherwise specified, all other chemicals were obtained from Sigma–Aldrich.

Western Blotting. Frozen non-MTLE and MTLE whole hippocampi were sonicated on ice in homogenization buffer (50

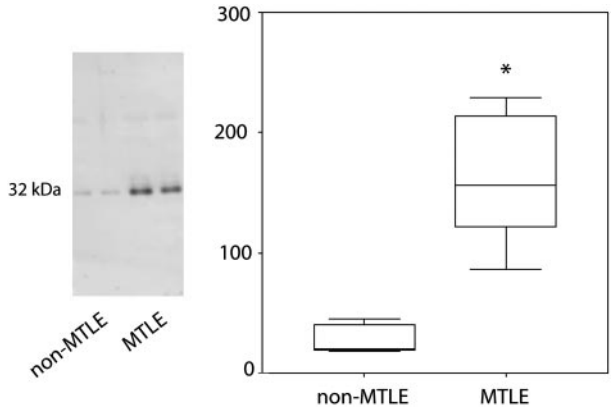

Fig. 1. There is an overall increase in AQP4 protein in the MTLE hippocampus. Western blots of representative non-MTLE and MTLE patient hippocampi immunostained with antibodies against AQP4 reveal single bands at the expected molecular mass of 32 kDa. The band intensities from six randomly selected non-MTLE and MTLE hippocampi (total of 12) were determined and visualized by box plots. The value of the *y* axis is the labeling intensity of AQP4 compared with a standard control of neocortical tissue (see *Materials and Methods* for details). A 360% increase in labeling intensity for AQP4 is evident in MTLE vs. non-MTLE (*, $P = 0.002$, two-tailed Mann–Whitney *U* test).

mM 3-[*N*-morpholino]propane-sulfonic acid·HCl/2 mM DTT, pH 7.6/3 mM EGTA/0.5 mM magnesium acetate/0.1 mM sodium orthovanadate/0.1 mM PMSF/20 μg/ml leupeptin/10 μg/ml pepstatin A/5 μg/ml aprotinin/0.32 M sucrose). Protein concentrations were determined with a BCA Protein Assay kit (Pierce). After being diluted in a sample loading buffer (50% sucrose/7.5% SDS/62.5 mM Tris, pH 6.8/2 mM EDTA/3.1% DTT/0.01% bromophenol blue), 10 μg of protein was added per lane, separated by electrophoresis on 12% polyacrylamide gels (MiniProtean II, Bio-Rad) and transferred onto poly(vinylidene difluoride) membranes. Membranes were blocked for 1 h in Tris-buffered saline (20 mM Tris/137 mM NaCl, pH 7.6) plus 0.1% Tween 20 (TBS-T) plus 5% blocking agent [Enhanced Chemifluorescence (ECH) kit, Amersham Biosciences], followed by overnight incubation in primary antibody (1 μg/ml AQP4; catalog no. AB3068, Chemicon). Membranes were subsequently incubated for 1 h in fluorescein-conjugated anti-rabbit antibodies (ECF kit, diluted 1:600), followed by a 1-h incubation in alkaline phosphatase-conjugated anti-fluorescein antibody (ECF kit, diluted 1:2,500). All steps were carried out at room temperature with antibodies diluted in TBST plus 1% milk powder.

After each incubation, membranes were washed in TBS-T. The chemifluorescent signal was detected with a laser scanner (Molecular Imager FX, Bio-Rad). For each blot, a global background subtraction was performed that removed the high-frequency, low-intensity pixels. After magnification, individual pixels were visible, and each band was traced manually by using the same background pixel intensity immediately adjacent to the band as a cutoff. Similarly, a standard curve was constructed for each blot with increasing concentrations (within the linear range of the curve) of SDS-homogenized human neocortex from a non-MTLE patient, with the highest concentration set at 100%. The volume values (volume = sum of intensities of the pixels within the volume boundary × pixel area) of the bands were determined for AQP4 and the relative concentrations from the patient samples were determined by comparison with the standard curve.

Preembedding Immunohistochemistry for Light Microscopy. Vibratome sections were processed free-floating according to the avidin–biotin complex method of Hsu *et al*. (13) as described in ref. 14 with the following modifications: Incubation in the primary antibodies was done for 18 h at room temperature at dilutions of 1:10,000 for anti-AQP4 and 1:5,000 for anti-dystrophin; a commercially available kit (VECTASTAIN Elite, Vector Laboratories) was used for the remaining procedure.

Freeze Substitution. Small tissue blocks ($0.3 \times 0.5 \times 1$ mm^3) of area CA1 were dissected from the 500-μm Vibratome sections and subjected to freeze substitution (15). Briefly, the tissue blocks were cryoprotected in glycerol and rapidly frozen in liquid propane at −190°C. The frozen tissue was immersed into anhydrous methanol containing 0.5% uranyl acetate at −90°C in an automatic freeze substitution unit (EMAFS, Leica, Vienna, Austria). The blocks were infiltrated with Lowicryl HM20 Resin (Lowi, Waldkraiburg, Germany) at −30°C, polymerized by UV light, sectioned at 60 nm, transferred to 500-mesh nickel grids, and processed for ImmunoGold electron microscopy.

Postembedding ImmunoGold Electron Microscopy and Specificity Controls. On-grid immunolabeling of AQP4 was carried out in six non-MTLE and six MTLE cases according to the procedure of Laake *et al*. (16) with some modifications. Briefly, the sections were incubated for 2 h or overnight with the AQP4 antiserum (raised in rabbit) diluted 1:100, followed by incubation for 2 h with 10-nm colloidal gold-conjugated secondary antibodies to rabbit IgG diluted 1:20 (EMGFAR, BB International, Cardiff,

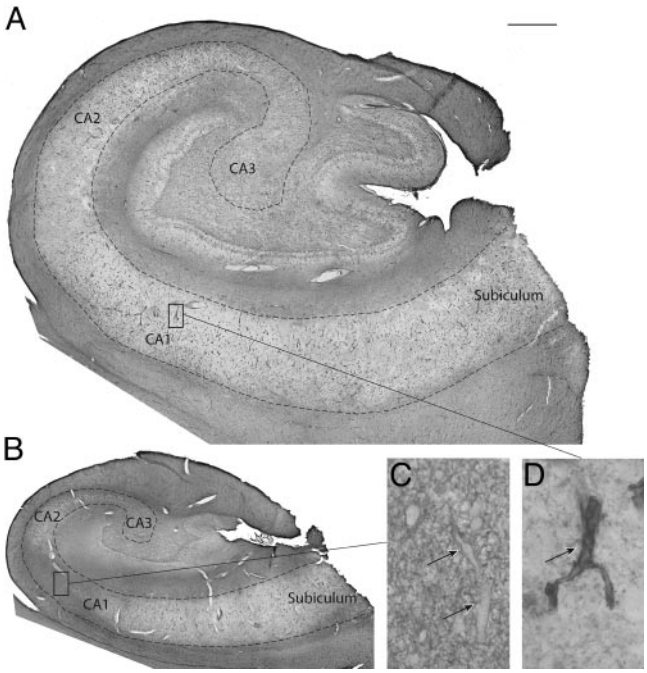

Fig. 2. Although AQP4 is preferentially distributed around blood vessels in the non-MTLE hippocampus, this localization is lost in MTLE. AQP4 is demonstrated by preembedding immunohistochemistry on Vibratome sections of a representative non-MTLE (*A* and *D*) and MTLE (*B* and *C*) hippocampus. (*A*) In the non-MTLE hippocampus, immunoreactivity for AQP4 in the pyramidal layer of Ammon's horn (the area within the dashed line) is preferentially distributed around blood capillaries. (Scale bar, 1 mm.) (*D*) This finding is demonstrated in the high-power field of CA1, where the arrow indicates a strongly immunopositive capillary amidst a weakly labeled neuropil. (Magnification, ×6 selected portion of *A*.) (*B*) In the MTLE hippocampus, the preferential distribution of AQP4 around blood capillaries is lost in the pyramidal layer in areas of sclerosis (such as CA1). Scale is the same as in *A*. (*C*) In the high-power field of CA1 moderate immunolabeling for AQP4 is present throughout the neuropil and also around blood capillaries, which are indicated by arrows. (Magnification, ×6 selected portion of *B*.)

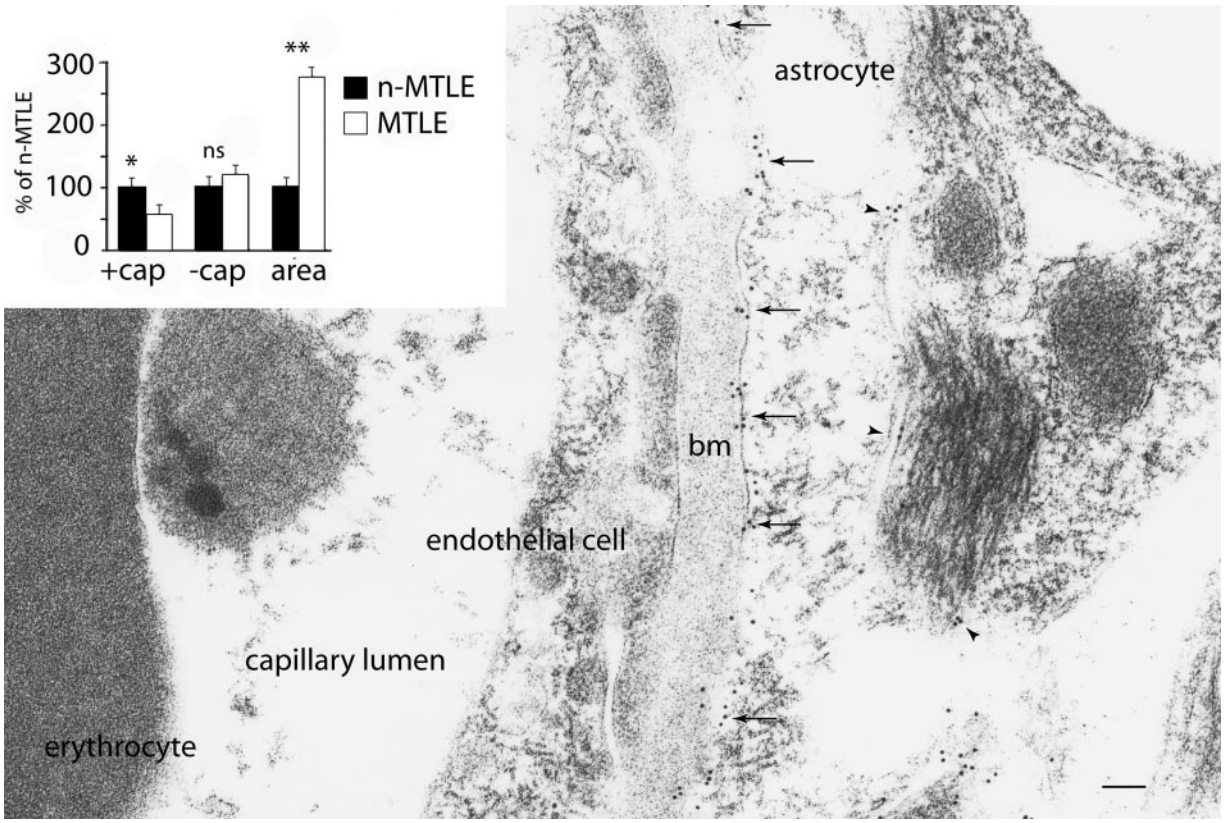

Fig. 3. Quantitative ImmunoGold electron microscopy reveals significant loss of AQP4 from the perivascular astrocyte membrane in MTLE vs. non-MTLE hippocampi. ImmunoGold electron microscopy of the endothelial–astrocyte interface in CA1 of a representative non-MTLE hippocampus demonstrates that AQP4 (arrows) is enriched on the astrocyte membrane facing the endothelial cell. Considerably less labeling is present on the astrocyte membrane facing the neuropil (arrowheads). (*Inset*) Quantitation of gold particle densities in random fields from area CA1 of six non-MTLE (n-MTLE) and six MTLE hippocampi. Gold particle counts for MTLE are given as percent of non-MTLE ± SEM: astrocyte membranes facing the endothelial cell (+cap; particles per μm), 56 ± 16% (*, P = 0.01); astrocyte membranes facing the neuropil (−cap; particles per μm), no change. The number of gold particles per unit area of neuropil (particles per μm^2) was 273 ± 23% (**, P = 0.013). A two-tailed Mann–Whitney U test was used for statistical analysis. bm, basal lamina; ns, not significant. (Scale bar, 100 nm.)

U.K.). The sections were counterstained with uranyl acetate followed by lead citrate or lead nitrate before being examined in a transmission electron microscope (Jeol EM 300). Substitution of the primary antibodies with normal serum or preimmune sera completely abolished the staining.

Statistical Analysis. A two-tailed Mann–Whitney U test was used to examine the differences in the Western blot results. In the postembedding experiments, gold particle densities were calculated per unit plasma membrane of randomly selected astrocyte profiles that were facing (*i*) the perivascular compartment or (*ii*) the neuropil. Gold particles were included in the counts as long as they touched the membrane, even if their center of gravity projected outside the plasma membrane. In addition, the total number of gold particles per unit area was calculated from particle counts in five randomly selected areas (total ≈60 μm^2) of the neuropil from each patient. Analysis was performed on electron micrographs that were digitized and analyzed by the Neurolucida system (Microbrightfield, Burlington, VT). Gold particle counts from six non-MTLE and six MTLE patients were used in the analysis.

Results

The level of AQP4 protein in hippocampal specimens from six non-MTLE and six MTLE patients was assessed by quantitative Western blotting. AQP4 was elevated by 360% in MTLE than in non-MTLE (P = 0.002, two-tailed Mann–Whitney U test) (Fig. 1). This finding is in accord with RT-PCR experiments of patient hippocampi in which the content of AQP4 mRNA is elevated by 257% in MTLE vs. non-MTLE (5). The increase in AQP4 in MTLE is proportional to the increase in the astrocyte marker glial fibrillary acidic protein (5); thus, the overall increase in AQP4 in MTLE can be explained by the proliferation of astrocytes typical of hippocampal sclerosis.

Immunocytochemistry was carried out to determine whether the increase in AQP4 was associated with a subcellular redistribution of AQP4. Light microscopic analysis revealed that AQP4 was enriched near blood vessels in non-MTLE hippocampi, consistent with a preferential localization of AQP4 in the perivascular endfeet of astrocytes (n = 11) (Fig. 2 *A* and *D*). In CA1 of the MTLE hippocampus (n = 13), the perivascular localization of AQP4 was disrupted (Fig. 2 *B* and *C*). Detailed analysis by ImmunoGold electron microscopy confirmed that the AQP4 labeling was confined to the plasma membrane of astrocytes in non-MTLE (n = 6) (Fig. 3) and MTLE (n = 6) hippocampi. Quantitation revealed that the labeling density was reduced by 44% on the perivascular astrocyte membrane in MTLE vs. non-MTLE (Fig. 3) hippocampi. In contrast, the labeling density of the astrocyte membrane facing the neuropil was the same in both patient categories. As expected from the increased number of astrocyte profiles in MTLE the gold particle density per unit area in randomly selected fields of the neuropil was 173% higher in MTLE hippocampi than in non-MTLE hippocampi (Fig. 3).

Anchoring of AQP4 to the perivascular astrocyte endfoot membrane depends on interactions with proteins of the dystro-

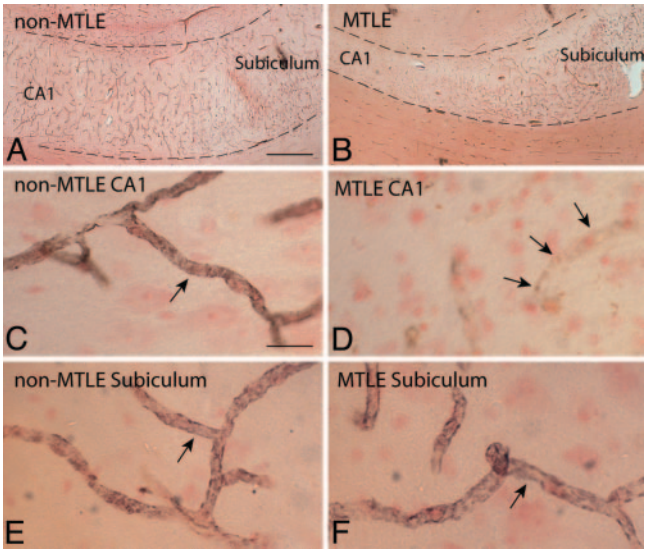

Fig. 4. Loss of perivascular AQP4 in the MTLE hippocampus is associated with a deficiency in perivascular dystrophin. Adjacent sections from the non-MTLE (*A*, *C*, and *E*) and MTLE (*B*, *D*, and *F*) hippocampi shown in Fig. 1 were immunolabeled with an antibody against the astrocyte-specific isoform of dystrophin (Dp71) and counterstained with neutral red. (*A* and *B*) The low-power micrographs from non-MTLE (*A*) and MTLE (*B*) depict the CA1-subiculum-transition, with the pyramidal layer between the dashed lines. (Scale bar, 500 μm.) (*C*, *D*, and *E*) In CA1 (*C*) and subiculum (*E*) of the non-MTLE hippocampus, there is strong immunolabeling for dystrophin around blood capillaries (arrows in *C* and *E*), whereas in the MTLE hippocampus, pericapillary immunolabeling for dystrophin is reduced in CA1 (arrows in *D*). (Scale bars, 40 μm.) (*F*) The validity of this finding is attested by the presence of numerous strongly dystrophin-positive capillaries in the subiculum of MTLE. (Scale bar, 40 μm.)

phin complex (17). Notably, deficiency in either dystrophin (18) or α-syntrophin (6) leads to loss of perivascular AQP4. Moreover, patients with Becker muscular dystrophy, a disorder characterized by defective expression of dystrophin, have increased incidence of epilepsy (19). In a recent microarray analysis of mRNA expression of nine dystrophin-associated proteins, only dystrophin was significantly lower by 68% in MTLE vs. non-MTLE hippocampi, whereas α-syntrophin mRNA was unchanged (5). To evaluate whether the deficiency of dystrophin in MTLE is related to the redistribution of AQP4, we localized dystrophin by immunohistochemistry with an antibody against the carboxyl terminus of the molecule. This antibody recognizes the 71-kDa major brain dystrophin isoform, Dp71, which is expressed in astrocytes (20). In agreement with animal studies, in the non-MTLE hippocampus, the immunolabeling for dystrophin was preferentially localized near blood vessels throughout all hippocampal subfields (Fig. 4 *A*, *C*, and *E*). In the MTLE hippocampus, the perivascular labeling for dystrophin was reduced in sclerotic areas (e.g., CA1) (Fig. 4 *B*, *D*, and *F*), despite the presence of numerous blood vessels in the latter (data not shown). In nonsclerotic areas of the MTLE hippocampus (Fig. 4 *B* and *F*), the labeling for dystrophin was similar to that of non-MTLE hippocampi (Fig. 4 *A* and *E*).

Discussion

As pointed out in the Introduction, hippocampi removed from patients with MTLE show evidence of an impaired water and K^+ homeostasis (1–3). This finding has obvious pathophysiological implications, because any buildup of K^+ in the extracellular space would increase neuronal excitability and contribute to the epileptogenicity of the relevant hippocampal subfields (21, 22). A reduced capacity to handle excess K^+ is likely to be particularly deleterious once a seizure has been precipitated. In such a situation a loss of K^+ homeostasis could easily set up a vicious cycle leading to a prolongation and aggravation of the epileptic seizures (23).

According to experimental studies, the processes responsible for clearance of extracellular K^+ are compromised by removing perivascular AQP4 (6). The most parsimonious interpretation of the latter observation is that K^+ homeostasis depends on the integrity of the mechanisms that are responsible for water flux through the perivascular astrocyte membrane. Functionally, the perivascular membrane domain is coupled in series with the astrocyte membrane domain that faces the neuropil and is likely to be critically involved in mediating water and K^+ efflux from the extracellular space surrounding active synapses (6). Corroborating the functional coupling between water transport and K^+ clearance, it has long been known that synaptic activation causes not only an increase in extracellular K^+ but also a decrease in extracellular space volume (24, 25). The exact mechanism underlying the coupling between K^+ and water transport is not known, but it has been proposed that the two transport processes are coupled through the activation of glial bicarbonate uptake (26). What is clear is that K^+ is not fluxed through AQP4 itself because AQP4 shows no evidence of a K^+ conductance in experimental models (27).

Mice lacking perivascular AQP4 after the removal of the anchoring protein α-syntrophin do not show any reduction in the total level of AQP4 in brain tissue (28). Quantitative electron microscopical studies have provided an explanation of this finding: The loss of AQP4 from the perivascular membrane domain is compensated for by a sustained or increased complement of AQP4 in the remainder of the astrocyte plasma membrane (28). Our previous finding that the brains of these mice display obvious deficiencies in water and K^+ transport underlines the fact that astrocytes are functionally polarized and that their normal function depends on a correct compartmentation of their membrane molecules (6). Specifically, the mislocalization of AQP4 induced by α-syntrophin deletion interferes with homeostatic processes that require a serial coupling between endfeet and non-endfeet astrocyte plasma membranes (29).

The question addressed in the present study is whether epileptogenic hippocampi from patients with MTLE display a mislocalization of AQP4 similar to that found to be associated with increased seizure vulnerability in transgenic mice. Our data indeed show that MTLE tissue mimics tissue from $syn^{-/-}$ animals by displaying a reduced density of AQP4 in perivascular membranes. Moreover, as in $syn^{-/-}$ animals, the tissue level of AQP4 is not decreased but significantly increased.

The most pressing question is whether the changes observed are responsible for the observed loss of K^+ and water homeostasis in the epileptogenic hippocampus. Extrapolation from the transgenic studies discussed above suggests that such a mechanistic coupling may exist. For obvious reasons this question cannot be subjected to direct experimental testing. It should be pointed out, however, that the present study provides the first evidence that a perturbed expression pattern of a membrane molecule could underlie the deficiency in water and K^+ homeostasis in MTLE. Whether other molecular mechanisms also contribute will have to be resolved in future studies.

What could be the mechanism underlying the loss of perivascular AQP4 in MTLE hippocampi? That this loss reflects a general depletion of AQP4 is ruled out by the finding that the tissue level of AQP4 increases rather than decreases. It was logical to look for changes in the dystrophin complex, which is known to be responsible for anchoring of AQP4 at perivascular membranes (17). Specifically, we tested whether tissue deficient in perivascular AQP4 showed a concomitant loss of perivascular DP71, the major dystrophin isoform in the brain (20). The finding that AQP4 and DP71 were similarly mislocalized suggests that the loss of perivas-

cular AQP4 may be secondary to a dissolution of the dystrophin complex. One possible mechanism underlying a dissolution of this complex is activation of extracellular proteases (such as metalloproteinases) that could sever the coupling to the laminin of the perivascular basal lamina that normally keeps the dystrophin/aquaporin complex in place (30, 31). Activation of extracellular metalloproteinases is a common pathophysiological response e.g., to infections and stroke in the CNS (32).

Based on the present findings, we conclude that mislocalization of AQP4 might contribute to the epileptogenicity of the MTLE hippocampi. This conclusion does not necessarily mean that the changes observed are primary events in the pathogenesis of MTLE. It could well be that the mislocalization develops rather late in the sequence of events that culminates in epilepsy. However, the changes are not merely a trivial consequence of gliosis, given that they are not reproduced in gliosis associated with other pathological conditions (33). Irrespective of the temporal course of events, our findings have identified a molecular mechanism that could be targeted pharmacologically to reduce brain excitability.

We thank Ms. Ilona Kovacs for excellent technical assistance and Dr. Jung Kim for providing neuropathological diagnoses of brain tumors in the non-MTLE patients. This work was supported by National Institutes of Health Grants NS 048434 (to N.C.d.L.) and HL48268 and EY11239 (to P.A.) and by the European Cooperation in Scientific and Technological Research, the Norwegian Research Council, and the Nordic Council through the establishment of the Center for Water Imbalance-Related Disorders (to O.P.O.).

1. Bordey, A. & Sontheimer, H. (1998) *Epilepsy Res.* **32,** 286–303.
2. Hinterkeuser, S., Schroder, W., Hager, G., Seifert, G., Blumcke, I., Elger, C. E., Schramm, J. & Steinhauser, C. (2000) *Eur. J. Neurosci.* **12,** 2087–2096.
3. Schroder, W., Hinterkeuser, S., Seifert, G., Schramm, J., Jabs, R., Wilkin, G. P. & Steinhauser, C. (2000) *Epilepsia* **41,** Suppl. 6**,** S181–S184.
4. Hugg, J. W., Butterworth, E. J. & Kuzniecky, R. I. (1999) *Neurology* **53,** 173–176.
5. Lee, T., Eid, T., Mane, S., Kim, J. H., Spencer, D. D., Ottersen, O. P. & de Lanerolle, N. C. (2004) *Acta Neuropath. (Berlin)* **108,** 493–502.
6. Amiry-Moghaddam, M., Williamson, A., Palomba, M., Eid, T., de Lanerolle, N. C., Nagelhus, E. A., Adams, M. E., Froehner, S. C., Agre, P. & Ottersen, O. P. (2003) *Proc. Natl. Acad. Sci. USA* **100,** 13615–13620.
7. Niermann, H., Amiry-Moghaddam, M., Holthoff, K., Witte, O. W. & Ottersen, O. P. (2001) *J. Neurosci.* **21,** 3045–3051.
8. Holthoff, K. & Witte, O. W. (1996) *J. Neurosci.* **16,** 2740–2749.
9. Paulson, O. B. & Newman, E. A. (1987) *Science* **237,** 896–898.
10. Spencer, D. D. & Spencer, S. S. (1991) *Surgery for Epilepsy* (Blackwell, Boston).
11. de Lanerolle, N. C., Kim, J. H., Williamson, A., Spencer, S. S., Zaveri, H. P., Eid, T. & Spencer, D. D. (2003) *Epilepsia* **44,** 677–687.
12. Lidov, H. G. (1996) *Brain Pathol.* **6,** 63–77.
13. Hsu, S., Raine, L. & Fanger, H. (1981) *J. Histochem. Cytochem.* **29,** 577–580.
14. de Lanerolle, N. C., Brines, M. L., Kim, J. H., Williamson, A., Philips, M. F. & Spencer, D. D. (1992) in *Molecular Neurobiology of Epilepsy*, eds. Engel, J., Jr., Wasterlain, C., Cavalheiro, E. A., Heinemann, U. & Avanzini, G. (Elsevier, Amsterdam), pp. 205–220.
15. Hjelle, O. P., Chaudhry, F. A. & Ottersen, O. P. (1994) *Eur. J. Neurosci.* **6,** 794–804.
16. Laake, J. H., Takumi, Y., Eidet, J., Torgner, I. A., Roberg, B., Kvamme, E. & Ottersen, O. P. (1999) *Neuroscience* **88,** 1137–1151.
17. Neely, J. D., Amiry-Moghaddam, M., Ottersen, O. P., Froehner, S. C., Agre, P. & Adams, M. E. (2001) *Proc. Natl. Acad. Sci. USA* **98,** 14108–14113.
18. Vajda, Z., Pedersen, M., Fuchtbauer, E. M., Wertz, K., Stodkilde-Jorgensen, H., Sulyok, E., Doczi, T., Neely, J. D., Agre, P., Frokiaer, J. & Nielsen, S. (2002) *Proc. Natl. Acad. Sci. USA* **99,** 13131–13136.
19. Goodwin, F., Muntoni, F. & Dubowitz, V. (1997) *Eur. J. Paediatr. Neurol.* **1,** 115–119.
20. Chelly, J., Hamard, G., Koulakoff, A., Kaplan, J. C., Kahn, A. & Berwald-Netter, Y. (1990) *Nature* **344,** 64–65.
21. Traynelis, S. F. & Dingledine, R. (1988) *J. Neurophysiol.* **59,** 259–276.
22. Moody, W. J., Futamachi, K. J. & Prince, D. A. (1974) *Exp. Neurol.* **42,** 248–263.
23. McNamara, J. O. (1994) *J. Neurosci.* **14,** 3413–3425.
24. Lux, H. D., Heinemann, U. & Dietzel, I. (1986) *Adv. Neurol.* **44,** 619–639.
25. Dietzel, I., Heinemann, U., Hofmeier, G. & Lux, H. D. (1980) *Exp. Brain Res.* **40,** 423–432.
26. Nagelhus, E. A., Mathiisen, T. M. & Ottersen, O. P. (2004) *Neuroscience* **129,** 905–913.
27. Jung, J. S., Bhat, R. V., Preston, G. M., Guggino, W. B., Baraban, J. M. & Agre, P. (1994) *Proc. Natl. Acad. Sci. USA* **91,** 13052–13056.
28. Amiry-Moghaddam, M., Otsuka, T., Hurn, P. D., Traystman, R. J., Haug, F. M., Froehner, S. C., Adams, M. E., Neely, J. D., Agre, P., Ottersen, O. P. & Bhardwaj, A. (2003) *Proc. Natl. Acad. Sci. USA* **100,** 2106–2111.
29. Newman, E. A. (1986) *Ann. N.Y. Acad. Sci.* **481,** 273–286.
30. Guadagno, E. & Moukhles, H. (2004) *Glia* **47,** 138–149.
31. Amiry-Moghaddam, M. & Ottersen, O. P. (2003) *Nat. Rev. Neurosci.* **4,** 991–1001.
32. Fukuda, S., Fini, C. A., Mabuchi, T., Koziol, J. A., Eggleston, L. L., Jr., & del Zoppo, G. J. (2004) *Stroke* **35,** 998–1004.
33. Ingelsson, M., Fukumoto, H., Newell, K. L., Growdon, J. H., Hedley-Whyte, E. T., Frosch, M. P., Albert, M. S., Hyman, B. T. & Irizarry, M. C. (2004) *Neurology* **62,** 925–931.

Comments to Paper 3

This study suggest that loss of AQP4 may underlie deficient water and K+ homeostasis and contribute to the epileptogenicity of the MTLE hippocampi in humans. I performed the quantitative electron microscopy and made bar-plot in figure 3. In the postembedding experiments, gold particle densities were calculated per unit plasma membrane of randomly selected astrocyte profiles that were facing the perivascular compartment or the neuropil. Gold particles ere included in the counts as long as they touched the membrane, even if their center of gravity was projected outside the plasma membrane. In addition, the total number of gold particles per unit area was calculated from particle counts in five randomly selected areas (total $\approx 60\ \mu m^2$) of the neuropil from each patient. Analysis was performed on electron micrographs that were digitized and analyzed. Gold particle counts from six non-MTLE and six MTLE patients were used in the analysis.

Focus of the thesis

In this thesis I have chosen to focus on my work with glial glutamate transporters in the human epileptic hippocampus. I have contributed to other projects (see abstract 1, and Paper 2-3), but this is the project that I have been singly responsible for. I have done the research and writing on my own and feel that this project has given me the chance to be part of the whole research process; from idea to the finished product.

Introduction

Glutamate is the major excitatory neurotransmitter in the brain and is implicated in the pathogenesis of neurodegenerative diseases. High extracellular glutamate concentrations have been identified as a likely trigger of epileptic seizures in mesial temporal lobe epilepsy (MTLE), and these high glutamate levels could be the result of malfunctioning and /or down-regulation of glutamate transporters. The aim of the present study is to further explore the differences in glial glutamate transporter distribution in the hippocampus between non-sclerotic and sclerotic hippocampi in TLE patients. The two glial transporters (EAAT1 and EAAT2) were studied by immunoblotting, immunohistochemistry and electron microscopic methods.

Glutamate

The neurotransmitter glutamate mediates most of the excitatory (stimulating, activating) signals in the central nervous system. This does not only include signals involved in perception, cognition and movements, but also for cell survival, elimination, migration and differentiation, as well as for synapse formation and elimination (Fonnum, 1984; Ottersen and Storm-Mathisen, 1984; Collingridge and Lester, 1989; Headley and Grillner, 1990). Further, glutamate affects brain energy consumption, free radical formation, cell volume and water transport. Glutamate has a role in the signal transduction in the nervous systems of apparently all complex living organisms, including man, and is considered to be the major mediator of excitatory signals in the mammalian central nervous system. From this it follows that glutamate has to be present in the right concentrations in the right places for the right time. Both too much and too little

glutamate is harmful. This implies that glutamate is both essential and highly toxic at the same time.

Glutamate is one of the ordinary 20 amino acids which are used to make proteins and takes parts in typical metabolic functions like energy production and ammonia detoxification in addition to protein synthesis. Glutamate forwards its signaling function by binding to and thereby activating receptor on cells that are programmed to respond when exposed to glutamate. Several subtypes of glutamate receptors have been identified: NMDA, AMPA/kainate and metabotropic receptors (mGluR). Most of the nerve cells, and even glial cells, have glutamate receptors (Hösli and Hösli, 1993; Steinhauser and Gallo, 1996; Vernadakis, 1996; Conti et al., 1999; Shelton and McCarthy, 1999; Bergles et al., 2000).

The normal concentration of glutamate in the extracellular fluid is low, in the order of a few micromolar. In contrast, the glutamate concentration inside the cells is several thousand times higher. The highest glutamate concentrations are found in nerve terminals (Storm-Mathisen et al., 1992; Ottersen et al., 1996) and the concentration inside synaptic vesicles may be as high as 100 millimolar. Glutamate is therefore almost exclusively located inside the cells and the intracellular location of some 99.99 % of brain glutamate is the reason why the huge amount of the transmitter is not toxic for the brain (Danbolt, 2001). This is essential because glutamate receptors can only be activated by glutamate binding to them from the outside. Hence, glutamate is relatively inactive as long as it is intracellular.

There is uptake of glutamate into both glial cells and nerve terminals. Glutamate taken up by astroglial cells is converted to glutamine. Glutamine is inactive in the sense that it cannot activate glutamate receptors, and is released from the glial cells into to extracellular fluid. Nerve terminals take up glutamine and convert glutamine back to glutamate (Van den Berg and Garfinkel, 1971). This process is referred to as the glutamate-glutamine, and is important because it allows glutamate to be inactivated by glial cells and transported back to neurons in an inactive (non-toxic) form (Gjessing et al., 1972; Hamberger et al., 1983; Hamberger and Nyström, 1984).

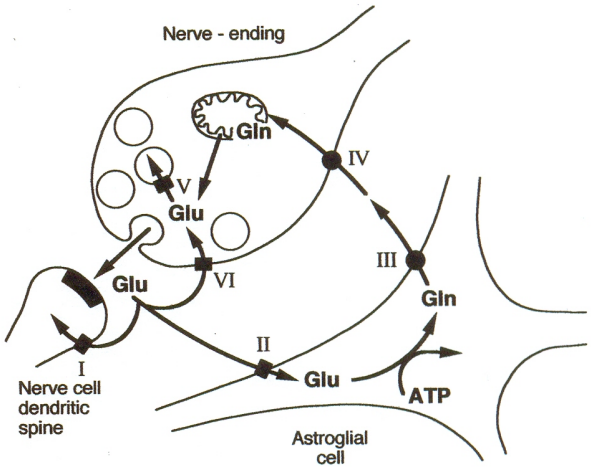

Fig. 1. The glutamate-glutamine cycle. This pathway represents a way of recycling transmitter glutamate. Glutamate released from a nerve terminal by exocytosis (which is ATP and Ca2 + dependent) is taken up by glutamate transporters present presynaptically (VI), postsynaptically (I) and extrasynaptically in astroglial cells (II). Astroglia detoxifies glutamate by converting it to glutamine in an ATP-dependent process. Glutamine is subsequently released from the glial cells by means of glutamine transporter (III) and taken up by neurons by means of other glutamine transporter (IV). Neurons convert glutamine back to glutamate. Synaptic vesicles are loaded with glutamate from cytosol by means of a vesicular glutamate transporter (V).

Glutamate transporters

Controlling the extracellular concentration of the neurotransmitter glutamate is crucial, but the mechanisms controlling glutamate are hard to study because glutamate is involved in so many different and interconnected processes. Evidence suggests that the control mechanisms of glutamate play key roles in the disease processes ultimately leading to the nerve cell damage, disabilities and suffering (for review see: Danbolt, 2001).

Synaptically released glutamate is normally taken up by astrocytes and, as mentioned, rapidly converted to the non-excitotoxic amino acid glutamine (Broman et al., 2000). The glutamate uptake system (for review see Danbolt, 2001) consists of five different transporter proteins and represents the only (significant) mechanism for removal of glutamate from the extracellular fluid in the brain. Five different glutamate (excitatory amino acid) transporters have been identified: EAAT1 (GLAST) (Storck et al., 1992; Tanaka, 1993), EAAT2 (GLT) (Pines et al., 1992), EAAT3 (EAAC1) (Kanai and Hediger, 1992), EAAT4 (Fairman et al., 1995), and EAAT5 (Arriza et al., 1997). EAAT1 and EAAT2 are expressed by astrocytes (Danbolt et al., 1992; Levy et al., 1993;

Chaudhry et al., 1995; Lehre et al., 1995), while EAAT3 is neuronal and probably predominantly postsynaptic (Rothstein et al., 1994). EAAT4 is a neuronal postsynaptic glutamate transporter in Purkinje cell spines (Yamada et al., 1996; Nagao et al., 1997; Dehnes et al., 1998) and EAAT5 is primarily expressed in the retina (Arriza et al., 1997). Although both neurons and glia contain glutamate transporters, it is generally accepted that more than 90 % of the forebrain glutamate uptake activity is mediated by EAAT2 (Danbolt et al., 1992; Haugeto et al., 1996; Tanaka et al., 1997; For review and discussion see Danbolt 2001).

The uptake process is driven by the electrochemical gradient across the cell membrane. Sodium is required for glutamate binding while potassium is required for net transport (Kanner and Sharon, 1978a; Roskoski, 1979; Barbour et al., 1988: Sarantis and Attwell, 1990: Szatkowski et al., 1991). The process is electrogenic (net positive charge moving in) and it is thereby stimulated by a negative membrane potential. The electrogenicity of the process implies that it generates a current, which can be measured with electrophysiological techniques. The transporters utilize the ion gradients of both sodium and potassium, and also H^+ (Billups et al., 1996; Zerangue and Kavanaught, 1996a; Levy et al., 1998b) as energy sources for the transport process. The EAAC and GLT glutamate transporters have the following stoichiometry: one glutamate is taken up together with three Na^+ and one H^+ in exchange for K^+ (Zerangue and Kavanaught, 1996a; Levy et al., 1998). In the only published study of the stoichiometry of GLAST (Klöckner et al., 1993) no conclusions were made concerning H+/OH-, but a stoichiometry of three Na^+, one glutamate and one K^+ was suggested.

Localization of the glial transporter subtypes

GLAST (EAATl) is expressed in astroglia throughout the central nervous system (Lehre et al., 1995; Chaudhry et al., 1995; Schmitt et al., 1997; Ullensvang et al., 1997). GLAST is present in all regions of the brain, with a relatively high level in the olfactory bulb, hippocampus, cerebral cortex and striatum, and lower concentrations in diencephalon and brainstem (Lehre et al., 1995). The GLAST protein concentration is particularly high in the Bergmann glia, in the molecular layer of cerebellum where it is the quantitatively dominating transporter (Lehre and Danbolt, 1998).

Fig. 2. Types of glutamate transporters at glutamatergic synapses. I. Glutamate transporters in glial cell plasma membranes, GLT and GLAST as well as some EAAC, remove glutamate from the extracellular fluid. This implies that they remove the glutamate that has already escaped from the synaptic cleft. GLT and EAAC pump one glutamate together with three Na^+ and one H^+ in to the cells in the exchange of one K^+. GLT is the most abundant of the so far molecularly identified glutamate transporters. GLAST is, however, the major transporter in some regions, including cerebellum (molecular layer) and retina. II. Glutamate transporters are also found post synaptically in the plasma membranes of dendritic spines. These transporters, which include EAAT4 (only in cerebellar Purkinje cells) and EAAC (throughout the brain), have a relatively high associated CI- channel activity. III. The glutamate transporter in glutamatergic nerve terminals has still not been molecularly identified and the exact stoichiometry of the transport cycle is not known. Because it is reversal of this transporter that is responsible for release of most of the glutamate during ischemia and because the ease by which it reverses depends on the stoichiometry, precise information of the stoichiometry is important to obtain. IV. Synaptic vesicles are loaded with glutamate from cytosol by means of a glutamate transporter located in the plasma membrane of synaptic vesicles. The energy driving this transporter comes from the action of a vesicular Mg^{2+}-dependent ATPase in the vesicular membrane pumping H^+ into the vesicles. V. Cystine, which is essential for the synthesis of glutathione (an important antioxidant), is transported into cells in exchange with glutamate.

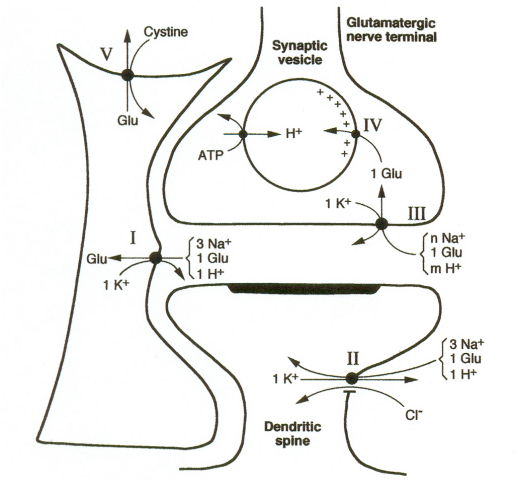

GLAST appears to be the quantitatively dominating glutamate transporter also in retina, where it is found in Müller cells and astrocytes (Derouiche and Rauen, 1995; Rauen et al., 1996; Lehre et al., 1997; Harada et al., 1998; Eliasof et al., 1998). There is a high degree of consistency between the localization of GLAST protein and GLAST mRNA as determined by immunoblotting, immunocytochemistry, and in situ hybridization.

GLT (EAAT2) has only been found in astroglia in the normal postnatal and adult central nervous system (Danbolt et al., 1992; Levy et al., 1993; Rothstein et al., 1994; Lehre et al., 1995; Chaudhry et al., 1995; Schmitt et al., 1996; Ullensvang et al., 1997), with the exception of retina (Rauen and Kanner, 1994; Rauen et al., 1996; Harada et al., 1998). It is the quantitatively dominating glutamate transporter in the forebrain (Lehre and Danbolt, 1998). It is found in the same astroglial cell membranes as GLAST (Lehre et al., 1995; Haugeto et al., 1996), and both GLT and GLAST are found at higher concentrations in the parts of the cell membranes facing neuropil (axons, nerve terminals, and small dendrites) than in membranes facing capillaries, pia, or large dendrites (Chaudhry et al., 1995). The regional distribution of GLT, however, is different from that of GLAST: The GLT concentration is highest in hippocampus, cerebral cortex and

striatum, with lower levels in diencephalon and mesencephalon, and only a low level in the olfactory bulb and cerebellum (Lehre et al., 1995). In spite of the exclusive astroglial localization, a clear GL T mRNA signal is also found in neurons in the adult brain, including pyramidal cells in hippocampus CA3 and pyramidal cells in the cerebral cortex (Torp et al., 1994; Schmitt et al., 1996; Torp et al., 1997; Berger and Hediger, 1998). Nevertheless, with these notable exceptions there is general consistency between the immunoblot data, immunocytochemistry, and in situ hybridization data for the regional distribution of GL T in the brain. Certain conditions apparently induce the expression of GLT protein in some neurons. This has been observed during prenatal development (Furuta et al., 1997a; Yamada et al., 1998; Northington et al., 1998), hypoxia (Martin et al., 1997), and in cell cultures (Mennerick et al., 1998; Brooks-Kaya1 et al., 1998).

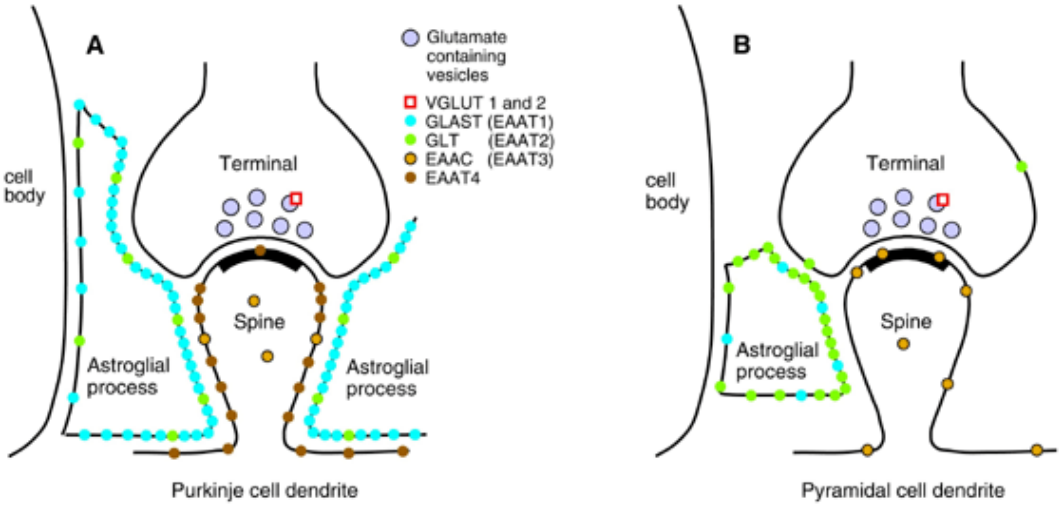

Fig. 3. Schematic representation of the detailed localization of glutamate transporters in the vicinity of the glutamatergic synapses. (A) Parallel fiber to Purkinje cell dendritic spine synapses in the cerebellar molecular layer. These synapses are completely surrounded by astroglial membranes containing GLAST and GLT at average densities of 4700 and 740 molecules per μm^2 membrane, respectively (Lehre and Danbolt, 1998). The concentrations are highest towards neuropil and lower towards other structures like cell bodies, vascular endothelium, large dendrites and pia mater. EAAT4 is concentrated in the glia-covered parts of the membranes of Purkinje cell dendrites, highest at the spines and thinner dendrites. EAAC is present in Purkinje cell membrane as well as cytoplasm (Conti et al., 1998; Kugler and Schmitt, 1999), but quantitative data and information on the precise subcellular distribution of this are currently unavailable. (B) Glutamatergic synapse in the hippocampus (e.g. Schaffer collateral to pyramidal cell synapse). The synapses are only contacted and not surrounded by astroglia. GLT and GLAST are present in the astroglial membranes at average densities of 8500 and 2300 molecules per μm^2 membrane, respectively, with highest concentration towards neuropil. Quantitative information is neither available on EAAC nor on the molecularly unidentified transporter in the glutamatergic nerve endings.

Temporal lobe epilepsy

Although there are many types of epilepsy of both genetic and acquired forms, temporal lobe epilepsy (TLE) is among the most common of the chronic seizure disorders (Hauser et al., 1975; Engel et al., 2001), and the one most intensely studied. Temporal lobe epilepsy (TLE) was defined in 1985 by the International League Against Epilepsy (ILAE) as a condition characterized by recurrent unprovoked seizures originating from the medial or lateral temporal lobe. Despite a wealth of descriptive data obtained from patient histories, imaging techniques, electroencephalographic recording, depth recording before and during surgery, and from histological study of surgical and autopsy tissues, the epileptogenic process remains poorly understood.

Patients with TLE exhibit neuronal loss and a network imbalance that presumably causes the clinical condition. It is believed that when the hippocampus is found to be asymmetrically atrophic on initial imaging (figure 4), the shrunken hippocampus is a likely source of epileptic seizures in TLE (Engel et al., 2001). The presence of a shrunken hippocampus is also a predictive indicator of the medically refractory state of the disease (Semah et al., 1998). Depth electrode recordings demonstrate hypersynchronous electrical activity in the hippocampus that is often associated with auras that can spread to cause clinical seizures (Engel et al., 2001).

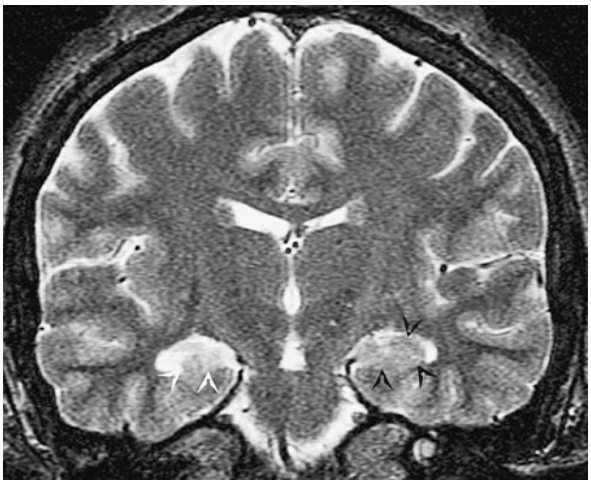

Figure 4
Mesial temporal lobe epilepsy (MTLE). The EEG suggested a right temporal lobe focus. Coronal high-resolution T2-weighted fast spin echo magnetic resonance image obtained through the body of the hippocampus demonstrates abnormal high signal intensity in the right hippocampus (white arrows; compare with the normal hippocampus on the left, black arrows) consistent with mesial temporal sclerosis (The McGraw-Hill Companies).

Since this form of epilepsy is often intractable (Chadwick, 1990) many of these patients undergo anteromedial temporal lobectomy with hippocampectomy for seizure control (Spencer et al., 1984). Approximately 70% of the resected hippocampi are characterized by pronounced neuronal loss and astroglial proliferation, especially in areas CA1, CA3 and the dentate hilus (de Lanerolle et al., 1994). The CA2 region is, on the other hand relatively spared. These neuropathological features are the hallmarks of hippocampal sclerosis, a distinctive characteristic of patients with mesial temporal lobe epilepsy (MTLE) (Sommer, 1880) (figure 5).

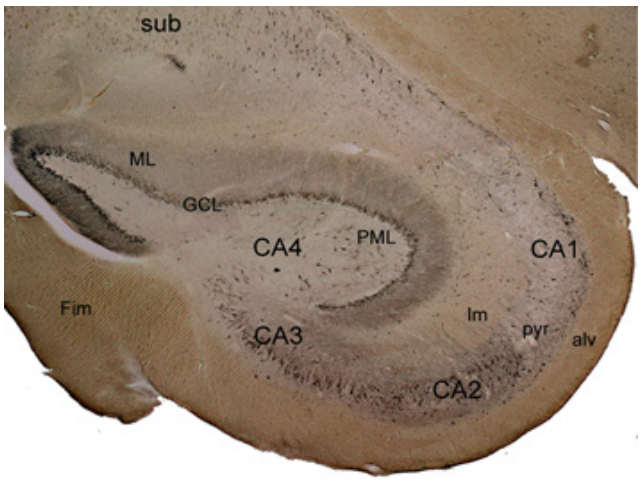

Figure 5
Photomicrographs of EAAT3 (EAAC)-like immunoreactivity in MTLE hippocampus. This low power view of the entire cross-section of a MTLE hippocampus shows the hallmarks of hippocampal sclerosis. The immunoreactivity is seen in the granule cell layer (GCL), molecular layer (ML), throughout the Ammon's horn (CA4, CA3, CA2, CA1) in the pyramidal cells and subiculum. The hippocampus is characterized by pronounced neuronal loss in areas CA1, CA3 and the dentate hilus (CA4), so there are less labeling in these regions. The CA2 region and subiculum are spared. Only neurons are labeled (granule cells and pyramidal cells). Pyr, stratum pyramidale; lm, lacunosum moleculare; alv, alveus; fim, fimbra. (LPB)

Hippocampal sclerosis is believed to play a key-role in the generation of seizures in MTLE (Mathern et al., 1997; de Lanerolle and Lee, 2005), but we do not really know precisely which cell populations, when lost, cause the network imbalance in TLE, or which cells generate the seizure discharges. Nor do we have an effective drug treatment that both points to the identity of the defective component and corrects the network imbalance to an extent that produces symptomatic improvement (Sloviter, 2005).

If the assumption that the hippocampus is a frequent source of seizures is correct, the observation that typical hippocampal sclerosis involves an extensive loss of dentate

hilar neurons and CA1 and CA3 pyramidal cells (Meldrum et al., 1992), logically focuses attention on surviving dentate granule cells (Tauck et al., 1985) and (Nadler et al., 2003) and subicular neurons (Cohen et al., 2002) as likely candidates for neurons that become the seizure generators. One perspective ("epileptogenic" mossy fiber sprouting) posits that a trauma- or seizure-induced loss of vulnerable dentate hilar neurons causes granule cells to redirect their axonal output to each other, resulting in a recurrent excitatory network (Tauck et al., 1985; Nadler et al., 2003). A second perspective ('inhibitory' mossy fiber sprouting) focuses on the postsynaptic targets of vulnerable hilar neurons, which include both granule cells and inhibitory neurons (Sloviter et al., 1992).

Glutamate transporters in epilepsy

Glutamate has long been thought to play a major role in the initiation and spread of seizure activity (Meldrum, 1994). Animal studies have shown that the administration to the hippocampus of glutamate or glutamate analogues triggers seizures, while co-injection of glutamate antagonists blocks the seizures (Olney JW., 1978; Olney *et al*, 1986).

In the sclerotic hippocampus changes in NMDA and AMPA receptors have been observed (de Lanerolle *et al.*, 1998; Musshoff *et al.*, 2000) and intracellular recordings from dentate granule cells in the human MTLE hippocampus have revealed a glutamate dependent hyperexcitability in these neurons (Williamson, 1995). Elevated levels of extracellular glutamate are observed in patients with various epilepsies (e.g. Janjua *et al.*, 1992; Ferrie *et al.*, 1999) and in vivo microdialysis studies of patients with MTLE have shown that the extracellular concentration of glutamate rises in sclerotic hippocampi just before a seizure and remains high for at least 15 minutes after the cessation of electrographic seizure activity (During and Spencer, 1993). These results indicate that there may be an impaired glutamate uptake capacity and thus possible malfunctioning and/or down-regulation of glutamate transporters (Meldrum *et al.*, 1999).

Reduced expression of glutamate transporters has been shown to cause or be associated with seizures in animal models. A relationship between glutamate transporter dysfunction and epilepsy was established by Tanaka and colleagues, who found that mutant mice lacking EAAT2 had increased extracellular glutamate levels and developed

spontaneous seizures (Tanaka *et al.*, 1997). Several studies on animal models have later linked glutamate transporter expression and epilepsy, but the results of these studies have been contradictory. The majority show a decrease in EAAT1 and EAAT2 mRNA and protein (e.g. Samuelsson *et al.*, 2000; Ueda *et al.*, 2001; Ingram *et al.*, 2001), and an increase in EAAT3 mRNA and protein (e.g. Ghijsen *et al.*, 1999; Ueda *et al.*, 2001; Crino *et al.*, 2002;Gorter *et al.*, 2002) in animal epileptic models. Some have on the other hand found an increase in EAAT1 mRNA (Nonaka *et al.*, 1998) and decreased EAAT3 mRNA (Akbar *et al.*, 1998), while Simantov et al. found a down-regulation of EAAT3 and a modest increase in expression of EAAT2 in restricted hippocampal regions (Simantov *et al.*, 1999).

There are a few studies reporting on glutamate transporters in human epileptic patients. Tessler and colleagues (Tessler *et al.*, 1999) found no change in the level of the mRNA or protein, by using *in situ* hybridization and Western blotting techniques respectively, for EAAT1 and EAAT2 in hippocampus and temporal cortex in temporal lobe epilepsy (TLE) patients compared to post mortem controls. In a study by Mathern and colleagues using immunocytochemical methods coupled with neuronal counting and image analysis, no changes in EAAT1 immunoreactivity (IR) were observed in hippocampi from TLE patients with hippocampal sclerosis compared with TLE patients without hippocampal sclerosis. Decreased EAAT2-IR was, in the same study, associated with neuronal loss. An increased EAAT3-IR was seen in areas where neurons were spared and a decrease in areas with neuronal loss (Mathern *et al.*, 1999). A recent study from Proper et al. showed a general decrease in EAAT1-IR and EAAT2-IR in the sclerotic hippocampus when compared with the non-sclerotic hippocampus or post mortem controls (Proper *et al.*, 2002). This decrease was accompanied by a decrease in mRNA levels for both transporters. An increase in neuronal EAAT3 protein levels in the resistant areas (CA2, granule cell layer and subiculum) in the hippocampal sclerosis group was also observed. Using immunohistochemistry and quantitative western blots Eid et al. found no difference in EAAT2 expression between non-MTLE and MTLE hippocampi (Eid *et al.*, 2004).

Materials and Methods

Patient Tissue

Patients with medically intractable temporal lobe epilepsy underwent phased presurgical evaluation at the Yale-New Haven Hospital, and appropriate candidates underwent anteromedial temporal lobectomy with hippocampectomy according to standard procedures (Spencer, 1984). Informed consent from each patient and institutional approval were obtained for the use of tissue in this project. The surgically resected hippocampi were classified into two groups: (1) mesial temporal lobe epilepsy (MTLE) and (2) non-MTLE as described by Eid et al. (Eid *et al.*, 2004). The MTLE hippocampus was characterized by pronounced neuronal loss (>50%) and extensive astroglial proliferation most pronounced in the hippocampal subfields CA1, CA3, and hilus (Kim, 2001). Reorganization of peptidergic neurons (neurons containing dynorphin, somatostatin, neuropeptide Y, and substance P) in the dentate gyrus was also seen (de Lanerolle *et al.*, 1994). On the other hand the non-MTLE hippocampi were recognized by a modest (<25%) neuronal loss throughout all hippocampal subfields, minimal astroglial proliferation, and no reorganization of peptidergic neurons in the dentate gyrus (Kim, 2001). They were obtained from patients with a mass lesion in the temporal lobe outside the hippocampus (MaTLE) and those with no clear etiology, described previously as paradoxical temporal lobe epilepsy –PTLE (de Lanerolle *et al.*, 1997).

Tissue preparation

Immediately after surgical resection two 5 mm thick slices were cut from the mid-portion of the hippocampus. One of the samples was immersed into a fixative containing 4 % formaldehyde and 15 % (v/v) of a saturated picric acid solution in 0.1 M phosphate buffer pH 7.4 (PB) for 1 hour, followed by immersion into 5 % acrolein in PB for 3 hours. Thereafter the tissue was rinsed and stored in PB at 4 °C. Fifty-micrometer coronal sections were cut on a Vibratome and processed for immunohistochemistry. The other sample was rapidly frozen on dry ice, stored at –80 °C, and later used for Western blots.

Hippocampal Nomenclature

The mesial temporal lobe consists of the hippocampus, parahippocampal gyrus, entorhinal cortex and amygdala. The hippocampus is commonly divided into the subiculum, Ammon's horn and dentate gyrus (Lorente de Nó, 1934). The Ammon's horn is further subdivided into the areas CA1, CA2 and CA3, while the dentate gyrus is subdivided into the hilus, granule cell layer and molecular layer (Amaral and Insauti, 1990).

Antisera and chemicals

Antibodies against GLAST and GLT were prepared by immunizing rabbits with synthetic peptides (A522-541 (PYQLIAQDNEPEKPVADSET) for GLAST and B563-573 (SVEEEPWKREK) for GLT) coupled to keyhole limpet hemocyanin with glutaraldehyde (Lehre *et al.*, 1995; Danbolt *et al.*, 1998). The corresponding anti-peptide antibodies were referred to as anti-A522 (rabbit 8D0161; Ab, 314) and anti-B563 (rabbit 1B0707; Ab, 355). These antibodies were tested and characterized by Western blotting (Fig. 1) and immunohistochemical methods, and cross-reacted with human GLAST and GLT, respectively. Unless otherwise specified, all other chemicals were obtained from Sigma-Aldrich (St. Louis, MO).

Immunohistochemistry and electron microscopy

Vibratome sections were incubated free-floating in anti-A522 (200 ng/ml) or anti-B563 (200 ng / ml) antibodies for 24 hours (RT), and then processed according to the avidin-biotin peroxidase method (Hsu *et al.*, 1981) using a commercially available kit (Vectastain Elite, Vector Laboratories, Burlingame, CA). Immunstained sections from each patient were mounted on slides, dehydrated and coverslipped for light microscopic analysis. Control sections incubated without the primary antibody or by replacing it with preimmune sera were not immunostained. Additional immunostained sections were processed for electron microscopy. After immunostaining as described above the sections were treated with 2 % osmium tetroxide in PB, stained *en bloc* with 2 % uranyl acetate in water, dehydrated and flat-embedded in Durcupan ACM. Sections were cut on an ultramicrotome, transferred to 500-mesh copper grids (Electron Microscopic Sciences,

Fort Washington, PA, USA), contrast-stained with lead citrate and examined in a transmission electron microscope (Jeol 1200 EX II) at 60 kV.

Western blot Analysis

Sections containing all hippocampal subregions were cut from frozen non-MTLE and MTLE specimens. The tissue was homogenized in 10 tissue volumes of SDS-solubilization buffer (1 % SDS with 150 mM NaCl and 10 mM PB pH 7.4, 5mM EDTA, and 1 mM PMSF) using a FastPrep® Instrument (Qbiogene, Inc., Ca) and the FastRNA® Pro Green Kit (Qbiogene, Inc., Ca). The homogenates were then incubated for 10 min and centrifuged (1000 x g, 10 min, 15°C). The supernatant solutions were stored at 80°C. The sample protein concentrations were determined using BCA Protein Assay Kit (Pierce, #23227) and the determination was preformed according to manufacturer's protocol. Bovine serum albumin (BSA) was used as standard and the spectrophotometer (GeneQuant pro, Amersham) was set to 562 nm. The extracts were then subjected to SDS-PAGE (Laemmli, 1970) and electroblotted (Towbin *et al.*, 1979) to nitrocellulose (100v, 1h). The Protein homogenates were diluted to a final protein concentration of 2 mg/ml in a loading buffer (10 % sucrose, 2 % (w/v) SDS (pure C12; Pierce 28312), 0.001 % (w/v) bromophenol blue, 62.5 mM Tris-HCl pH 6.8, and 5% 2-mercaptoethanol) and applied at different concentration on precast polyacrylamide gels (Criterion, 10% Tris-HCl, BIORAD). The gels were run (200V, 40 min) in Criterion^{TM} Cell Electrophoresis Module (BIORAD). Immunostaining of blots was done as previously described (Lehre *et al.*, 1995) at room temperature. The immunolabeling of the blots was preformed using Supersignal West Dura Extended Duration Substrate (Pierce, cat#34075). First the nitrocellulose blots were washed (1x1min) in TBST (150mM NaCl, 0.05% (v/v) Tween 20, 0.05% (w/v) sodium azide and 10mM Tris-HCl pH 8), blocked (30 min) in TBST with 4 % (w/v) skimmed milk powder (Nestle, Carnation, instant nonfat dry milk), washed (1 x 1 min) with TBST and incubated (overnight) with primary antibodies (200 ng / ml anti-A522 or 200 ng / ml anti-B563) in TBST with 1% BSA (Sigma A-7888) and 0.05% (w/v) sodium azide. The blots were washed (1x1 min and 3x5-10 min) in TBST without azide, incubated 1 hour with peroxidase conjugated (HRP-Conjugated) anti-rabbit IgG (Anti-rabbit IgG peroxidase conjugate, A-1949, Sigma, diluted 1:30000) in

TBST with 4 % dry milk (without azide) on a shaker. The blots were incubated for 5 min in Supersignal Substrate according to manufacturers protocol (Pierce, Prod # 34075), after they had been washed (1x1 min and 3x5-10 min) with TBST (without azide). The blots were read at a Kodak Image 2000 R and the intensity of the bands was calculated for GLAST and GLT using the Kodak software. A standard curve was made with increasing concentrations of homogenized hippocampal tissue from a non-MTLE patient to determine the linear range and 3, 6, and 12 µg protein were used from each patient. Both antibodies gave a strong single band consistent with the expected molecular mass of the glial glutamate transporters. Substitution of the primary antibodies with normal serum completely abolished the staining. The blots were assessed using a two-tailed Mann-Whitney U test (Statview Software, SAS Institute, NC).

Results

Clinical characteristics of patients

The demographic and clinical characteristics of the patients used in this study were similar to those in a larger sample reported previously (de Lanerolle *et al.*, 2003) (Table 1). Similar numbers of males and females were studied in the non-MTLE group, but the male:female relationship was 5:8 in the MTLE group. Eight of the 10 non-MTLE hippocampi were of the PTLE category (Table 1). The ages at surgery of the patients in the MTLE group were not significantly different (MTLE mean 37 years ± 4 SEM and non-MTLE 26 years ± 5 SEM, $p = 0.082$, Mann-Whitney U, two-tailed test). The duration of seizure history prior to surgery was also not significantly different (MTLE 27 ±2 and non-MTLE 19 ±4 years, $p = 0.0585$, Mann-Whitney U, two-tailed test). All MTLE patients had hippocampal sclerosis characterized by significant neuronal loss easily seen in area CA1 (neuronal counts not shown) compared to non-MTLE. There was no difference between groups as regards the antiepileptic drugs they were on at the time of surgery.

Table 1 – Patient Characteristics

Patient and classification	Gender	Age at Surgery (years)	Years since first seizure to surgery	Antiepileptic drugs at surgery	Pathology
Non-MTLE					
1	M	24	24	GBP, PHT, TPM	PTLE
2	F	34	21	CBZ	PTLE
3	F	5	5	PHT	Ischemic stroke
4	F	15	15	LEV, OXC	Cortical dysplasia
5	F	50	42	LEV	PTLE
6	M	5	4	CLP, ZNS, TPM,	PTLE
7	M	34	21	CBZ	PTLE
8	F	43	34	CBZX, LTG, TPM	PTLE
9	M	10	10	LTG, PHT	PTLE
10	M	44	18	CBZX, CZP	PTLE
MTLE					
11	M	37	31	CBZ	Hippocampal Sclerosis
12	F	40	38	GBP, LTG, LEV	Hippocampal Sclerosis
13	F	18	17	CBZX	Hippocampal Sclerosis
14	F	39	36	CBZ, PRM	Hippocampal Sclerosis
15	F	25	25	CBZX	Hippocampal Sclerosis
16	F	52	27	PHT, VPA	Hippocampal Sclerosis
17	F	51	40	CBZ	Hippocampal Sclerosis
18	F	52	33	CBZX	Hippocampal Sclerosis
19	M	47	10	LTG, LEV, CBZX	Hippocampal Sclerosis
20	M	17	17	CBZ, PHT	Hippocampal Sclerosis
21	M	53	50	CBZ, PRM	Hippocampal Sclerosis
22	M	28	26	CBZ, PHT	Hippocampal Sclerosis
23	F	26	26	CBZ	Hippocampal Sclerosis

Table 1: Characteristics of patients selected for the study. Abbreviations for anti-epileptic drugs: Carbamazepine/Tegretol (CBZ), Gabapentin/Neurontin (GBP), Phenytoin/Dilantin (PHT), Topiramate/Topamax (TPM), Lamotrigine/Lamictal (LTG), Levetiracetam/Keppra (LEV), CarbamzepineXR (CBZX), Primidone/Mysoline (PRM), Valproic Acid/Depakote (VPA), Clorazepate/Tranxene (CLP), Oxcarbazepine/Trileptal (OXC)

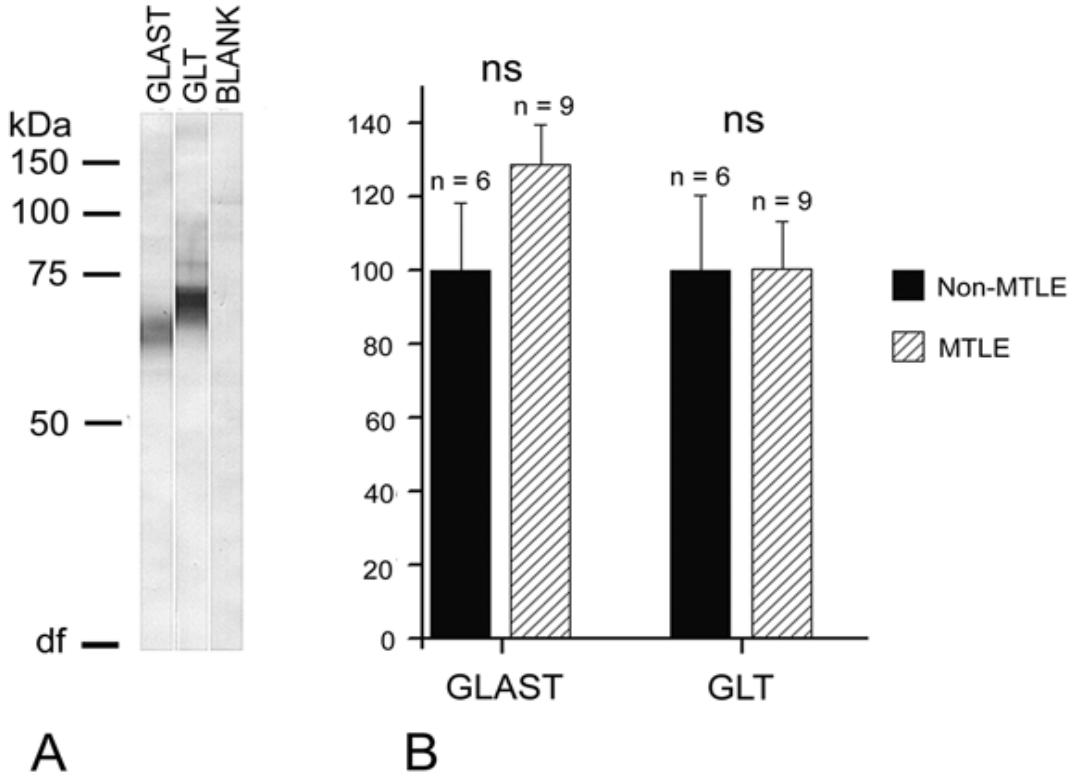

Figure 1
(A) Immunoblots of crude SDS extracts of human neocortex which were subjected to SDS-PAGE (~ 50 µg protein/lane) and reacted with EAAT1 (GLAST) (anti A522, 200 ng/ml, lane 1) and EAAT2 (GLT) (anti-B563, 200 ng/ml, lane 2) antibodies followed by alkaline phosphatase conjugated secondary antibodies. Both antibodies gave a band at the expected molecular weight for each of the glutamate transporters. Substitution of normal serum for the primary antibodies abolished staining (lane 3). Molecular mass markers (kDa) are shown alongside the blots. (B) A bar plot showing the relative amounts of EAAT1 (GLAST) and EAAT2 (GLT) (expressed as a percentage of the non-MTLE mean) quantified from Western blots for non-MTLE (n=6) and MTLE (n=9) hippocampi. No significant differences in GLAST (EAAT1) or GLT (EAAT2) were detected between patient groups.

Western blotting

Western blot studies of the transporters GLAST and GLT were carried out on whole hippocampal sections from non-MTLE and MTLE hippocampi to determine if there was an overall difference in the levels of these transporters between patient groups (figure 1). No statistically significant difference in the expression of GLAST and GLT between the non-MTLE and MTLE hippocampi was observed (GLAST: $p = 0.27$, GLT: $p = 0.95$, Mann-Whitney U, two-tailed test). However, since such a result may also be produced in the face of regional changes in distribution, which may be compensatory, an immunohistochemical study of the distribution of GLAST and GLT was undertaken.

Cellular localization of GLAST and GLT

In both non-MTLE and MTLE hippocampi both EAAT1 and EAAT2 were localized to astrocytes, being seen in both somata and processes of these cells (Fig. 2D, 2E, 3D, 3E). The staining was around neurons sometimes outlining them (Fig. 2C-F, 3C-F). No neuronal labeling was detected.

At the ultrastructural level localization of EAAT1 and EAAT2 the immunoreactivity was studied in area CA1 of the hippocampus in both MTLE and non-MTLE patients (Fig. 4). CA1 was chosen as sclerosis is most prominent in this area of the hippocampus. Only astrocytes were labeled, processes (Fig.4A) as well as somata. Labeled astrocytic processes could be seen to separate unlabeled pyramidal cell bodies and terminals (Fig. 4B, C, D). The immunostained somata contained the organelles typical for astrocytes. Though they were adjacent to strongly labeled astrocytic processes, the axon terminals themselves always appeared completely unlabeled (Fig. 4B, 4D). The labeling was entirely intracellular. In moderately reacted preparations the diaminobenzidine reaction product appeared concentrated close to the inner surface of the plasma membrane sparing the outer lamina (Fig 4E). The extracellular space always was free of reaction product. Fibrous astrocytes in white matter were also labeled (Fig. 4F). Strong immunolabeling for EAAT1 and EAAT2 was also seen at the endothelial-astrocyte interface with the labeling on the astrocyte membrane (Fig. 4E). Such labeling was seen in both non-MTLE and MTLE tissue.

Regional distribution of immunolabeling

The pattern of immunolabeling for EAAT1 and EAAT2 in non-MTLE differed somewhat from the MTLE group. Overall, there was weaker EAAT1 than EAAT2 immunostaining. EAAT1 and EAAT2 were expressed in all subfields of both non-MTLE and MTLE hippocampi. The immunoreactivity was homogeneous and seen in all sublayers, but a patchy pattern, was seen in some subareas such as CA1 for both EAAT1 and EAAT2 in non-MTLE and MTLE (Fig. 2A, 2B, 3A, 3B), as earlier described for GLT in post mortem material (Milton *et al.*, 1997; Proper *et al.*, 2002).

Dentate gyrus and hilus

The staining of both GLAST and GLT was mainly around pyramidal cells in hilus (not shown) and granule cells (figure 2c-d and 3c-d), outlining the neurons, and individual labeled astrocyte cell bodies were seen in the dentate molecular layer and polymorphic layer (not shown) in both non-MTLE (Fig. 2C, 3C) and MTLE (Fig. 2D, 3D). In MTLE compared to non-MTLE a loss of GLAST immunoreactivity was visually observed throughout these two regions (Fig. 2B). The immunoreactivity for GLT in the molecular layer of MTLE hippocampi, was less uniform than in the non-MTLE, with some regions of the molecular layer showing even stronger labeling (Fig. 3B).
Some areas of the hilus in MTLE also retained EAAT1 and EAAT2 immunoreactivity and individual labeled astrocytes were seen in these resistant areas (not shown). Blood vessels were outlined by the immunostaining for both EAAT1 and EAAT2 in all hippocampi (Fig 2C, 2D, 3C, and 3D).

Hippocampal area CA1

The CA1 region in the MTLE is clearly sclerotic and smaller in size then the non-MTLE hippocampus (Fig 2B, 3B). The staining of both EAAT1 and EAAT2 were mainly around pyramidal cells in non-MTLE (Fig 2E, 3E). The neurons were outlined, but not as clearly as around the granule cells. It was hard to distinguish individual astrocytes due to an intricate meshwork of labeling in stratum radiatum, stratum pyramidale, and stratum oriens in non-MTLE hippocampi (not shown). In the MTLE hippocampi, the intensity of immunoreactivity for both GLAST and GLT appeared reduced in astrocyte cell bodies compared the non-MTLE area CA1, and this was associated with the neuronal loss and astroglial proliferation in CA1 (Fig. 2F, 3F).

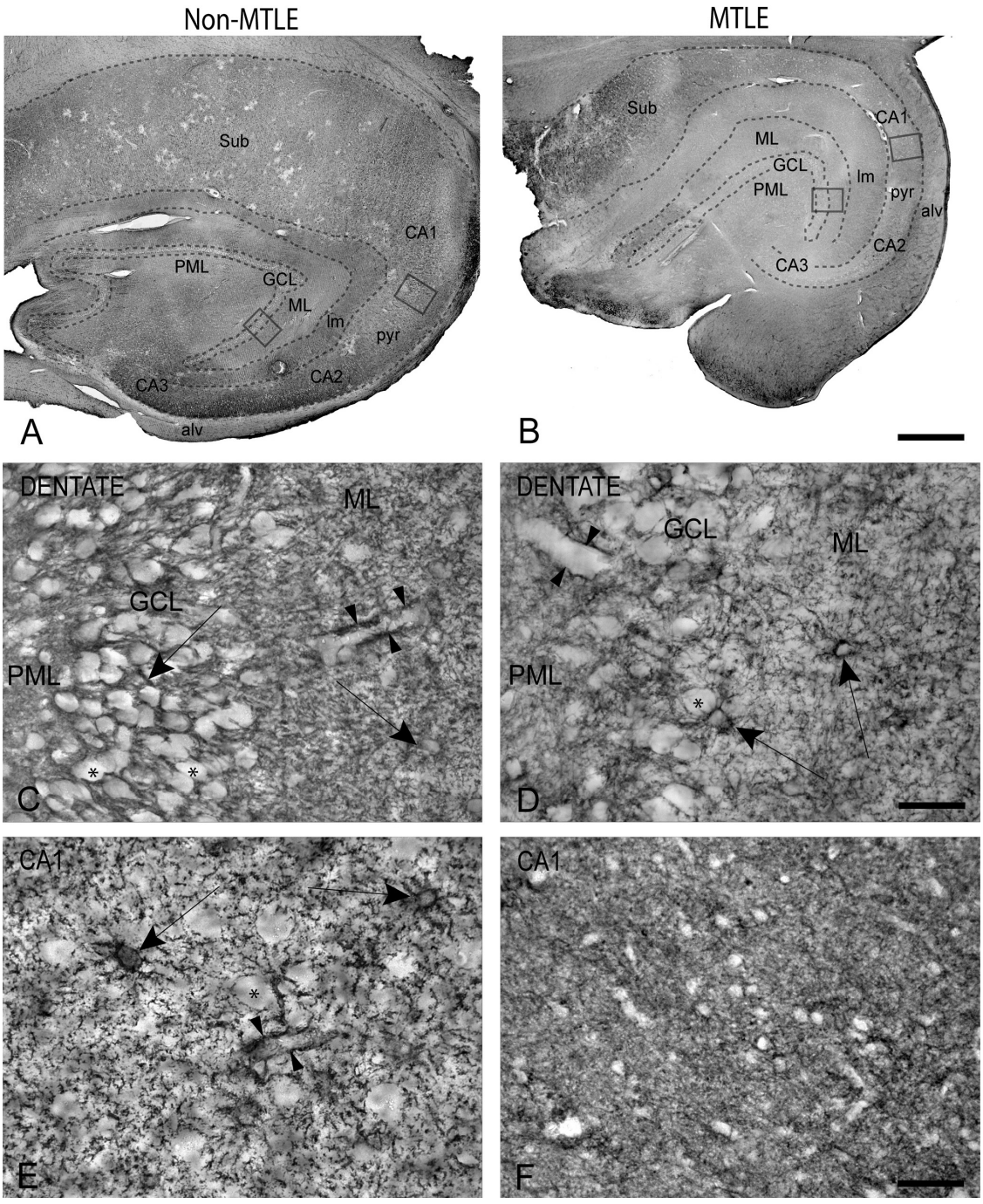
Non-MTLE
MTLE
Sub
CA1
PML
GCL
ML
lm
pyr
CA3
CA2
alv
A
B
DENTATE
ML
GCL
PML
C
DENTATE
GCL
ML
PML
D
CA1
E
CA1
F

Figure 2

Hippocampal area CA3, CA2 and subiculum

The immunostaining for both GLAST and GLT in these regions was also mainly in fine processes around pyramidal neurons, but individual astrocytes were seen in stratum radiatum, stratum oriens, and subiculum in both non-MTLE and MTLE (not shown). Blood vessels were outlined by the staining for both GLAST and GLT in both groups of hippocampi, specially pronounced in subiculum. In the MTLE hippocampi, weaker immunoreactivity for GLAST was apparent in CA3 and CA2, whereas for GLT no noticeable differences were observed. The subiculum did not show any loss of immunoreactivity for either transporter in either group of hippocampi (Fig. 2B, 3B). Individual astrocytes cell bodies labeled for GLAST and GLT were observed in MTLE. (not shown).

White matter and alveus

A few astrocytes labeled with GLAST and GLT were seen in alveus and the white matter in both non-MTLE and MTLE groups (not shown).

Figure 2 (page 16)
Photomicrographs of EAAT1 (GLAST)-like immunoreactivity in non-MTLE (PTLE) and MTLE hippocampi. (A) and (B) are low power views of the entire cross-section of a non-MTLE and MTLE hippocampus respectively. At this magnification the immunoreactivity appears as darkened areas in these figures. In the non-MTLE (A) the immunoreactivity is seen in the dentate ML, throughout the Ammon's horn (CA3, CA2, CA1) and subiculum. In Ammon's horn and the subiculum immunoreactivity appears patchy as previously reported (Milton et al. 1997). In the MTLE (B) the immunoreactivity appears weaker except in the subiculum. (C) and (D) are higher magnifications of the dentate gyrus showing parts the granule cell layer (GCL), polymorphic layer (PML) and molecular layer (ML) in non-MTLE and MTLE respectively showing fine immureactive processes around the granule cells (asterisks) and blood vessels (arrow heads) as well as astrocytic cell bodies (arrows). (E) and (F) are portions of area CA1 in non-MTLE and MTLE hippocampi showing immunoreacitve astrocytes (arrows) and processes, some of which surround blood vessels (arrow heads) (E), which are more diffusely stained in MTLE hippocampi (F). Bar = 100 μm in A and B, and 20 μm in C-F.

Figure 3 (page 18)
Photomicrographs of EAAT2 (GLT)-like immunoreactivity in non-MTLE (PTLE) and MTLE hippocampi. (A) and (B) are low power views of the entire cross-section of a non-MTLE and MTLE hippocampus respectively. At this magnification the immunoreactivity appears as darkened areas in these figures. In the non-MTLE (A) the immunoreactivity is seen more prominently in the dentate ML, and throughout the Ammon's horn (CA3, CA2, CA1) and subiculum. In the MTLE (B) the immunoreactivity appears weaker in the hilus, CA3, CA2 and CA1 but more intense in the subiculum. (C) and (D) are higher magnifications of the dentate gyrus showing parts the granule cell layer (GCL), polymorphic layer (PML) and molecular layer (ML) in non-MTLE and MTLE respectively, In both types of hippocampi fine immunoreactive processes surround the granule cells (asterisks) and blood vessels (arrow heads). Labeled astrocytic cell bodies (arrows) are also seen. (E) and (F) are portions of area CA1 showing immunoreacitve astrocytes (arrows) and processes which strongly surround blood vessels (arrow heads (E). The immunostaining is more diffuse in MTLE hippocampi (F). Bar = 100 μm in A and B, and 20 μm in C-F.

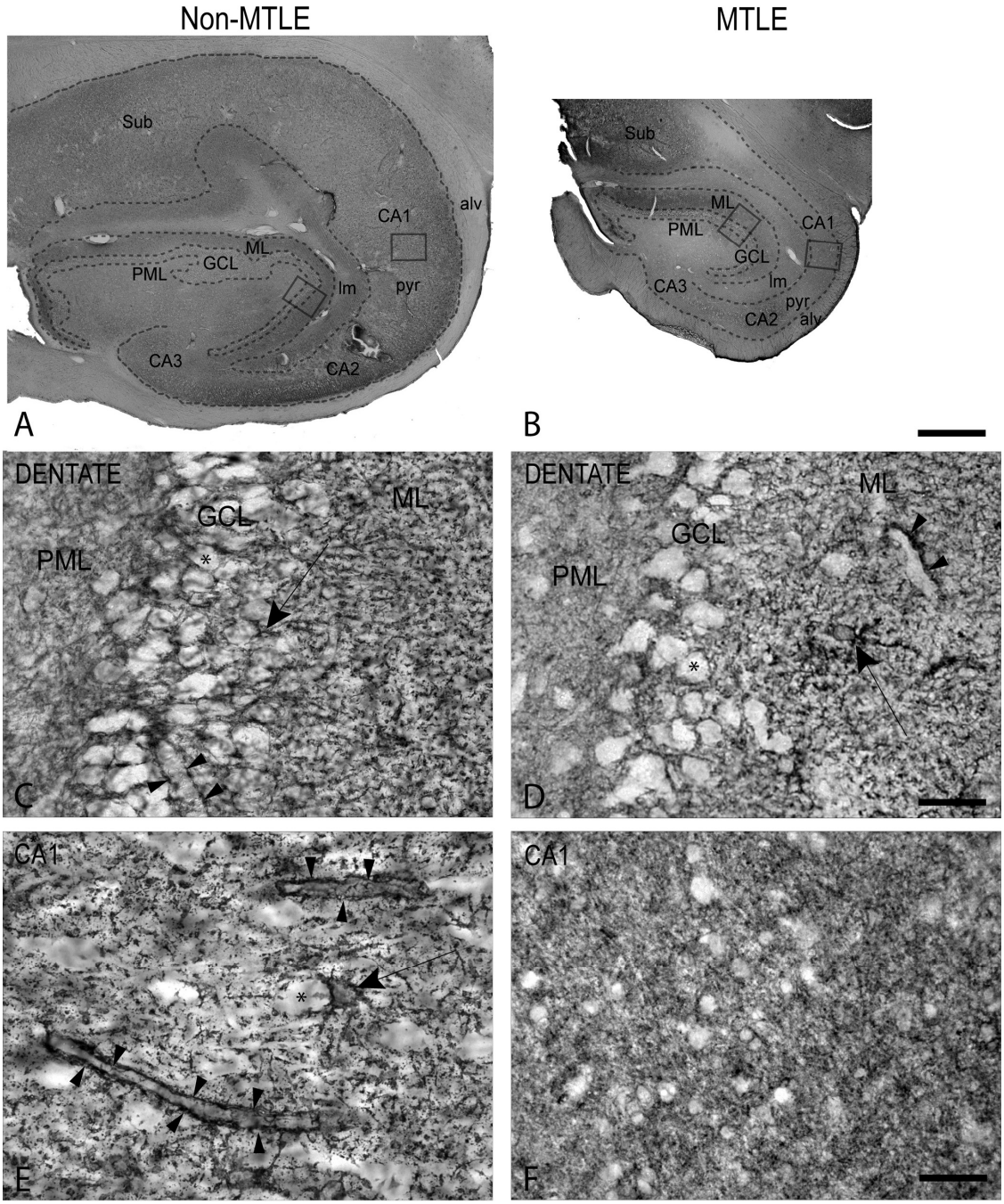
Non-MTLE
MTLE
Sub
alv
CA1
ML
PML
GCL
lm
pyr
CA3
CA2
A
B
DENTATE
GCL
ML
PML
C
D
CA1
E
F

Figure 3

Discussion

In this study we demonstrate both at the light microscopic and ultrastructural level that in the human hippocampus both EAAT1 and EAAT2 are found in astrocytes. No immunoreativity for these two proteins was observed in neurons. This finding is fully consistent with the localization of EAAT1 and EAAT2 in the rat hippocampus (Lehre *et al.*, 1995). In contrast, one study of the human hippocampus has reported EAAT2 mRNA in neurons as well. This has not been corroborated in the immunohistochemical studies by these same workers or by in situ hybridization or immunohistochemistry in any other studies (Lehre *et al.*, 1995; Mathern *et al.*, 1999; Tessler *et al.*, 1999).

Prior studies of the distribution of EAAT1 and EAAT2 in surgically removed human sclerotic hippocampi compared to non-sclerotic hippocampi have concluded that there is a reduction in EAAT2 (Proper *et al.*, 2002; Mathern *et al.*, 1999), a slight or no reduction in EAAT1 (Proper *et al.*, 2002; Mathern *et al.*, 1999) or essentially no-change in these transporters (Tessler *et al.*, 1999). The Western blot data presented in the current study suggests that there is no change in the levels of either EAAT1 or EAAT2, though immunohistochemical localization shows weaker staining in sclerotic regions like CA1 and the hilus compared to that in non-sclerotic hippocampi. This apparent discrepancy needs explanation.

Careful perusal of previous reports of reduced astrocyte glutamate transporters in the sclerotic hippocampus from patients with TLE, show that the actual evidence for such reduction is not compelling. Firstly the two studies that report a reduction of glutamate transporters, especially of EAAT2, do so on the basis of immunohistochemistry on fixed tissue (4% formaldehyde for 24 - 48 hr), whereas those that assessed transporter levels in parallel with immunoblots report no change (Tessler *et al.*, 1999 and this study). It is well known that fixatives reduce the antigenicity of molecules and do not provide a reliable basis for quantification (Danbolt, 2001).

Evaluation of immunohistochemical data also presents further issues for discussion. The data presented in Proper et al (Proper *et al.*, 2002) show that staining levels for EAAT1 quantified as a Relative Optical Density (ROD) measure show a reduction only for the dentate polymorphic layer (PML) in the sclerotic compared to the non-sclerotic

hippocampus, despite the demonstration in their immunohistochemical photomicrographs of reductions in staining in area CA1 and CA3/CA2 (see Fig. 2 Proper *et al.*, 2002). Mathern et al (Mathern *et al.*, 1999) also find no difference in EAAT1 immunostaining levels between sclerotic and non-sclerotic hippocampi. Thus in essence all previous studies concur with our data that there is no difference in EAAT1 levels. Comparisons that report reductions relative to autopsy controls must be interpreted with caution as postmortem changes are in general likely to results in changes of glutamate transporter levels due to autolytic effects (Beckstrøm *et al.*, 1999).

EAAT2 is the predominant glutamate transporter in the hippocampus (Danbolt et al., 1992; Haugeto et al., 1996; Tanaka et al., 1997; For review and discussion see Danbolt, 2001). Proper et al (Proper *et al.*, 2002) report on the basis of immunohistochemical staining that EAAT2 levels in areas CA1, CA2, CA3 and CA4 were reduced. Unlike for EAAT1, the immunohistochemical patterns and well as their ROD quantification are generally in concordance for EAAT2. However, in situ hybridization studies by the same group show no quantitative change in EAAT2 in areas CA1 and CA2 (Fig 6B Proper *et al.*, 2002) between sclerotic and non-sclerotic hippocampi. Even though the granule cell layer in the sclerotic hippocampus appears visually to have a considerable reduction in mRNA (see Fig. 5F and 5G Proper *et al.*, 2002) no quantitative difference is recorded (Fig. 6B Proper *et al.*, 2002). Thus the data for EAAT2 as presented in this study is equivocal at best. In a study using similar surgical tissue and patient types and fixed similar to that of the study by Proper et al., Mathern and co-workers found a reduction in EAAT2 only in the hilar area of sclerotic hippocampi (see Fig. 11 Mathern *et al.*, 1999).

No depletion of EAAT2 is shown for CA1 either in gray value measures or immunoreactivity pattern shown in the illustrated figures (Fig 6E and F Mathern *et al.*, 1999). Tessler et al (1999) also found no difference in EAAT2 levels between epileptic hippocampi and postmortem controls; this study did not distinguish between sclerotic and non-sclerotic hippocampi (Tessler *et al.*, 1999). On the basis of these studies it would be reasonable to conclude that there is no appreciable difference in EAAT2 levels as well between sclerotic and non-sclerotic hippocampi.

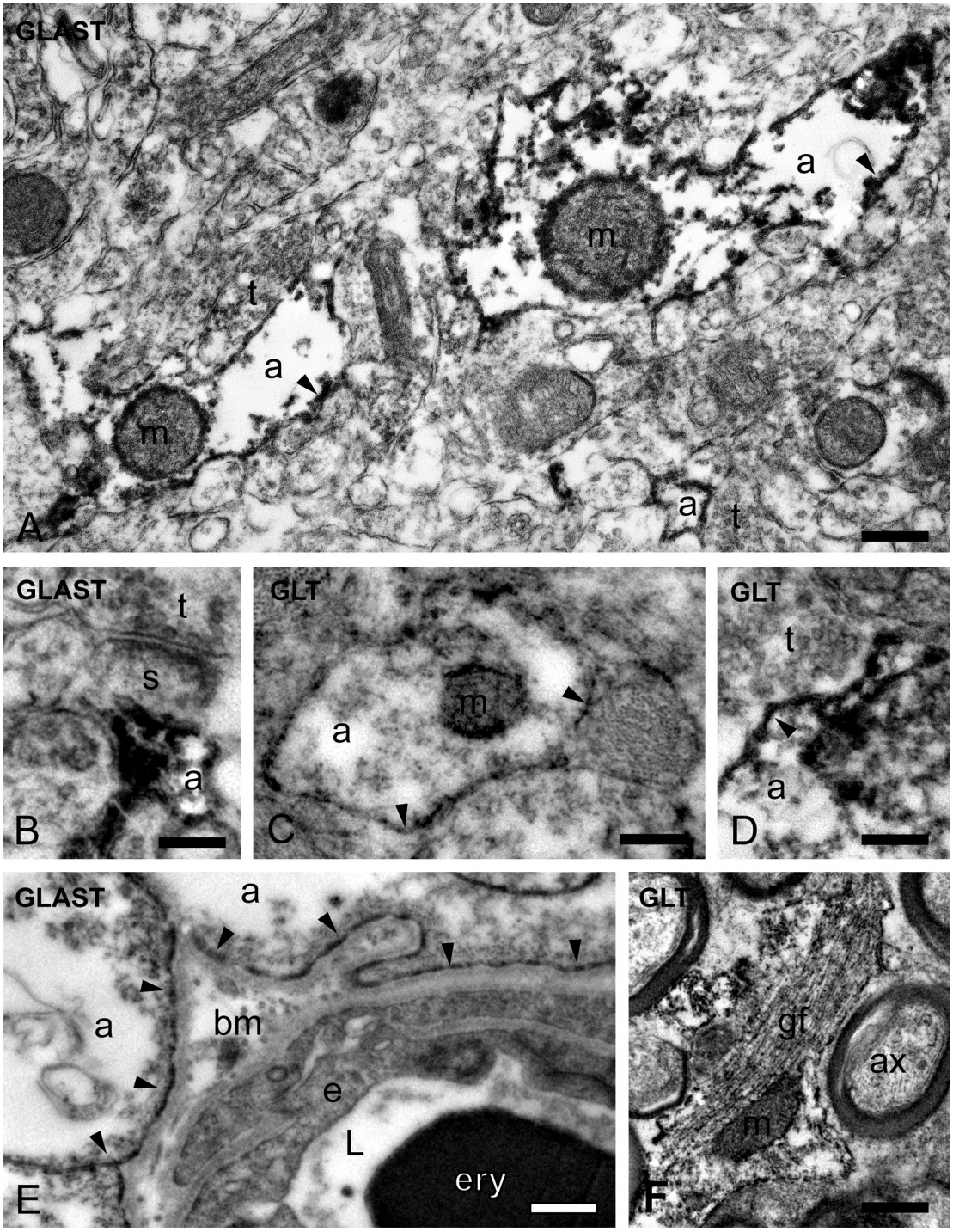

Figure 4
Electron micrographs of GLAST and GLT immunoreactivity in CA1 of hippocampus in non-MTLE and MTLE patients demonstrating labeling of astrocytic processes (a). Similar staining pattern was found for both antibodies in non-MTLE and MTLE. A, B, D, and E are from CA1 of a representative non-MTLE hippocampus, while C and F are from MTLE. Both A and C show a large stained astrocytic cell process, while B and D show small processes adjacent to axospinous synapses. Note that the staining appears concentrated close to the inside of glial membranes (arrowheads) and that axospinous synapses (s, t) are always unlabeled. Electron microscopy of the endothelial-astrocyte interface in CA1 of a representative

non-MTLE hippocampus (E) demonstrates strong labeling on the astrocyte membrane facing the endothelial cell. Labeling with GLAST and GLT gave the same perivascular astrocytic staining pattern in both non-MTLE and MTLE hippocampi. F shows GLAST labeling in fibrous astrocyte (gf) in alveus of CA1. Abbreviations: a, astrocytic cell process; ax, myelinated axon; bm, basal lamina; e, endothelial cell; ery, erythrocyte; gf, fibrils in astroglial process; m, mitochondrium; t, axon terminal; s, dendritic spine; L, capillary lumen;. Antibodies: Anti-A522 1 µg/ml (A, B, and G) and anti-B563 3 µg/ml (D and E). Scale bars: A, 800 nm, C, D, and F, 500 nm, B and D, 200 nm.

However, in the immunohistochemical localization studies shown in this paper as well as others, why does there appear to be reduced immunoreactivity in areas such as CA1 and the hilus in sclerotic hippocampi, while immunoblot analyses show no difference? There are some possible explanations for this. The first may be that in areas such as CA1 where there is an apparent reduction in staining intensity, this may only be reflective of a redistribution of the transporter throughout the astrocytic processes in the sclerotic hippocampi rather than a true reduction in level. Evidence in support of this is that ultrastructural localization studies show EAAT2 immunoreactivity throughout astrocytic process despite apparent loss suggestive in light microscopy (present study). Likewise confocal immunohistochmical studies reveal EAAT2 immunoreactivity throughout astrocyte processes, even though staining in somata is reduced (Eid *et al.*, 2004). Such redistribution of EAAT2 transporter in epileptic surgical tissue has previously been suggested by others (Tessler *et al.*, 1999). An alternative possibility is that there may be compensatory changes in the expression of transporters in its different regions. Such a possibility is recognized in suggestive upregulation of transporter in subiculum and molecular layer (our study) with the apparent down regulation in other areas.

Previous studies of the distribution of glutamate transporters (Proper *et al.*, 2002; Mathern *et al.*, 1999) have postulated a reduction in glutamate transporters to explain the striking physiological observation that there are elevated levels of extracellular glutamate in the epileptogenic (sclerotic) hippocampus (During and Spencer, 1993; Cavus *et al.*, 2005) during seizures. Our own findings, like those of Tessler et al. (Tessler *et al.*, 1999) find little support for a role of glutamate transporters in this phenomenon.

On the contrary, there are several plausible alternative explanations for such elevated extracellular glutamate levels. One possibility may be related to the down regulation of glutamine synthetase in astrocytes in sclerotic areas of the hippocampus,

which has been argued as a possible cause (Eid *et al.*, 2004). Alternatively, or in addition, increased levels of inflammatory factors such as interleukin 1β and chemokines in sclerotic hippocampi are now recognized as able to cause the release of glutamate from astrocytes, which may be the source of the increased glutamate (data reviewed in de Lanerolle and Lee, 2005). These mechanisms may be more pertinent to elevated extracellular glutamate in sclerotic seizure foci than alterations in transporter levels or their function and certainly merit further study.

Results other papers

Results Abstract 1

Rats were stressed by immobilization for 7 hours and the transporter immunoreactivities were then determined in hippocampus, hupotahlamus and frontal cortex by quantitative immunoblotting 3, 7, 15, and 24 hours after termination of immobilization stress. We found the GAT1 immunoreactivity was significantly increased in hippocampus by a maximum of 57 ± 18 % (mean ± SEM) after 3 hours. This effect was still detectable after 24 hours. There were no significantly effects on the immunoreactivities of the other transporters, with a possible exception of GAT3 in the hypothalamus. Injection (i.p) of corticosterone-21-acetate (10 mg / kg) did not result in a similar up-regulation of GAT1. In conclusion, our data show that immobilization stress up-regulates GAT1 in the hippocampus, but we now think that newer methods (ECL) and accurate measurements (pipetting robot) might show changes in other transporters. We are planning to repeat this experiment.

Results Paper 2

Animals were immunized with synthetic peptides corresponding to different parts of the EAAT3-sequence. Because the antibodies were affinity purified, all antibodies used in this paper recognized the peptides used to generate them. In order to produce good anti-peptide antibodies, we show that the key factor is to select the right parts of the sequence for peptide synthesis.

The anti-C479, anti-C491, and the anti-C510 antibodies labeled the same broad fuzzy band around 70 kDa on immunoblotting, while other antibodies generated by immunization and purification (C1-13, C1-18, C39-58, C81-94 and C468-482) did not recognize EAAT3. In addition to the 70 kDa band the anti-C479 antibodies labeled a broad band just below the 66 kDa marker. The identity of the lower anti-C479 positive band was uncovered by testing the antibodies for reactivity toward proteins present in high concentrations in axons. A strong and specific reaction to tubulin was observed, but no to any of the other proteins tested, including another abundant cytoskeletal protein,

actin. This result indicated that the anti-C479 antibodies recognized both tubulin and EAAT3 despite of being affinity purified against the corresponding peptide. The antibodies to EAAT3 and to tubulin were separated by absorption of crude serum from the original immunized rabbit on columns containing glutaraldehyde-treated bovine serum protein, KLH (carrier protein to which the peptide was conjugate during immunization), tubulin, and the C479-498 peptide. The antibodies that were eluted from the last column with the C479-498 peptide did not recognize the lover band labeled by the non-absorbed anti-C497 antibodies. Absorption against tubulin removed the antibodies labeling labeling the lower band.

To verify that the band expected to represent EAAT3 really did so, the antibodies were tested by immunoblotting with protein extracts from wild-type and EAAT3 knock-out mice. The band detected in the wild type were exactly as would be observed in rat tissue, while neither the absorbed anti-C479 nor anti-C491 antibodies showed any bands on the blots from the EAAT3 knock-out mice.

The results illustrate that immunization with an antigen may lead to the generation or antibodies that recognize not only the antigen, but also molecules that appear completely unrelated to the antigen. The conclusions are that not all antibodies to synthetic peptides recognize the native protein and that the specificity of an antibody is hard to predict. Unwanted reactivity can be highly specific and thereby hard to recognize. In this case, cross-reactivity was discovered because antibodies to different epitopes gave different epitopes gave different labeling patterns.

Results Paper 3

Hippocampi removed from patients with mesial temporal lobe epilepsy show evidence of impaired water and K+ homeostasis. *According to* experimental studies, the processes responsible for clearance of extracelluar K+ are compromised by removing perivascular AP4. This suggests that an efficient clearance of K+ depends on a concomitant water flux through astrocyte membranes. Therefore, we hypothesized that loss of perivascular AQP4 might be involved in the pathogenesis of MTLE. Whereas Western blot analysis showed an overall increase in AQP4 levels in MTLE compared

with non-MTLE hippocampi, quantitative ImmunoGold electron microscopy revealed that the density of AQP4 along the perivascular membrane domain of astrocytes was reduced by 44% in area CA1 of MTLE vs. non-MTLE hippocampi. There was no difference in the density of AQP4 on the astrocyte membrane facing the neuropil. Because anchoring of AQP4 to the perivascular astrocyte endfoot membrane depends on the dystrophin complex, the localization of the 71 kDa brain-specific isoform of dystrophin was assessed by immunohistochemistry. In non-MTLE hippocampus, dystrophin was preferentially localized near blood vessels. However, in the MTLE hippocampus, the perivascular dystrophin was absent in sclerotic areas, suggesting that the loss of perivascular AQP4 is secondary to a disruption of the dystrophin complex.

Based on the present findings, we conclude that mislocalization of AQP4 might contribute to the epileptogenicity of the MTLE hippocampi. This conclusion does not necessarily mean that the changes observed are primary events in the pathogenesis of MTLE. It could well be that the mislocalization develops late in the sequence of events that culminates in epilepsy. Irrespective of the temporal course of events, our findings have identified a molecular mechanism that could be targeted pharmacologically to reduce brain excitability.

References

Akbar, M.T., Rattray, M., Williams, R.J., Chong, N.W.S., and Meldrum, B.S., 1998. Reduction of GABA and glutamate transporter messenger RNAs in the severe-seizure genetically epilepsy-prone rat, Neuroscience, 85, pp. 1235-1251.

Amaral, D. G. and Insauti, R., 1990. Hippocampal Formation, In: The Human Nervous System, Ed: G. Paxinos, Academic Press, New York, pp. 711-756.

Arriza, J.L., Eliasof, S., Kavanaugh, M.P., and Amara, S.G., 1997. Excitatory amino acid transporter 5, a retinal glutamate transporter coupled to a chloride conductance, Proceedings of the National Academy of Sciences of the United States of America, 94, pp. 4155-4160.

Barbour, B., Brew, H., and Attwell, D., 1988. Electrogenic glutamate uptake in glial cells is activated by intracellular potassium, Nature, Sep 29, 335(6189), pp. 433-435.

Beckstrøm, H., Julsrud, L., Haugeto, Ø., Dewar, D., Graham, D.I., Lehre, K.P., Storm-Mathisen, J., and Danbolt, N.C., 1999. Interindividual differences in the levels of the glutamate transporters GLAST and GLT, but no clear correlation with Alzheimer's disease, Journal of Neuroscience Research, 55, pp. 218-229.

Berger, U.V., Hediger, M.A., 1998. Comparative analysis of glutamate transporter expression in rat brain using differential double in situ hybridization, Anatomy and Embryology (Berl), 198, pp. 13-30.

Bergles, D.E., Roberts, J.D., Somogyi, P., and Jahr, C.E., 2000. Glutamatergic synapses on oligodendrocyte precursor cells in the hippocampus, Journal of Neurochemistry,405, (6783), pp. 187-191.

Billups, B., Rossi, D., and Attwell, D. 1996. Anion conductance behavior of the glutamate uptake carrier in salamander retinal glial cells. Journal of Neuroscience, Nov 1, 16(21), pp. 6722-6731.

Broman, J., Hassel, B., Rinvik, E., Ottersen, O.P., 2000. Biochemistry and anatomy of transmitter glutamate. In: Ottersen, O.P., Storm-Mathisen, J., eds. Glutamate, Elsevier Science, Amsterdam, pp. 1-44.

Brooks-Kayal, A.R., Munir, M., Jin, H., Robinson, M.B., 1998. The glutamate transporter, GLT-1, is expressed in cultured hippocampal neurons. Neurochemistry International, 33, pp. 95-100.

Cavus, I., Kasoff, W.S., Cassaday, M.P., Jacob, R., Gueorguieva, R., Sherwin, R.S., Krystal, J.H., Spencer, D.D., and Abi-Saab, W.M., 2005. Extracellular metabolites in the cortex and hippocampus of epileptic patients, Annals of neurology, 57, pp. 226-35.

Chadwick, D., 1990. The epidemiology of drug resistant epilepsy and adverse effects of antiepileptic drugs, Acta Neurochirurgica Supplement (Wien), 50, pp. 32-37.

Chaudhry, F.A., Lehre, K.P., van Lookeren Campagne, M., Ottersen, O.P., Danbolt, N.C., and Storm-Mathisen, J., 1995. Glutamate transporters in glial plasma membranes: highly differentiated localizations revealed by quantitative ultrastructural immunocytochemistry, Neuron, 15, pp. 711-720.

Cohen, I., Navarro, V., Clemenceau, S., Baulac, M. and Miles, R., 2002. On the origin of interictal activity in human temporal lobe epilepsy in vitro, Science, 298, pp. 1418–1421.

Collingridge, G.L. and Lester, R.A., 1989. Excitatory amino acid receptors in the vertebrate central nervous system, Pharmacol Rev, Jun, 41(2), pp.143-210.

Conti, F., DeBiasi, S., Minelli, A., Rothstein, J. D., and Melone, M., 1998. EAAC1, a high-affinity glutamate tranporter, is localized to astrocytes and gabaergic neurons besides pyramidal cells in the rat cerebral cortex, Cerebral Cortex, Mar, 8(2), pp.108-116.

Conti, F. and Weinberg, R. J., 1999. Shaping excitation at glutamatergic synapses, Trends in Neurosciences, 22, (10), pp. 451-458.

Crino, P.B., Jin, H., Shumate, M.D., Robinson, M.B., Coulter, D.A., and Brookskayal, A.R., 2002. Increased expression of the neuronal glutamate transporter (EAAT3/EAAC1) in hippocampal and neocortical epilepsy, Epilepsia, 43, pp. 211-218.

Danbolt, N.C., Storm-Mathisen, J., and Kanner, B.I., 1992. An [$Na^+ + K^+$] coupled L-glutamate transporter purified from rat brain is located in glial cell processes, Neuroscience, 51, pp. 295-310.

Danbolt, N.C., Lehre, K.P., Dehnes, Y., Chaudhry, F.A., and Levy, L.M., 1998. Localization of transporters using transporter-specific antibodies, Methods in Enzymology, 296, pp. 388-407.

Danbolt, N.C., 2001. Glutamate uptake, Progress in Neurobiology, 65, pp. 1-105.

de Lanerolle, N.C., Eid, T., von Campe, G., Kovacs, I., Spencer, D.D., and Brines, M., 1998. Glutamate receptor subunits GluR1 and GluR2/3 distribution shows reorganization in the human epileptogenic hippocampus, European Journal of Neuroscience, 10, pp. 1687-1703.

de Lanerolle, N.C., Kim, J.H., Williamson, A., Spencer, S.S., Zaveri, H.P., Eid, T., and Spencer, D.D., 2003. A retrospective analysis of hippocampal pathology in human temporal lobe epilepsy: evidence for distinctive patient subcategories, Epilepsia, 44, pp. 677-687.

de Lanerolle, N.C. and Lee, T.S., 2005. New facets of the neuropathology and molecular profile of human temporal lobe epilepsy, Epilepsy and Behavior, 7, pp. 190-203.

de Lanerolle, N.C., Williamson, A., Meredith, C., Kim, J.H., Tabuteau, H., Spencer, D.D., and Brines, M.L., 1997. Dynorphin and the kappa 1 ligand, Epilepsy Research, 28, pp. 189-205.

de Lanerolle, N.C., Kim, J.H., Brines, M.L., 1994. Cellular and molecular alterations in partial epilepsy, Clinical Neuroscience, 2, pp. 64-81.

Dehnes, Y., Chaudhry, F.A., Ullensvang, K., Lehre, K.P., Storm-Mathisen, J., Danbolt, N.C., 1998. The glutamate transporter EAAT4 in rat cerebellar Purkinje cells: a glutamate-gated chloride channel concentrated near the synapse in parts of the dendritic membrane facing astroglia, Journal of Neuroscience, 18, pp. 3606-3619.

Derouiche, A., Rauen, T., 1995. Coincidence of L-glutamate/L-aspartate transporter (GLAST) and glutamine synthetase (GS) immunoreactions in retinal glia: evidence for coupling of GLAST and GS in transmitter clearance. Journal of Neuroscience Research, 42, pp. 131-143.

During, M.J. and Spencer, D.D., 1993. Extracellular hippocampal glutamate and spontaneous seizure in the conscious human brain, Lancet, 341, pp. 1607-1610.

Eid, T., Thomas, M.J., Spencer, D.D., Runden-Pran, E., Lai, J.C., Malthankar, G.V., Kim, J.H., Danbolt, N.C., Ottersen, O.P., de Lanerolle, N.C., 2004. Loss of glutamine synthetase in the human epileptogenic hippocampus: possible mechanism for raised extracellular glutamate in mesial temporal lobe epilepsy, Lancet, 363(9402), pp. 28-37.

Eliasof, S., Arriza, J.L., Leighton, B.H., Kavanaugh, M.P., Amara, S.G., 1998. Excitatory amino acid transporters of the salamander retina: identification, localization, and function, Journal of Neuroscience, 18, pp. 698-712.

Engel, J.Jr., 2001. Mesial temporal lobe epilepsy: what have we learned?, Neuroscientist, 7, pp. 340–352.

Fairman, W.A., Vandenberg, R.J., Arriza, J.L., Kavanaugh, M.P., and Amara, S.G., 1995. An excitatory amino-acid transporter with properties of a ligand-gated chloride channel, Nature, 375, pp. 599-603.

Ferrie, C.D., Bird, S., Tilling, K., Maisey, M.N., Chapman, A.G., and Robinson, R.O., 1999. Plasma amino acids in childhood epileptic encephalopathies, Epilepsy Research, 34, pp. 221-229.

Fonnum, F., 1984, Glutamate: a neurotransmitter in mammalian brain, Journal of Neurochemistry, 42, pp. 1-11.

Furuta, A., Rothstein, I.D., Martin, L.J., 1997a. Glutamate transporter protein subtypes are expressed differentially during rat CNS development, Journal of Neuroscience, 17, pp. 8363-8375.

Ghijsen, W.E.J.M., Belo, A.I.D.A., Zuiderwijk, M., and da Silva, F.H.L., 1999. Compensatory change in EAAC1 glutamate transporter in rat hippocampus CA1 region during kindling epileptogenesis, Neuroscience Letters, 276, pp. 157-160.

Gjessing, J., Renal failure in acute pancreatitis, 1972. British Medical Journal, Nov 11, 4(836), pp. 359-60.

Gorter, J.A., Van Vliet, E.A., Proper, E.A., De Graan, P.N.E., Ghijsen, W.E.J.M., Da Silva, F.H.L., and Aronica, E., 2002. Glutamate transporters alterations in the

reorganizing dentate gyrus are associated with progressive seizure activity in chronic epileptic rats, Journal of Comparative Neurology, 442, pp. 365-377.

Hamberger, A., Berthold, C-H., Karlsson, B., Lehmann, A. and Nyström, B., 1983. Extracellular GABA, glutamate and glutamine in vivo - perfusion-dialysis of rabbit hippocampus, Neurology and Neurobiology, 7, pp. 473-492.

Hamberger, A. and Nyström, B., 1984. Extra- and intracellular amino acids in the hippocampus during development of hepatic encephalopathy, Neurochemical Research; 9, (9): 1181-1192.

Harada, T., Harada, C., Watanabe, M., Inoue, Y., Sakagawa, T., Nakayama, N., Sasaki, S., Okuyama, S., Watase, K., Wada, K., Tanaka, K., 1998. Functions of the two glutamate transporters GLAST and GLT-1 in the retina, Proc Natl Acad Sei, U S A, 95, pp. 4663-4666.

Haugeto, Ø., Ullensvang, K., Levy, L.M., Chaudhry, F.A., Honoré, T., Nielsen, M., Lehre, K.P., Danbolt, N.C.,1996. Brain glutamate transporter proteins form homomultimers. Journal of Biological Chemistry, 271, pp. 27715-27722.

Hauser, W.A., Kurland, L.T., 1975. The epidemiology of epilepsy in Rochester, Minnesota, 1935 through 1967, Epilepsia., 16(1), pp. 1-66.

Headley, P.M. and Grillner, S., 1990. Excitatory amino acids and synaptic transmission: the evidence for a physiological function, Trends Pharmacol Sci, May, 11(5), pp. 205-211.

Hsu, S., Raine, L., Fanger, H., 1981. The use of avidin-biotin-peroxidase complex (ABC) in immunoperoxidase techinques: a comparison between ABC and unlabeled antibody (PAP) procedures, Journal of Histochemistry and Cytochemistry, 29, pp. 577-580.

Hösli, E., Krogsgaard-Larsen, P., and Hösli, L., 1983. Binding sites for the glutamate-analogue [^{3}H]AMPA in cultured rat brainstem and spinal cord, Brain Research, 268, pp.177-180.

Ingram, E.M., Wiseman, J.W., Tessler, S., and Emson, P.C., 2001. Reduction of glial glutamate transporters in the parietal cortex and hippocampus of the EL mouse, Journal of Neurochemistry, 79, pp. 564-575.

Janjua, N.A., Itano, T., Kugoh, T., Hosokawa, K., Nakano, M., Matsui, H., Hatase, O., 1992. Familial increase in plasma glutamic acid in epilepsy, Epilepsy Research., 11(1), pp. 37-44.

Kanai, Y. and Hediger, M.A., 1992. Primary structure and functional characterization of a high-affinity glutamate transporter, Nature, 360, pp. 467-471.

Kanner, B. I. and Sharon, I., 1978. Active transport of L-glutamate by membrane vesicles isolated from rat brain, Biochemistry, Sep 19, 17(19), pp. 3949-3953.

Kim, J.H., 2001. Pathology of epilepsy, Experimental and Molecular Pathology, 70(3), pp. 345-367.

Klöckner, U., Storck, T., Conradt, M., and Stoffel, W., 1993. Electrogenic L-glutamate uptake in Xenopus laevis oocytes expressing a cloned rat brain L-glutamate/L-aspartate transporter (GLAST-1), Journal of Biological Chemistry, Jul 15, 268(20), pp. 14594-14596.

Kugler, P. and Schmitt, A., 1999. Glutamate transporter EAAC1 is expressed in neurons and glial cells in the rat nervous system, Glia, Aug, 27(2), pp.129-142.

Laemmli, U.K., 1970. Cleavage of structural proteins during the assembly of the head of bacteriophage T4, Nature, 227, pp. 680-685.

Lehre, K.P., Levy, L.M., Ottersen, O.P., Storm-Mathisen, J., and Danbolt, N.C., 1995. Differential expression of two glial glutamate transporters in the rat brain: quantitative and immunocytochemical observations, Journal of Neuroscience , 15, pp. 1835-1853.

Lehre, K.P., Davanger, S., Danbolt, N.C., 1997. Localization of the glutamate transporter protein GLAST in rat retina. Brain Research, 744, pp. 129-137.

Lehre, K.P., Danbolt, N.C., 1998. The Number of Glutamate Transporter Subtype Molecules at Glutamatergic Synapses: Chemical and Stereological Quantification in Young Adult Rat Brain, Journal of Neuroscience, 18, pp. 8751-8757.

Levy, L.M., Lehre, K.P., Rolstad, B., and Danbolt, N.C., 1993. A monoclonal antibody raised against an [Na^+ - K^+]coupled L- glutamate transporter purified from rat brain confirms glial cell localization, FEBS Letters, 317, pp. 79-84.

Levy, L.M., Attwell, D., Hoover, F., Ash, J.F., Bjoras, M., and Danbolt, N.C., 1998. Inducible expression of the GLT-1 glutamate transporter in a CHO cell line selected for low endogenous glutamate uptake, FEBS Letters, Feb 6, 422(3), pp. 339-342.

Lorente de Nó, R., 1934. Studies on the structure of the cerebral cortex: II continuation of the study of the ammonic system, Journal of Psychology and Neurology (Leipzig), 46, pp. 113-77.

Martin, L.J., Brambrink, A.M., Lehmann, C., Portera-Cailliau, C., Koehler, R., Rothstein, J., Traystman, R.J., 1997. Hypoxia-ischemia causes abnormalities in glutamate transporters and death of astroglia and neurons in newbom striatum, Annals of Neurology, 42, pp. 335-348.

Mathern, G.W., Mendoza, D., Lozada, A., Pretorius, J.K., Dehnes, Y., Danbolt, N.C., Nelson, N., Leite, J.P., and Chimelli, L., 1999. Hippocampal GABA and glutamate transporter immunoreactivity in patients with temporal lobe epilepsy, Neurology, 52, pp. 453-472.

Mathern, G.W., Babb, T.L., Armstrong, D.L., 1997. Hippocampal sclerosis, In: Engel, J., Pedley, T.A., eds. Epilepsy: a comprehensive textbook, Lippincott-Raven, Philadelphia, pp. 133-155.

Meldrum, B.S. and Bruton, C.J., 1992. Epilepsy. In: J.H. Adams and L.W. Duchen, eds, Greenfield's Neuropathology, Oxford University Press, New York, pp. 1246–1283.

Meldrum, B.S., 1994. The role of glutamate in epilepsy and other CNS disorders, Neurology, 44, pp. 14-23.

Meldrum, B.S., Akbar, M.T., and Chapman, A.G., 1999. Glutamate receptors and transporters in genetic and acquired models of epilepsy, Epilepsy Research, 36, pp. 189-204.

Mennerick, S., Dhond, R.P., Benz, A., Xu, W., Rothstein, I.D., Danbolt, N.C., Isenberg, K.E., Zorumski, C.F., 1998. Neuronal expression of the glutamate transporter GLT-l in hippocampal microcultures, Journal of Neuroscience, 18, pp. 4490-4499.

Milton, I.D., Banner, S.J., Ince, P.G., Piggott, N.H., Fray, A.E., Thatcher, N., Horne, C.H.W., and Shaw, P.J., 1997. Expression of the glial glutamate transporter EAAT2 in the human CNS: an immunohistochemical study, Molecular Brain Research, 52, pp. 17-31.

Musshoff, U., Schünke, U., Köhling, R., and Speckmann, E.J., 2000. Alternative splicing of the NMDAR1 glutamate receptor subunit in human temporal lobe epilepsy, Molecular Brain Research, 76, pp. 377-384.

Nadler, J.V., 2003. The recurrent mossy fiber pathway of the epileptic brain, Neurochemistry Research, 28, pp. 1649–1658.

Nagao, S., Kwak, S., and Kanazawa, I., 1997. EAAT4, a glutamate transporter with properties of a chloride channel, is predominantly localized in Purkinje cell dendrites, and forms parasagittal compartments in rat cerebellum, Neuroscience, 78, pp. 929-933.

Nonaka, M., Kohmura, E., Yamashita, T., Shimada, S., Tanaka, K., Yoshimine, T., Tohyama, M., and Hayakawa, T., 1998. Erratum to: Increased transcription of glutamate-aspartate transporter (GLAST/glut-1) mRNA following kainic acid-induced limbic seizure [vol 55 (1998), pp. 54-60], Molecular Brain Research, 60, p. 310.

Northington, F.J., Traystman, R.J., Koehler, R.C., Rothstein, I.D., Martin, L.J., 1998. Regional and cellular expression of glial (GLTl) and neuronal (EAAC1) glutamate transporter proteins in ovine fetal brain. Neuroscience, 85, pp. 1183-1194.

Olney, J.W., 1978. Neurotoxicity of exitatory amino acids, In: McGeer, E.G., Olney, J.W., McGeer, P.L., eds. Kaini acid as a tool in neurobiology, Raven Press, New York, pp. 37-70.

Olney, J.W., Collins, R.C., Sloviter, R.S., 1986. Excitotoxic mechanisms of epileptic brain damage, Advances in Neurology, 44, pp. 857-77.

Ottersen, O.P. and Storm-Mathisen, J., 1984. Neurons containing or accumulating transmitter amino acids. Bjorklund, A., Hökfelt, T., and Kuhar, M.J., Handbook of

Chemical Neuroanatomy: Classical Transmitters and transmitter receptors in the CNS. Elsevier Science Publishers B.V., Amsterdam, 3, Part II, pp.141-246.

Ottersen, O.P., Laake, J.H., Reichelt, W., Haug, F.M. and Torp, R., 1996. Ischemic disruption of glutamate homeostasis in brain: quantitative immunocytochemical analysis, Journal of Chemical Neuroanatomy, 12, pp. 1-14.

Pines, G., Danbolt, N.C., Bjørås, M., Zhang, Y., Bendahan, A., Eide, L., Koepsell, H., Storm-Mathisen, J., Seeberg, E., and Kanner, B.I., 1992. Cloning and expression of a rat brain L-glutamate transporter, Nature, 360, pp. 464-467.

Proper, E.A., Hoogland, G., Kappen, S.M., Jansen, G.H., Rensen, M.G., Schrama, L.H., van Veelen, C.W., van Rijen, P.C., van Nieuwenhuizen, O., Gispen, W.H., and de Graan, P.N., 2002. Distribution of glutamate transporters in the hippocampus of patients with pharmaco-resistant temporal lobe epilepsy, Brain, 125, pp. 32-43.

Rauen, T., Kanner, B.I., 1994. Localization of the glutamate transporter GLT-1 in rat and macaque monkey retinae, Neuroscience Letters, 169, pp. 137-140.

Rauen, T., Rothstein, I.D., Wassle, H., 1996. Differential expression of three glutamate transporter subtypes in the rat retina, Cell Tissue Research, 286, pp. 325-336.

Roskoski, R.Jr., 1979. Net uptake of aspartate by a high-affinity rat cortical synaptosomal transport system. Brain Research, Jan 5, 160(1), pp. 85-93.

Rothstein, J.D., Martin, L., Levey, A.I., Dykes-Hoberg, M., Jin, L., Wu, D., Nash, N., and Kuncl, R.W., 1994. Localization of neuronal and glial glutamate transporters, Neuron, 13, pp. 713-725.

Samuelsson, C., Kumlien, E., Flink, R., Lindholm, D., and Ronne-Engstrom, E., 2000. Decreased cortical levels of astrocytic glutamate transport protein GLT-1 in a rat model

of posttraumatic epilepsy, Neuroscience Letters, 289, pp. 185-188.

Sarantis, M. and Attwell, D., 1990, Glutamate uptake in mammalian retinal glia is voltage- and potassium-dependent, Brain Research, May 21, 516(2), pp. 322-325.

Schmitt, A., Asan, E., Puschel, B., Jons, T., Kugler, P., 1996. Expression of the glutamate transporter GLT1 in neural cells of the rat central nervous system: non-radioactive in situ hybridization and comparative immunocytochemistry, Neuroscience, 71, pp. 989-1004.

Schmitt, A., Asan, E., Puschel, B., Kugler, P., 1997. Cellular and regional distribution of the glutamate transporter GLAST in the CNS of rats: nonradioactive in situ hybridization and comparative immunocytochemistry, Journal of Neuroscience, 17, pp. 1-10.

Semah, F., Picot, M.C., Adam, C., Broglin, D., Arzimanoglou, A., Bazin, B., Cavalcanti, D. and Baulac, M., 1998. Is the underlying cause of epilepsy a major prognostic factor for recurrence?, Neurology, 51, pp. 1256–1262.

Shelton, M.K. and McCarthy, K.D., 1999. Mature hippocampal astrocytes exhibit functional metabotropic and ionotropic glutamate receptors in situ, Glia, Mar, 26(1), pp. 1-11.

Simantov, R., Crispino, M., Hoc, W., Broutman, G., Tocco, G., Rothstein, J.D., and Baudry, M., 1999. Changes in expression of neuronal and glial glutamate transporters in rat hippocampus following kainate-induced seizure activity, Molecular Brain Research, 65, pp. 112-123.

Sloviter, R.S., 1992. Possible functional consequences of synaptic reorganization in the dentate gyrus of kainate-treated rats, Neuroscience Letters, 137, pp. 91–96.

Sloviter, R.S., 2005. The neurobiology of temporal lobe epilepsy: too much information, not enough knowledge, Comptes Rendus Biologies, 328, pp. 143-153.

Sommer W., 1880. Erkrankung des Ammonshorns as aetiologisches Momnet der Epilepsie, Archiv fur Psychiatrie und Nervenkrankheiten, 10, pp. 631-675.

Steinhauser, C. and Gallo, V., 1996. News on glutamate receptors in glial cells, Trends in Neurosciences, 19, (8), pp. 339-345.

Spencer, D.D., Spencer, S.S., Mattson, R.H., Williamson, P.D., Novelly, R.A., 1984. Access to the posterior medial temporal lobe structures in the surgical treatment of temporal lobe epilepsy, Neurosurgery, 15(5), pp. 667-671.

Storck, T., Schulte, S., Hofmann, K., and Stoffel, W., 1992. Structure, expression, and functional analysis of a Na^+-dependent glutamate/aspartate transporter from rat brain, Proceedings of the National Academy of Sciences of the United States of America, 89, pp. 10955-10959.

Storm-Mathisen, J., Danbolt, N.C., Rothe, F., Torp, R., Zhang, N., Aas, J.E., Kanner, B.I., Langmoen, I. and Ottersen, O.P., 1992. Ultrastructural immunocytochemical observations on the localization, metabolism and transport of glutamate in normal and ischemic brain tissue, Progress of Brain Research, 94, pp. 225-41.

Szatkowski, M., Barbour, B., and Attwell, D., 1991. The potassium-dependence of excitatory amino acid transport: resolution of a paradox, Brain Research, Aug 2, 555(2), pp. 343-345.

Tanaka, K., 1993. Cloning and expression of a glutamate transporter from mouse brain, Neuroscience Letters, 159, pp. 183-186.

Tanaka, K., Watase, K., Manabe, T., Yamada, K., Watanabe, M., Takahashi, K., Iwama, H., Nishikawa, T., Ichihara, N., Hori, S., Takimoto, M., and Wada, K., 1997. Epilepsy and exacerbation of brain injury in mice lacking the glutamate transporter GLT-1, Science, 276, pp. 1699-1702.

Tauck, D.L. and Nadler, J.V., 1985. Evidence of functional mossy fiber sprouting in hippocampal formation of kainic acid treated rats, Journal of Neuroscience, 5, pp. 1016–1022.

Tessler, S., Danbolt, N.C., Faull, R.L.M., Storm-Mathisen, J., and Emson, P.C., 1999. Expression of the glutamate transporters in human temporal lobe epilepsy, Neuroscience, 88, pp. 1083-1091.

Torp, R., Danbolt, N.C., Babaie, E., Bjoras, M., Seeberg, E., Storm-Mathisen, J., Ottersen, O.P., 1994. Differentia1 expression of two glial glutamate transporters in the rat brain: an in situ hybridization study, European Journal of Neuroscience, 6, pp. 936-942.

Torp, R., Hoover, F., Danbolt, N.C., Storm-Mathisen, J., Ottersen, O.P., 1997. Differential distribution of the glutamate transporters GLT1and rEAACl in rat cerebral cortex and thalamus: an in situ hybridization analysis, Anatomy and Embryology (Berl), 195, pp. 317-326.

Towbin, H., Staehelin, T., and Gordon, J., 1979. Electrophoretic transfer of proteins from polyacrylamide gels to nitrocellulose sheets: Procedure and some applications, Proceedings of the National Academy of Sciences of the United States of America, 76, pp. 4350-4354.

Ueda, Y., Doi, T., Tokumaru, J., Yokoyama, H., Nakajima, A., Mitsuyama, Y., Ohyanishiguchi, H., Kamada, H., and Willmore, L.J., 2001. Collapse of extracellular glutamate regulation during epileptogenesis: down-regulation and functional failure of glutamate transporter function in rats with chronic seizures induced by kainic acid, Journal of Neurochemistry, 76, pp. 892-900.

Ullensvang, K., Lehre, K.P., Storm-Mathisen, J., Danbolt, N.C., 1997. Differential developmental express ion of the two rat brain glutamate transporter proteins GLAST and GLT, European Journal of Neuroscience, 9, pp. 1646-1655.

Van den Berg, C.J. and Garfinkel, D.A., 1971. A simulation study of brain compartments - metabolism of glutamate and related substances in mouse brain, Biochemical Journal, 123, pp. 211-218.

Williamson, A., Spencer, S.S., and Spencer, D.D., 1995. Depth electrode studies and intracellular dentate granule cell recordings in temporal lobe epilepsy. Annals of Neurology, Nov; 38(5), pp. 778-87.

Yamada, K., Watanabe, M., Shibata, T., Tanaka, K., Wada, K., and Inoue, Y., 1996. EAAT4 is a post-synaptic glutamate transporter at Purkinje cell synapses, Neuroreport, 7, pp. 2013-2017.

Yamada, K., Watanabe, M., Shibata, T., Nagashima, M., Tanaka, K., Inoue, Y., 1998. Glutamate transporter GLT-l is transiently localized on growing axons of the mouse spinal cord before establishing astrocytic expression, Journal of Neuroscience, 18, pp. 706-713.

Zerangue, N. and Kavanaugh, M.P., 1996. Flux coupling in a neuronal glutamate transporter, Nature, Oct 17, 383(6601), pp. 634-637.